The Cenozoic volcanism in the Kivu rift: Assessment of the tectonic setting, geochemistry, and geochronology of the volcanic activity in the South-Kivu and Virunga regions

André Pouclet, H Bellon, K Bram

Accepted Manuscript

The Cenozoic volcanism in the Kivu rift: Assessment of the tectonic setting, geochemistry, and geochronology of the volcanic activity in the South-Kivu and Virunga regions

A. Pouclet, H. Bellon, K. Bram

PII: S1464-343X(16)30177-7

DOI: 10.1016/j.jafrearsci.2016.05.026

Reference: AES 2585

To appear in: *Journal of African Earth Sciences*

Received Date: 19 November 2015

Revised Date: 2 April 2016

Accepted Date: 29 May 2016

Please cite this article as: Pouclet, A., Bellon, H., Bram, K., The Cenozoic volcanism in the Kivu rift: Assessment of the tectonic setting, geochemistry, and geochronology of the volcanic activity in the South-Kivu and Virunga regions, *Journal of African Earth Sciences* (2016), doi: 10.1016/j.jafrearsci.2016.05.026.

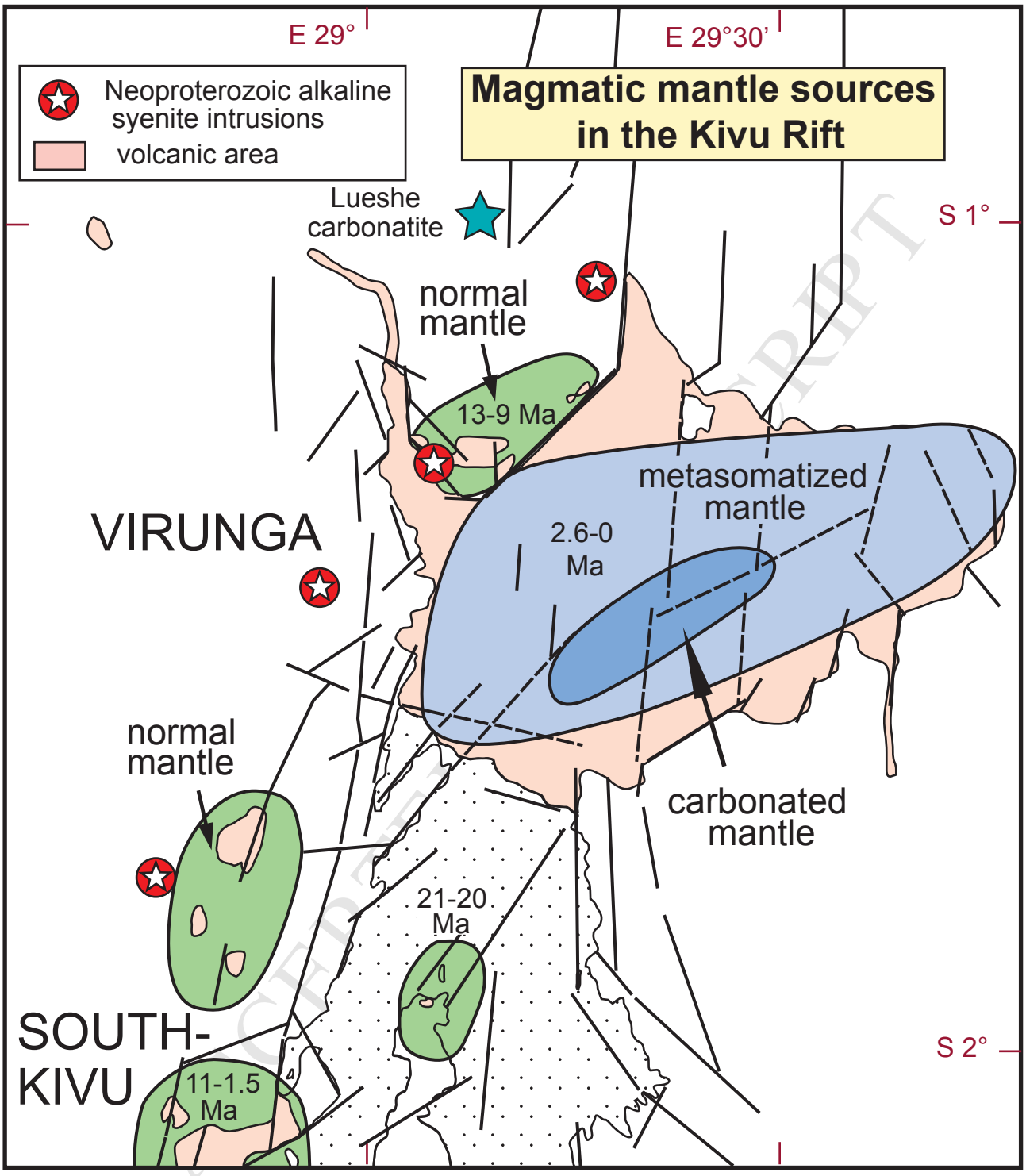
E 29°
E 29°30'
Magmatic mantle sources in the Kivu Rift
Neoproterozoic alkaline syenite intrusions
volcanic area
Lueshe carbonatite
S 1°
normal mantle
13-9 Ma
metasomatized mantle
2.6-0 Ma
VIRUNGA
normal mantle
carbonated mantle
21-20 Ma
SOUTH-KIVU
11-1.5 Ma
S 2°

The Cenozoic volcanism in the Kivu rift: Assessment of the tectonic setting, geochemistry, and geochronology of the volcanic activity in the South-Kivu and Virunga regions.

A. Pouclet[a]*, H. Bellon[b], K. Bram[c]

[a] 3 rue des foulques, 85860 Longeville-sur-mer, France

[b] Université européenne de Bretagne, Université de Brest, UMR Domaines océaniques, IUEM, 6 av. Le Gorgeu, 29238 Brest Cedex3, France

[c] Uhlenkamp 8, D-30916 Isernhagen, Germany

* Corresponding author. E-mail address: andre.pouclet@sfr.fr

Key words: East African Rift, Kivu, Virunga, tholeiitic, alkaline and potassic lavas, K-Ar age dating

ABSTRACT

The Kivu rift is part of the western branch of the East African Rift system. From Lake Tanganyika to Lake Albert, the Kivu rift is set in a succession of Precambrian zones of weakness trending NW-SE, NNE-SSW and NE-SW. At the NW to NNE turn of the rift direction in the Lake Kivu area, the inherited faults are crosscut by newly born N-S fractures which developed during the late Cenozoic rifting and controlled the volcanic activity. From Lake Kivu to Lake Edward, the N-S faults show a right-lateral en echelon pattern. Development of tension gashes in the Virunga area indicates a clockwise rotation of the constraint linked to dextral oblique motion of crustal blocks. The extensional direction was W-E in the Mio-Pliocene and ENE-WSW in the Pleistocene to present time.

The volcanic rocks are assigned to three groups: (1) tholeiites and sodic alkali basalts in the South-Kivu, (2) sodic basalts and nephelinites in the northern Lake Kivu and western Virunga, and (3) potassic basanites and potassic nephelinites in the Virunga area. South-Kivu magmas were generated by melting of spinel+garnet lherzolite from two sources: an enriched lithospheric source and a less enriched mixed lithospheric and asthenospheric source. The latter source was implied in the genesis of the tholeiitic lavas at the beginning of the South-Kivu tectono-volcanic activity, in relationships with asthenosphere upwelling. The ensuing outpouring of alkaline basaltic lavas from the lithospheric source attests for the abortion of the

asthenorpheric contribution and a change of the rifting process. The sodic nephelinites of the northern Lake Kivu originated from low partial melting of garnet peridotite of the sub-continental mantle due to pressure release during swell initiation. The Virunga potassic magmas resulted from the melting of garnet peridotite with an increasing degree of melting from nephelinite to basanite. They originated from a lithospheric source enriched in both K and Rb, suggesting the presence of phlogopite and the local existence of a metasomatized mantle. A carbonatite contribution is evidenced in the Nyiragongo lavas.

New K-Ar ages date around 21 Ma the earliest volcanic activity made of nephelinites. A sodic alkaline volcanism took place between 13 and 9 Ma at the western side of the Virunga during the doming stage of the rift and before the formation of the rift valley. In the South-Kivu area, the first lavas were tholeiitic and dated at 11 Ma. The rift valley subsidence began around 8 to 7 Ma. The tholeiitic lavas were progressively replaced by alkali basaltic lavas until to 2.6 Ma. Renewal of the basaltic volcanism happened at ca. 1.7 Ma on a western step of the rift. In the Virunga area, the potassic volcanism appeared ca. 2.6 Ma along a NE-SW fault zone and then migrated both to the east and west, in jumping to oblique tension gashes.

The uncommon magmatic evolution and the high diversity of volcanic rocks of the Kivu rift are explained by varying transtensional constraints during the rift history.

1. Introduction

The Kivu Rift is the middle part of the western branch of the East African Rift system (**Fig. 1**). This branch separated from the main rift to the north of Lake Malawi and outlined a westward curved path from Lake Rukwa to Lake Albert. The rift valley is discontinuous in displaying a succession of deep lacustrine basins and structural heights commonly overlain by volcanic rocks, *i. e.* from south to north: Rungwe volcanic area, Rukwa and Tanganiyka basins, South-Kivu volcanic area, Kivu basin, Virunga volcanic area, Edward basin, Toro-Ankole volcanic area, and Albert basin.

The East African rift system is commonly explained as the result of one or two mantle plumes beneath Afar and Kenyan Plateaux (Ebinger and Sleep, 1998; Rogers et al., 2000; Furman et al., 2006). It is assumed that the plateaux are dynamically supported by convective activity in the underlying asthenosphere (Ebinger et al., 1989), providing heat transfer for partial melting of the sub-continental lithospheric mantle. Numerous chemically distinctive, but dominately alkaline sodic volcanic provinces emplaced along the entire length of extensional fracture systems across the Ethyopian and Kenyan domes. In return, the western

wranch displays limited and localized volcanic products with a great diversity of chemical compositions including potassic lavas which are rare in the eastern branch. Moreover, the time and space distribution of these various lavas, from oversaturated to undersaturated, sodic to potassic and per-potassic, is problematical and hardly understandable. No "conventional" timing of the magmato-tectonic evolution of the rift can be evidenced. Which kind of rift may provide such a diversity of magmatic rocks with unclear time-related setting? What happened in the western branch of the East African Rift system?

To document this question, it is necessary to constrain the volcano-tectonic evolution, to comfort the geochemical data, and to obtain numerous age markers. Many years ago, we sampled and studied all the volcanic rocks of the South-Kivu and Virunga areas (Pouclet, 1973, 1976, 1980; Pouclet et al., 1981, 1983, 1984; Marcelot et al., 1989). We provided the first significant age data set and discovered the North Idjwi nephelinites, the oldest lavas of the rift (Bellon and Pouclet, 1980). Since that time, a lot of papers were published, some of them providing new and accurate geochemical data (references therein in section 3).

In this study, we expose an updated synthesis of the volcano-tectonic features of the Kivu rift on the base of unpublished maps of the Kivu Lake area, Kahuzi horst, Tshibinda Volcanic Chain, Virunga area, and West-Virunga area (**Figs. 2 to 6**). We complete the analytical data set if necessary for some badly known volcanic series (**Table. 1**) and investigate the magmatological characteristics of the various volcanic series on the base of a revised nomenclature. We perform seventeen new K/Ar age measurements (**Table 2**) and improve the geodynamical history of the Kivu rift. We discuss about the varying behaviour of the rift tectonic constraints, the subsequent conditions of magma genesis from heterogenous mantle sources, and the role of carbonate metasomatism.

2. Volcano-tectonic features of the Kivu Rift

2.1. Background

The Kivu Rift is linked with a large lithospheric swell centred in the Lake Kivu region. It encompasses two volcanic areas: the South-Kivu area to the south, around the city of Bukavu, and the Virunga area to the north, close to the city of Goma (Fig. 1). The main structural features consist of interplayed two fault patterns: a NW-SE trending fault set and a NE-SW to NNE-SSW trending fault set. Some of these faults are reworked fractures of the Precambrian crust which played as normal faults when a large uplift event affected the eastern Congo. The

NW-SE faults control the rift section from Lake Rukwa to north of Lake Tanganyika. They are inherited from Palaeoproterozoic Rusizian and Ubendian structural patterns. Clearly, the rift extends along the Ubendian Belt, a prominent NW-SE crustal structural weakness between the Archaean Bangweulu Block and the Tanzania Craton (Boven et al., 1999; Tack et al., 2010). The NE-SW faults dominate the Lake Kivu region. They belong to the Mesoproterozoic Karagwe-Ankole Belt and are overprinted, to the west of Lake Kivu, by NNE-SSW faults of the Neoproterozoic Itombwe Synclinorium which reoriented the rift direction (Villeneuve, 1987: Villeneuve and Chorowicz, 2004). At the NW to NNE turn of rift direction, from Tanganyika to Kivu lakes, the two fault sets are crosscut by newly born N-S fractures constituting a third set, which developed during late stage of the rift tectonic process. The rift is asymmetric. The western edge is larger and higher than the eastern edge, and east-facing faults are more abundant than the west-facing ones. Similar half-graben structure is described in the Tanganyika rift and explained by the flexural cantilever model (Kusznir and Ziegler, 1992), implying isostatic response of the lithosphere to a continental extension by planar faulting in the upper crust. The E-W crustal extension is estimated to be less than 16 km (Ebinger,1989a, b). The offset of the rift axis between the Tanganyika and Kivu lakes is accommodated by oblique-slip transfer faults along the Rusizi valley. Besides, we explain the southwestern segment of Mwenga by a southwestward propagation of the rift, based on age dating of the basaltic lavas (see geochronological section).

The South-Kivu volcanic area is centred at the crossing of the NW-SE and NNE-SSW fault sets in a classical accommodation zone (Ebinger et al., 1999). It consists of abundant lava flows of olivine tholeiites and sodic alkali basalts, and of few trachy-phonolitic extrusions, all being dated from late Miocene to Pleistocene. The Virunga volcanic area is located at a WSW-ENE dextral shift of the rift, and also in an accommodation zone. It consists of eight large strato- and shield-volcanoes, Nyamuragira (3,058 m), Nyiragongo (3,470 m), Mikeno (4,437 m), Karisimbi (4,507 m), Visoke (3,711 m), Sabinyo (3,634 m), Gahinga (3,500 m), and Muhavura (4,127 m), from south-west to north-east. Mikeno and Sabinyo are the oldest volcanoes and are dated, respectively, to late Pliocene and to Early Pleistocene. Nyiragongo and Nyamuragira are presently active. The other volcanoes were active from Middle Pleistocene to recent time. Two different magmatic suites are displayed: leucite-bearing basanites and evolved lavas at Nyamuragira, Karisimbi, Visoke (*pro parte*), Sabinyo, Gahinga and Muhavura, and leucite-melilite nephelinites and nepheline-leucitites at Nyiragongo, Mikeno and Visoke (*pro parte*) (Pouclet et al., 1981, 1983, 1984). In addition, remnants of basaltic lava flows, dated to Miocene, are preserved at the upper western edge of the rift. They

predated the major fault motion of the rift shoulder and the building of the great volcanoes of the main Virunga area (Pouclet, 1975, 1977).

2.2. Main features of the Lake Kivu and South-Kivu volcanic area

2.2.1. Tectonic pattern

The tectonic evolution of the Kivu rift is witnessed by the Lake Kivu structural and sedimentological features. Dating the sedimentary deposition pattern is the best way for defining the tectonic events. Oscillations of the water level are related to climatic phases but also to tectonic pulses and lava damming of outlets. For these reasons, we draw the tectonic map of the Lake Kivu of the Figure 2, after the bathymetric map and the geophysical data of Degens et al. (1973) and Wong and Von Herzen (1974). The Kahuzi Mountain is another key sector for timing the doming of the rift and the subsidence of the rift valley, because it is the source of the Lugulu flows, a large lava pile running down to the west (Fig. 1). For that reason, a field work was done and we draw a sketch map of the volcanic source area in the Figure 3. The youngest volcano-tectonic activity took place in a western upper step of the rift, east of the Kahuzi horst and built a chain of strombolian volcanoes. We mapped this chain in the Figure 4, in order to illustrate its tectonic relationships.

The Lake Kivu is made of a northern basin and two western and eastern basins. The northern basin is a tectonic trough including 400 m of lacustrine sediments. According to the sedimentation rate, the basin may be dated back to about 5 Ma (Degens et al., 1973). The sediment substratum is at around 600 m of elevation. The mountainous edges reaching 3,000 m, the relative vertical motion is calculated at 2,400 m (Pouclet, 1975). The western and eastern basins, on both sides of the Idjwi Island, were former valleys, with rivers flowing down to the northern basin. These valleys were flooded after the damming of the lake northern run-off, which resulted from building of the Nyiragongo and Nyamuragira volcanoes, in the late Pleistocene. The maximum water level reached 1,650 m, at the Bukavu shelf level, ca. 10,000 years ago (Denaeyer, 1954; Pouclet, 1975, 1978). Then, it lowered in furthering the excavation of the Rusizi canyon. The Lake Kivu southward overflow is recorded in the Lake Tanganyika sediments at 9,400 yr BP (Haberyan and Hecky, 1987) or 10,600 yr BP (Felton et al., 2007). The early Holocene high water level coincided with the formation of sub-lacustrine flank volcanoes in the Virunga area, at the northern shore of the lake. But this high level cannot explain the formation of the under-water hyaloclastite vents of South-Idjwi which are much older and thus related to a previous lacustrine basin (Pouclet,

1975, 1978). The present-day level of 1,462 m is stabilized by the hydroelectric dam of Bukavu.

The deep northern basin is crosscut by SW-NE tectonic steps (cross-section A-B, Fig. 2). The southern part consists of an alternation of horsts and basins trending SSW-NNE (cross-section C-D). All the fractures play as normal faults with horst uplifting, graben sinking, and tilting of the steps. The western edge culminates at Mount Kahuzi (3,308 m), which is a Neoproterozoic intrusive complex of acmite- riebeckite-bearing granite, syenite, and quartz-porphyry microgranite, as well as the neighbouring Mount Biega (2,790 m) (Ledent and Cahen, 1965; Kampunzu et al., 1985). These intrusions are dated between 800 and 700 Ma, according to the ages of neighbouring similar alkaline intrusions in the western edge of the rift (Van Overbeke et al., 1996; Kampunzu et al., 1998a).

The Kahuzi Mountain is the source area of important flows (Fig. 3). At its western and southern feet, basaltic flows poured out in westward direction from a fracture system, in the Miocene to Pliocene time. Four main lava flow units are distinguished. Doleritic facies are localized along NW-SE fractures, at the southern to south-western foot of the massif, indicating the feeder sites. Heating of the Kahuzi area by rising of this basaltic magma is probably responsible for rejuvenation to 134 and 55 Ma of K-Ar ages of the Kahuzi rocks (Bellon and Pouclet, 1980). At present, the Lugulu flows consist of a reverse topographic relief of elongated hills. The lava flowed down to the west, but not to the east. They poured out during the doming stage of the rift and predated the formation of the rift because they are cut by the major faults of the rift scarp. Indeed, to the eastern foot of the Kahuzi heights, on the Tshibinda step (Fig. 4), the Quaternary Tshibinda basaltic flows overlie metasediments of the Precambrian substratum, which is devoid of any older lava cover. We thus conclude that a true rift valley did not exist across the swell at the Kahuzi lava flowing time, and lavas only flowed down to the western slope of the dome.

The rift valley initiated in the latest Miocene. East of the western higher steps, Late Miocene lavas are preserved in the Kavumu lowland where they are partly overlain by the Tshibinda Quaternary flows (detailed in the following section). They widely flooded to the Lake Kivu and to the Bukavu and Bugarama grabens, and also poured out in the SSW segment of the rift, the Mwenga graben (Figs. 1 and 2). The western basin of the Lake Kivu is the continuation of the Bukavu Graben. The Idjwi Island is the northern prolongation of the Mushaka horst that separated the Bukavu and Bugarama-Bitare grabens. There is not a single rift valley. However, the deepest part locates in the eastern basin of the lake, where the main rift axis can be assumed to be, in the continuation of the Bitare-Bugarama Graben (Fig. 1).

Fault associated mineral hot springs are abundant (Fig. 2). Many of the faults are more or less presently active as illustrated by the Frebuary 3, 2008 earthquake along the Luhini Fault (Fig. 4).

2.2.2. Volcanic activity

The South-Kivu volcanic activity mainly consisted of basaltic flow piling from fissural eruptions, in the Late Miocene to Late Pliocene (10 to 2.6 Ma; Kampunzu et al., 1998b). In the Pleistocene, a renewed strombolian volcanic activity has built the chain of Tshibinda (Bellon and Pouclet, 1980) (Fig. 4). In the stacked lava field, the old volcanic vents can be localized by their feeder dykes and by interbedded pyroclastic materials, which locally gain a few metres in thickness. Occurrences of intercalated tephra are common, but well-preserved scoria cones are absent or limited to the recent Tshibinda volcanic chain. Some metre-sized basaltic dykes are present in the western (Congo side) and eastern (Rwanda side) upper steps and also in the Mwenga area. They are trending N-S to NE-SW. These features are consistent with linear basaltic eruptions along cracks fringed with small scoria cones. Trachy-phonolitic extrusions are only known in the Bukavu Graben, into and close to the upper-Rusizi canyon. They are dated from 6.14 Ma to 5.05 Ma (Pasteels et al., 1989). In this area, we number five decametre- to hectometre-sized bodies, which intruded a lower basaltic pile and are overlain by flows of olivine basalt and hawaiite.

The Pleistocene chain of Tshibinda consists of numerous well-preserved scoria cones and lava flows (Fig. 4). The chain is named after the Tshibinda site, in its southern end, where the first scoria cones were discovered (Meyer and Burette, 1957). The cones are set at the border of the Tshibinda step, at the eastern foot of the Kahuzi upper shoulder. The chain is 33 km-long in a SSW-NNE direction, from Tshibinda to Leymera. During our mapping, we numbered sixty strombolian cones, 50- to 150 m-high. Most of them are opened and have supplied lava flows. A few flows run to the west, in following the slope of the tilted step, but most of them came down the fault scarp and spread towards the eastern lowlands. A prominent feature is the alignment of vents along SSE-NNW fractures (N 160° trend) in the Tshibinda and Tshibati sectors. This fracture system is consistent with a NE-SW left-lateral strike slip constraint, and an ENE-WSW extensional strain. We dated the Tshibinda chain activity from 1.9 to 1.6 Ma (Bellon and Pouclet, 1980). Younger ages have been suggested but not proved (Pasteels et al., 1989).

2.3. Main features of the Virunga volcanic area

2.3.1. Tectonic pattern

The Virunga volcanic area is located between the Kivu and Edward lakes on a structural height or shoal between two troughs (Fig. 5). The continuation of this shoal beneath the Nyiragongo and Nyamuragira volcanoes is based on sedimentological, volcanological and geophysical evidence (Pouclet, 1975). Its level averages 1,200 m, while the nearest higher topographical Mount Muhungwe rift edge reaches 2,990 m. Thus, the relative vertical motion of the rift floor is around 1,800 m. Subsidence of the Lake Kivu bottom reached approximately 600 m below the shoal level.

The tectonic pattern is linked to right lateral shift of the rift axis between Kivu and Edward lakes, which is underlined by the SW-NE **Tongo**, **Muhungwe,** and **Rutshuru faults**. However, motion along these faults is dominantly vertical. This motion is evidenced by the uprising of sedimentary terraces at the foot of the Tongo scarp to the west, and along the Rutshuru Fault to the east as shown in the Figure 6. These terraces contain Early to Middle Pleistocene littoral sediments of the Lake Edward. They recorded an uplifting of 1,000 m along the Tongo Fault, and of 500 m along the Rutshuru Fault (Pouclet, 1975). Taking into account a vertical motion of 500 m before the Early Pleistocene sediment deposition, the total vertical motion of the Tongo Fault is calculated around 1,500 m. The south-eastern side registered a vertical motion of 1,000 m at the Muhungwe Fault. This motion in evidenced along the N-S **Kisenyi Fault**, in the continuation of eastern border of the Lake Kivu northern trough. Meanwhile, at the eastern end of the Virunga area, vertical displacements are limited to a few hundred of metres along N-S and SSE-NNW faults.

The structure and nature of the volcanic substratum are constrained by the trends of the volcano-tectonic framework and the composition of the volcanic xenoliths. In the Virunga area, underlying cliffs moulded by lavas can explain some major topographic uneven differences. It is the case for the N-S west-facing scarp between the Karisimbi-Mikeno volcanoes, in the upper eastern side, and the Nyiragongo-Nyamuragira volcanoes, in the lower western side. This scarp is in the continuation of Rwandese east-Kivu Fault (Fig. 1) and is connected with the eastern fault of the Kirwa sedimentary terrace (Fig. 5). It is named the "**Virunga Fault**". This fault has right-lateral en echelon segments, as shown by shift of the Kirwa Fault to the fault of the low Rutshuru terrace. A sub-parallel less important scarp separates the Mikeno to the Karisimbi-Visoke, and is linked to a fault at the north-western border of the Precambtian substratum, south of the Rutshuru Fault. It is named the "**Mikeno Fault**". A third scarp is located between Sabinyo and Gahinga. To the lower southern flank of

Nyiragongo, a transverse WNW-ESE scarp is merely related to a fault between the Virunga shelf and the northern basin of Lake Kivu.

Two types of volcanic fractures are distinguished. Some fractures show radial distribution on the flank of the largest volcanoes. But many others are aligned independently of the volcano building shape. A SW-NE trend of fractures locates in the prolongation of the east fault of the M'Buzi peninsula. It reveals a major fault between Nyiragongo and Nyamuragira, the "**Kameronze Fault**", which is ascertained for many reasons. Firstly, the M'Buzi block is extended below the lava cover, according to gravimetric data (Evrard and Jones, 1963). Secondly, the xenoliths of Nyiragongo consist, solely, of granite rocks, while those of Nyamuragira are made of metashales, quartzites, and micaschists. Thus, the two volcanoes were emplaced in two geologically different steps of the rift floor. Thirdly, there is a deepening of focal depth of tectonic earthquakes from west, in the Nyamuragira area, to east, in the Nyiragongo area (Tanaka, 1983). Fourthly, the Kameronze fractures have provided original lava, the rushayite, an ultrabasic olivine-rich melilitite, which is unknown in the rest of Virunga. This rare lava could be originated from a deep cumulate zone of the Nyiragongo magma chamber or from an independent reservoir (see discussion in section 3.4.). Thus, the Kameronze Fault separates the low granitic step of Nyiragongo to the upper meta-sedimentary step of Nyamuragira. The two neighbouring volcanoes have very different lava compositions. Their different setting in two distinct crust compartments may explain their different way of magma feeding. A SSW-NNE fracture set is partly in the continuation of the Kameronze Fault to the north-east. But, its related eruptive vents produced Nyamuragira-type lavas. An important SW-NE fissural complex is located between Visoke and Sabinyo. In the same direction, main fractures crosscut the Mikeno, Visoke, and Sabinyo edifices. This complex is linked to a SW-NE major fault emplaced between the Mikeno NW-base and the Karisimbi-Visoke step, parallel to the Muhungwe Fault of the rift edge.

Undeniably, the most important present-day fracture system is the great NNW-SSE fracture zone or weakness zone of Nyamuragira that crosscuts the caldera and the shield volcano, reaching 20 km in length (Pouclet and Villeneuve, 1972; Pouclet, 1976, 1977). In many parts, this tectonic zone is a trench, 15 to 30 m wide and 20 to 30 m deep, limited by two parallel sub-vertical fractures. It is associated with slightly parallel secondary fissures, on the NNW and SSE upper flanks. It extended from Nyamuragira to the Nyiragongo area, across the Kameronze Fault, with large fissures at the NNW flank of this Nyiragongo. This tectonic system, having an axial direction of N 155°, can be considered as a mega tension

gash. In the NNW flank of the Nyamuragira caldera, there is a spectacular fan-shaped succession of fissures where thirteen eruptive events took place since the year 1900.

In addition, the Nyamuragira shield is crossed by N-S faults. In the northern wall of the caldera, a N-S fault shows a two metres-displacement of the lava pile and is intruded by a dyke. The fault motion has occurred after the setting up of the initial summit cone, but before the caldera collapse (Pouclet, 1976). In the SW upper flank, a N-S fault was active during the 1938 eruption that drained a large volume of lava from the caldera. The western flank of the shield displays a morphological lowering of 30 to 40 m. A less important lowering of the SSE flank is due to a N-S fault associated with the Kameronze Fault. Important N-S fractures also concern the southern flank of Nyiragongo. They were responsible for draining of the caldera lavas during the dramatic 1977 and 2002 eruptions (Pottier, 1978; Komorowski et al., 2002). It is concluded that the N-S fractures, not only controlled the structural pattern of the Virunga substratum (Virunga and Mikeno faults), but also play a present-day important role in the tectonic constraints triggering volcanic eruptions.

2.3.2. Volcanic activity

The Volcanic activity began in the Late Miocene. The oldest lavas are preserved as residual basaltic flows, above the western edge of the Bishusha-Tongo area as depicted in Figure 6. They are dated between 12.6 and 8.6 Ma (Bellon and Pouclet, 1980; Kampunzu et al., 1998b). They predated the 1,500 m vertical motion of the Tongo fault system, and then, the rifting process and the main volcanic activity of the Virunga area (Pouclet, 1977). For these lavas we use the term “pre-Virunga” magmatic activity because there is an important time gap and a drastic difference of composition between these Miocene lavas and the Quaternary Virunga lavas. We numbered and sampled a dozen of scattered outcrops of basaltic rocks at small hills in the Bishusha area, above and along the Mushebele scarp, and above the Tongo scarp (Fig. 6). They belong to different dissected and highly eroded lava flows, as it is attested by the various petrographical compositions (olivine basalt, basanite, hawaiite, mugearite, benmoreite) and frequent doleritic textures of the mafic rocks. The lava setting is controlled by NW-SE and NNW-SSE fractures, the same directions that were used by the two recent Mushari fractures of satellite eruptions of Nyamuragira. No field relationships between the flows, in term of succession order, can be inferred. In addition, a thick blanket of tephra coming from the numerous Nyamuragira flank eruptions overlies the entire area.

At the middle flank of Mount Mushebele, an olivine basalt lava flow seems to be overlain by a hawaiite flow that crops out at the top of the scarp. However, the hawaiite is dated at 12.6 ± 0.7 Ma (Bellon and Pouclet, 1980) and the basalt at 10.8 ± 1.7 Ma (Kampunzu et al., 1998b). The 12.6 Ma age was questioned because the hawaiite being at a higher altitude than the basalt must be younger (Kampunzu et al., 1983). There is an alternative explanation: The two lavas are separated by an important normal fault and the hawaiite was tectonically displaced above the basalt.

The other lavas of the west Virunga area are the Mweso valley flows and the Pinga flows (Fig. 1). The Mweso flows poured out in the Mokoto Bay. Their source is hidden by the recent flows of Nyamuragira (Fig. 6). The lavas extended along 32 km in the valley, from Mokoto to the NNW end of the flow system. Our sampling shows that the petrographical composition remains constant: olivine basalt with microphenocrysts of skeletal olivine and aggregated phenocrysts of diopside and labradorite. At the Pinga area, residual basaltic flows are pointed out in the Pinga village and 35 km west of this village, in the Oso valley, (De La Vallée-Poussin, 1933). These lavas cannot belong to the Mweso flow, for topographical evidences, but recalls the Numbi lava for their western position out of the rift. More accurate studies are needed for precising their petrographical and chemical compositions.

The volcanic activity of the Virunga main area began with Mikeno, in the middle part of the shelf between the Kivu and Edward troughs. This volcano was active around 2.6 Ma and maybe until 0.3 or 0.2 Ma (Guibert et al., 1975). The old age of Sabinyo, the second oldest volcano, is only attested by its erosional feature similar to that of Mikeno. Its base is totally covered by lavas from Gahinga and Visoke. It was active around 0.1 Ma (Bagdasaryan et al., 1973; Rançon and Demange, 1983; Brousse et al., 1983; Rogers et al., 1998). Thus, the erosion of Sabinyo may be recent and due to violent volcano-tectonic activities. Gahinga and Muhavura are dated between 0.29 and 0.03 Ma (Rançon and Demange, 1983; Rogers et al., 1998), but recent activities are suspected (Brousse et al., 1983). Visoke consists of two superposed stratovolcanoes (Ongendangenda, 1992). The upper one is as old as 0.08 Ma (Bagdasaryan et al., 1973). Its last eruption in 1957 produced the adventive cone of Mugogo on the lower north flank (Verhaeghe, 1958). Karisimbi is made of a shield volcano overlain by two successive upper flank large cones (De Mulder, 1985). It is dated between 0.14 and 0.01 Ma (De Mulder et al., 1986: De Mulder and Pateels, 1986). Nyiragongo and Nyamuragira emplaced since 12 ka on the lower steps of the Virunga shelf (Pouclet, 1978). Nyiragongo is a combination of three stratovolcanoes, from south to north: Shaheru,

Nyiragongo main cone and Baruta. Shaheru, the first volcano of the complex, may be as old as 0.1 Ma (Demant et al., 1994).

3. Geochemical composition of lavas

Numerous geochemical analyses of South-Kivu and Virunga lavas are available from the literature, though their accuracy is highly variable. Trace element and isotopic data are provided by Mitchell and Bell (1976), Vollmer and Norry (1983), Hertogen et al. (1985), Vollmer et al. (1985), De Mulder et al. (1986), Auchapt (1987), Auchapt et al. (1987), Marcelot et al. (1989), Toscani et al. (1990), Demant et al. (1994), Rogers et al. (1998), Furman and Graham (1999), Platz et al. (2004) and Chakrabarti et al (2009a). These data are reviewed and, when necessary, completed by new analyses (Table 1). The analytical set is used to discuss the petrological features and the magmato-tectonic relationships dealing with the rift formation and evolution. South-Kivu basalts derived from a heterogeneous lithosphere mantle source by variable degrees of melting (Auchapt et al. 1987; Furman and Graham, 1999). Both the leucite-basanite and leucite-nephelinite series of Virunga resulted from moderate or small amount of partial melting of mica-garnet-lherzolite lithospheric and/or asthenospheric mantle, with contribution of carbonatite for the more alkaline series (Pouclet, 1973; Furman and Graham, 1999; Chakrabarti et al., 2009a).

In the South-Kivu and Virunga area, it has been shown in the section 2 that volcanism and doming preceded the rifting, with the Kahuzi and pre-Virunga basalts. Asthenospheric upwelling caused uplift of the lithosphere and partial melting of various sources. However, to document that model, we have to clarify some intriguing questions, because the geochemical data from literature are, in many cases, incomplete and not representative, and sometimes inexact. The questions concern the early and late activity of South-Kivu, the poorly known volcanism of North-Idjwi between South-Kivu and Virunga, and the early activity of Virunga.

What is the composition of the earliest volcanic rocks in South-Kivu? Is it really tholeiitic? It is necessary to ascertain the existence, the age, and the tectonic location of true tholeiites, in one hand, and the timing of the rift formation, in the other hand. The Quaternary South-Kivu Tshibinda volcanoes erupted simultaneously with some Virunga volcanoes. Their basaltic composition is close to that of South-Kivu lavas. What is their place in the South-Kivu magmatic evolution? The early Miocene North-Idjwi lavas are the oldest dated lavas of the Kivu rift. They are not tholeiites but nephelinites. What is their magmato-tectonic meaning between the South-Kivu and Virunga areas? The Miocene pre-Virunga lavas predated the rift

formation, and may be contemporaneous with the first South-Kivu activities. They are very different from the Quaternary Virunga lavas. Their composition, tholeiitic to alkaline, is a matter of debate. What is the true composition of the pre-Virunga lavas? Is it similar to that of the South-Kivu? And, finally, what is the origin of the original features of the Virunga lavas?

3.1. South-Kivu lavas

South-Kivu lavas mainly consist of alkali basalts and tholeiites. The first question deals with the true composition of tholeiites and their meaning in the rift evolution. Then, we revise the composition and the nomenclature of the various volcanic rocks. Most of the activities are dated in the Miocene and Pliocene, but a renewal occurred during the Pleistocene in the Tshibinda site. New analytical data are provided for to better constrain this last magmatic event.

3.1.1. The tholeiite question

Tholeiite lavas have been pointed out at different parts of the South-Kivu volcanic area and in the pre-Virunga field, with various ages. They are very important in the debate about the tectono-magmatic history of the rift. But, examination of these lavas is problematic. Many "tholeiites" have been defined on the basis of their major element composition (low abundance of alkali elements), without mineralogical arguments. As they are always more or less altered, in having high loss on ignition, they could be former alkali basalts secondary depleted in alkali elements. It is tritely verified that altered olivine-rich basalt may display oversaturated norm composition. In addition, it is ascertain for tholeiites by Pasteels and Boven (1989) that many K-Ar ages are questionable, due to alteration (loss of K and/or Ar) and to magmatic argon excess. This tholeiite problem leads to three questions: 1) Are there true tholeiites? 2) Is there a space distribution of tholeiites from the border to the rift axis? 3) Is there a time relationship in the tholeiite and alkali basalt production?

The criteria for defining true tholeiites are their mineral content, crystallization order, and major and trace element composition. Early olivine phenocrysts are absent. Calcic plagioclase crystallizes before sub-calcic pyroxene. For that reason, the tholeiitic doleritic facies displays intersertal texture. Olivine only exists as residual and corroded xenocrysts. There is a single pyroxene of sub-calcic augite composition, or two coexisting pyroxenes that are augite and ferrous hypersthene. The norm calculation gives variable amount of quartz and more than

10% hypersthene. Trace element pattern of continental tholeiites exhibits moderate enrichment of the most incompatible elements. However, olivine-tholeiites contain microphenocrysts of ferrous olivine and partly syncrystallizing plagioclase and augite leading to intergranular or sub-ophitic textures in doleritic facies. Their norm composition is saturated with variable amount of hypersthene. The most incompatible elements are slightly more enriched than for tholeiites.

On the basis of these mineralogical and geochemical criteria, examination of the South-Kivu lavas indicates that true tholeiites are present at five sites: West-Kahuzi, South-Idjwi and Mushaka horst, Bitare-Buragama graben, lower-Rusizi (southern continuation of the Bugarama graben), and Mwenga. Olivine-tholeiites are present at the same sites, plus the Bukavu graben. The answer to the question of space and time distribution is more complicated. Tholeiites are localized along the rift axis, but also at distant fields, though they are concentrated close to the rift axis. Concerning the chronological setting of tholeiites versus alkali basalts, tholeiites are everywhere overlain by alkali basalts, but the transition is diachronic. For instance, at the Mwenga site, tholeiites are younger than the alkali basalts of Bukavu. On the whole, tholeiites predated alkali basalts, and, for that reason, they crop out in the most eroded topographical landscapes. Because the erosion process is variable, the distribution of tholeiites is not known for all the volcanic area.

3.1.2. Composition of lavas

To display relative abundances and features of tholeiitic rocks compared with alkaline lavas, a set of representative and accurate chemical analyses is provided in Table 1. Poorly described and altered lavas are eliminated. Thanks to this precaution, we adopt a normative classification slightly modified from Green (1969): 1) quartz-bearing and hypersthene-rich tholeiite, 2) olivine-tholeiite containing olivine and more than 15% hypersthene, 3) olivine basalt containing olivine and less than 15% hypersthene, 4) alkaline-basalt with 0 to 5% nepheline, 5) basanite with 5 to 15% nepheline, and 6) nephelinite having more than 15% nepheline. Classification of the South-Kivu, North-Idjwi, and Pre-Virunga lavas is accomplished using a tetrahedral diagram of normative proportions of Qtz, Hy, Ol, Ne+Le, and Ab+Or (**Fig. 7**). Compared with the tetrahedral diagram of Yoder and Tilley (1962), diopside is replaced by albite + orthose because the alkali amount is more significant than the calcium content, and the alkali abundance cannot be shown only by feldspathoids. True tholeiites plot in the Qtz – Hy – Ab+Or triangle. In the Ol – Hy – Ab+Or triangle, olivine-

tholeiites are discriminated to olivine basalts by Hy normative amount of more than 15 %. In the Ol – Ne – Ab+Or triangle, the alkali basalt - basanite and basanite - nephelinite limits are determined by Ne normative amounts of 5% and 15%, respectively. In this triangle, some basanites of the Mwenga site are characterized by high MgO contents (9-12 wt %). They are rich in olivine, although being not cumulative. Then they are termed “Mg-basanites”.

Trace element data of the new analyses (Table 1) are completed by those of Auchapt (1987), Auchapt et al. (1987), Marcelot et al. (1989), and Furman and Graham (1999). In the Primitive Mantle normalized incompatible elements diagram (**Fig. 8A**) tholeiites and olivine-tholeiites are moderately fractionated in the light rare earth elements. Their La/Yb ratios range from 8 to 13 and from 10 to 15, respectively. They are not enriched in Ba and Th, and are poor in Rb. Similar patterns are exhibited, with increasing trace element abundances and rare earth element fractionation, from tholeiites to olivine basalts (15<La/Yb<30), alkaline-basalts (20<La/Yb<35), basanites (25<La/Yb<40), and Mg-basanites (40<La/Yb<50). As already suggested by Auchapt et al. (1987), Marcelot et al. (1989) and Furman and Graham (1999), this is consistent with varying degree of partial melting of a lithospheric mantle source, which decreases from tholeiites to Mg-basanites, as shown by the Yb vs. La/Yb diagram (**Fig. 9A**). Auchapt (1987) has calculated the source composition from a set of tholeiitic and basanitic lavas of the Mwenga area. A first source, moderately enriched, (C1, **Table 3**) can be assumed for most of the lavas. A second less enriched source (C2, Table 3) is suitable for lavas that are poor in the most incompatible elements.

Having tested the accuracy of the Auchapt‘s results, we calculated the degrees of partial melting after the reverse method and the source composition C1, for all the South-Kivu mafic lavas and using light rare earth elements (LREE). We obtained the following values: tholeiites and olivine-tholeiites = 15 to 7%, olivine- and alkaline-basalts = 6 to 4%, basanites and Mg-basanites = 3 to 2%. However, to get consistency of partial melting degrees between large ion lithophile elements (LILE) and high field strength elements (HFSE), it is necessary to increase the bulk partition coefficient of heavy rare earth elements (HREE), particularly in the basanite case implying the presence of garnet in the source. This assertion is supported by increasing HREE depletion from alkaline-basalts to basanites characterized by increasing values of Tb_N/Yb_N normalized ratio from 1.78 to 2.27 locating the melting column in the garnet stability field. Indeed, due to the residual garnet effect, the Tb_N/Yb_N melt ratio passes beyond 1.8 at the spinel-garnet transition (Furman et al., 2004; Rooney, 2010).

Batch melting is calculated for the enriched source C1 and the less enriched source C2; results are shown in the La/Sm versus Sm/Yb diagram (**Fig. 9B**). Melt curves are drawn for

spinel-lherzolite, garnet-lherzolite, and a 50:50 mixture of spinel- and garnet-lherzolite. Modal compositions of spinel-lherzolite (olivine 53%, OPX 27%, CPX 17%, spinel 3%) and garnet-lherzolite (olivine 60%, OPX 20%, CPX 10%, garnet 10%) are after Kinzler (1997) and Walter (1998). Mineral/melt partition coefficients for basaltic liquids are after the compilation of Rollinson (1993). Tholeiites may have resulted from ca. 10% of partial melting of spinel-lherzolite from a moderately enriched source. But, globally, South-Kivu magmas may be generated by melting of spinel+garnet lherzolite, from enriched source between the C1 and C2 calculated compositions, assuming increasing amount of garnet, from tholeiites to basanites. Hence, melting took place in the spinel-garnet transition zone at depth surrounding 80 km. The more abundant garnet content in the basanite source locates its melting in the lower part of the transition zone. Partial melting degree of the C1 source decreases from 20% to 5%, from basalts to basanites, along the 50:50 spinel+garnet-lherzolite curve. Lower degrees of partial melting (8% to 2%) and lower amounts of garnet are determined with the C2 source. But, the large dispersion of plots suggests compositional heterogeneities and/or mixing in the melted sources.

Contribution of these different sources has to be tested by using all the incompatible elements. However, chemical bias may be due to crustal contamination and assimilation. This latter process can be evidenced in the Nb/Yb versus Th/Yb diagram (**Fig. 10**). Crustal effect is suspected in the case of thorium enrichment unrelated to magmatic processes. In this diagram, all the lavas plot in the Mantle array along the partial melting vector. No particular Th-enrichment is visible, precluding perceptible crustal assimilation. In addition, Sr-isotopic data of Furman and Graham (1999) do not display Sr anomalous pattern. Hence, the chemical scatter only resulted from magmatic processes, and the analytical data, namely the incompatible element values, can be used to discern magmatic patterns of the different lava suites.

To test the behaviour of incompatible elements, bivariate diagrams have been carried out. Results are illustrated in **Figure 11** with three selected diagrams. La versus Yb diagram shows data scatter between two partial melting curves: a low-Yb and high-La curve, and a low-La curve (1 and 2, Fig. 11A). The lack of significant Yb increase is due to garnet effect, mainly in basanites, which are the most LILE-enriched and-HREE-depleted lavas. The high-La curve evolves from basanites to olivine basalts and can be related to the enriched C1 source. The low-La trend characterizes tholeiites and some olivine basalts; it may be inherited from the less-enriched C2 source (3), as suggested above (Fig. 9B). Fractional crystallization is limited to few tholeiites and olivine basalts (see also Fig. 10A). The Ba versus La diagram

displays a high-Ba curve, a low-Ba curve and an intermediate high-Ba and high-La pattern (1, 2 and 3, Fig. 11B). Nb versus Zr diagram shows a low-Zr curve, a high-Zr curve and an intermediate trend (1, 2 and 3, Fig. 11C). It is concluded that high-Ba and low-Zr values (trend # 1) agree with the enriched source C1 and are best displayed in the Tshibinda Volcanic Chain. Low-Ba and high-Zr values (trend # 2), observed in tholeiitic lavas, comply with the C2 less enriched source. Thus, the double source model can be assumed. Intermediate trends and scattering of plots are explained by varying contributions of the two sources.

Existence of two source components is inferred from Sr-Nd isotopes (Furman and Graham, 1999). The lavas define a Sr-Nd isotope array between a high $^{143/144}$Nd and low $^{87/86}$Sr end-member and a low $^{143/144}$Nd and high $^{87/86}$Sr end-member. The latter end-member characterizes Tshibinda lavas, and complies with the C1 enriched source, that is the main source of these lavas. Further isotope features including the East Africa data by Furman and Graham (1999) indicate that this end-member belongs to the continental lithospheric mantle (CLM). In return, the isotopically depleted end-member is allotted to sub-lithospheric source. Its isotope values correspond to an asthenospheric mantle source much more depleted than the C2 source and close to the FOZO composition as redefined by Stracke et al. (2005). Then, the C2 composition is not an end-member, but probably a mixture of asthenospheric and lithospheric (C1) components.

In short, diversity of South-Kivu magmas results from interplay of three parameters: 1) mixing of two source components, a lithospheric enriched component and a sub-lithospheric (asthenospheric) less enriched or depleted component; 2) varying degree of partial melting as a function of melt depth; 3) modal composition of the melted source with varying amount of garnet. It is concluded that the South-Kivu magmas were generated in the sub-continental mantle at depth surrounding 80 km (spinel-garnet transition zone) with important degree of partial melting for tholeiites, and slightly below 80 km, with low degree of partial melting for basanites. Olivine- and alkaline-basalts were produced under intermediate conditions. It can be assumed that the magma genesis was initiated by upwelling of asthenospheric hot material and by decompression linked to extensional tectonic regime of the rift area.

3.1.3. The Tshibinda Volcanic Chain

According to previous chemical data (Meyer and Burette, 1957; Pouclet, 1976; Guibert, 1977; Villeneuve, 1978; Kampunzu et al., 1979; Bellon and Pouclet, 1980; Pasteels et al.,

1989), the lavas of the Tshibinda Volcanic Chain (TVC) share the composition of olivine basalt and alkaline-olivine basalt similar to that of the Mio-Pliocene alkaline lavas (Fig. 7). However, on the base of four samples from south of the volcanic chain, Furman and Graham (1999) emphasize significant differences in some trace element abundances between the Tshibinda lavas and the other South-Kivu lavas (higher Th/Nb, Nb/Zr, Ba/La, Ba/Nb), while Sr and Nd isotope ratios show that Tshibinda lavas form an end-member in the South-Kivu suite.

To better document the chemical data, we carried out new analyses along the chain (Table 1, Fig. 4). Compared with the South-Kivu alkaline lavas, the TVC lavas are significantly less enriched in less mobile HFS elements, but relatively more enriched in Ba (Fig. 8B). These features are exposed in the Nb versus Zr and Ba versus La covariation diagrams of Figure 11. Tshibinda magma resulted from 4 to 2.5% of partial melting of the C1 lithospheric source as discussed above (Fig. 9B). HREE fractionation points to low amount of garnet (Fig. 8B). Indeed, the Tb_N/Yb_N ratio ranges from 1.41 to 1.85, the higher values corresponding to the more alkali basalts. The source melted in upper level of the spinel-garnet transition zone. Chemical variations along the chain can be explained by increasing of melting degree from south (Tshibinda volcanoes) to the middle part (Tshibati volcanoes). However, in the northern part of the TVC, the Leymera volcanoes, which are set after a volcanic gap of 8 km (Fig. 4), show different chemical (Fig. 11) and isotopical features (Furman and Graham, 1999). The Leymera lava has more Zr, less Th, and is isotopically depleted. This feature is close to the depleted end-member attributed to upwelling asthenosphere, which is absent in the rest of the TVC. This strong difference in a single magmatic event exemplifies heterogeneity of the sources that resulted from mingling of asthenospheric blobs dispersed in the lithosphere.

3.2. North-Idjwi lavas

To the northern tip of Idjwi Island, two decametre-sized outcrops of maftic lava are situated on a hill above the Lake Kivu shore and in a small island, two miles from the mainland. These outcrops are residues of an old volcanic cover. The rock, a nephelinite, displays an intergranular texture with microphenocrysts of olivine and diopside in a nepheline-rich groundmass. Compositionally, the rock is highly undersaturated and sodic-rich (Bellon and Pouclet, 1980; Marcelot et al., 1989; Table 1; Fig. 7). Similar nephelinitic lava occurs on the upper western edge of the rift, in the Numbi area (Fig. 1) (Agassiz, 1954). But, unfortunately, we were not able to sample these outcrops. The Primitive Mantle

normalized incompatible element pattern (**Fig. 12**) shows high incompatible element abundances and strong fractionation (64<La/Yb<67) indicating low degree of melting of an enriched source. This source is clearly related to the garnet-lherzolite mantle (Figs. 9, 11A) complying with high values of the Tb_N/Yb_N ratio from 2.41 to 2.50. The partial melting degree is calculated at 2%.

Structural position of these nephelinites is peculiar in the Kivu Rift, far north to the South-Kivu volcanic area, and south to the Virunga area beyond the Lake Kivu. The nephelinites have been K-Ar dated at 28 Ma (Bellon and Pouclet, 1980). A new K-Ar age shows that the lavas are ca. 21 Ma (also see forward, geochronological section). Consequently, the first volcanic activity related to the western branch of the rift was nephelinitic, and took place somewhere between the South-Kivu and Virunga areas, a long time before the rifting and the Lake Kivu formation.

3.3. Pre-Virunga lavas

The Middle Miocene Pre-Virunga lavas consist of dismembered flows roosted on the western edge of the rift. Flows are cut by the Mushebele and Tongo faults (Fig. 6). First petrographical and chemical data allocated these lavas to basaltic alkaline and sodic series (Denaeyer, 1960; Pouclet, 1976). But, some other analyses were used to assume the presence of olivine-tholeiites (Kampunzu et al., 1983, 1998b), which is not supported by petrographical data. However, it is fitting to discard altered samples having high loss on ignition and displaying a false tholeiitic norm composition. Using criteria given above in the South-Kivu section, all the suspected lavas are olivine basalts and not tholeiites. We performed new analyses in the Bishusha and Tongo sectors (Fig. 6; Table 1). All the lavas belong to a sodic-rich basanite series highly fractionated in the light rare earth elements (44<La/Yb<49), Nb, Th, and Ba (Fig. 12). The convenient source must be garnet lherzolite (Fig. 9) taking into account high value of the Tb_N/Yb_N ratio of 2.92. This source may be the same than the lithospheric source of South-Kivu, but with smaller partial melting degrees of 4% to 2%.

In the Tongo sector, the new analyses confirm the presence of mugearite and benmoreite evolved lavas, and thus the occurrence of crustal reservoirs where differentiation processes could have worked. This implies a focusing of a long-lasting source melting.

An intriguing question is the initial geographical distribution of Pre-Virunga lavas. Present-day location of these lavas is limited to western upper step of the rift, west of Tongo Fault. Similar old lavas are totally lacking in the eastern edge, namely in the Muhungwe area.

But one may assume that such lavas may have poured out above the lower steps of the rift, presently overlain by the recent Virunga volcanoes. If it is the case, these lavas must have been sampled by the numerous eruptions of Virunga, and may be collected as xenoliths, like any basement rocks, in the Quaternary Virunga lavas. We have investigated the 107 flank and parasitic cones of Nyamuragira, many flank cones of Nyiragongo, and the Nyamuragira and Nyiragongo calderas. All our collected xenoliths (excluding the cognate xenoliths) only consist of quartzites, shales, and micaschists in the Nyamuragira sector and of granite in the Nyiragongo sector. No Pre-Virunga-like basalts were sampled. Only one sample of basaltic lava has been found in 1959, as ejected block in the inner pit of Nyiragongo. Petrography of this sample was done by Sahama (1978), but without any chemical analysis. The origin of this "basalt" remains questionable. It is concluded that the Pre-Virunga magmatic activity was restricted to the west part of the rift, between 13 and 9 Ma and before the rift valley formation. Volcanic activity of the Virunga area along the rift axis only began in the late Pliocene.

To the west of the rift, close to Pre-Virunga lavas, the Mweso lava flow has run along the valley, from south-east to north-west (Figs. 1, 5, 6). This flow highly post-dated the Pre-Virunga lavas that crop out at the hilltops. It is overlain by recent flows from Nyamuragira parasitic events. Poor chemical data are available for this lava flow (Table 1). However, its alkaline content is close to that of the neighbouring Nyamuragira lavas that belong to a potassic basanite series, and is very different to the sodic series of Pre-Virunga lavas.

3.4. Virunga lavas

Virunga lavas exhibit many outstanding compositions, such as high-potassium content shared with lavas of north part of the Kivu Rift in the Toro-Ankole volcanic area, but unmatched by any other lavas of the East African Rift, except some nephelinites and melilitites of North Tanzania. In this section, the analyzed rocks are distributed according their petrographical features in a simplified nomenclature. The geochemical groups are defined and the question of their magma sources is discussed.

3.4.1. Magma compositions

Virunga lavas are characterized by a potassic magmatic signature, but range in two contrasting series: a leucite basanite series and a leucite-melilite nephelinite series, illustrated

by the two currently active volcanoes, Nyamuragira and Nyiragongo. Because the nomenclature of potassic lavas was imprecise and confusing, we proposed a simplified taxonomic system (Pouclet, 1980, b; Pouclet et al., 1981, 1983, 1984) that has been adopted in most of the following studies of the Virunga lavas. We use the K-prefixed rock names of the sodic series commonly known in the international community: K-basanite, K-hawaiite, K-mugearite, K-benmoreite, and K-trachyte. Limits of the terms are defined by the differentiation index (DI) of Thornton and Tuttle (1960) values of 35, 50, 65, and 80. The more mafic terms (DI < 25) enriched in phenocrystic olivine and/or pyroxene, are named K-limburgite and K-ankaratrite, respectively. The K-basanite and K-hawaiite correspond to local terms of porphyritic kivite and kivite, respectively. The feldspathoid-rich lavas are named after their main mineral contents: olivine melilitite, olivine nephelinite, nepheline melilitite, melilite-leucite nephelinite, leucite nephelinite, and nepheline leucitite.

The leucite basanite series is located at Nyamuragira, Karisimbi, old Visoke, Sabinyo, Gahinga, and Muhavura. It is suspected at Shaheru. The leucite-melilite nephelinite series is located at Nyiragongo, Baruta, Mikeno, and young Visoke. Various compositions of these volcanoes are depicted by the Primitive Mantle normalized trace element diagrams (**Fig. 13**). Chemical data are given by Hertogen et al. (1985), De Mulder et al. (1986), Marcelot et al. (1989), Toscani et al. (1990), Rogers et al. (1992), Rogers et al. (1998), Platz et al. (2004), Chakrabarti et al. (2009a), and by new analyses (Table 1).

Nyamuragira lavas are characterized by moderate enrichment of large ion lithophile elements (LILE; La/Yb = 25-34), slight Sr-negative anomaly, and HREE depletion with Tb/Yb_N ratios ranging from 1.95 to 2.24 (Fig. 13A). All the mobile LILE are equally moderately enriched, including Rb. This last feature distinguishes the Nyamuragira-related western lavas of Kamatembe (N46) and Mushari (N572) from the Pre-Virunga lavas (Table 1; Figs. 5 and 6). These two successive magmatic activities (Pre-Virunga and W-Nyamuragira) came from very different sources (Figs. 12 and 13A). Compared to Pre-Virunga lavas, the Nyamuragira lavas are less enriched in LILEs with the noticeable exception of Rb. The basanitic volcanoes Karisimbi, early Visoke, Sabinyo, Gahinga, and Muhavura share the same trace-element patterns with Nyamuragira (Fig. 13B), though their evolved lavas are normally more enriched in the whole incompatible elements.

Nyiragongo lavas are much more enriched in incompatible elements than Nyamuragira lavas (Fig. 13C). Their La/Yb ratios range from 43 to 58 in the olivine nephelinites, 54 to 69 in the nephelinites and leucitites, and 63 to 73 in the melilitites. They are depleted in HREEs with Tb/Yb_N ranging from 1.93 to 2.86. A peculiar feature is the prominent depletion in Hf.

The other leucite nephelinite volcanoes, Baruta, Mikeno and young Visoke, share similar composition (Fig. 13D). It is worth noting that melilitites are the most enriched in incompatible elements. Leucite-rich leucitites show Rb (and K) enrichment and Ti (and Mg, Fe) depletion, but also high Hf depletion.

In Virunga lavas, HREE depletion points to low degree of partial melting with residual garnet in the source. By using similar approach than for the South-Kivu lavas, the magmatic source of the Virunga lavas may be a garnet peridotite with low or no content of spinel (**Fig. 14**). The nephelinitic magma originated from lower degree of partial melting than the basanitic magma.

Both K and Rb enrichments suggest the presence of phlogopite in the source (Furman, 2007), while low to moderate values of the K/Rb ratio (70-174 in K-basanite series and 117-202 in K-nephelinite series) preclude an amphibole-bearing source, as emphasized by Chakrabarti et al. (2009a and b). In the Ba/Rb vs. Rb/Sr diagram of Furman et al. (2006), elevated Rb/Sr ratios may indicate phlogopite or carbonatite metasomatism. High values are recorded in the K-basanite series (Rb/Sr = 0.06-0.11), excluding the crustal contaminated evolved lavas analyzed by De Mulder et al. (1986) and by Rogers et al. (1998), while the values of the K-nephelinite series are moderate (Rb/Sr = 0.04-0.09). Zr/Hf ratios (41-47) of the K-basanites are consistent with low partial melting of a garnet-clinopyroxene bearing mantle source (Dupuy et al., 1992; Chakrabarti et al., 2009a) and do not indicate carbonate contribution. A phlogopite contribution is retained for K-basanites. Very high Zr/Hf ratios in the Nyiragongo leucite-nephelinites and leucitites (Zr/Hf = 47-94) may be a consequence of carbonatite metasomatism (Dupuy et al., 1992). We show that high Zr/Hf values are due to Hf depletion (**Fig. 15**). This implies contribution of a Hf-poor component in the Nyiragongo source. According to analytical data of Andrade et al. (2002), Zr- and Hf-contents in carbonatites display very large range of values and ratios. This is explained by heterogeneities in the mantle source that are amplified by very low degrees of partial melting of the carbonatite melt. Hf-poor carbonatites with super-chondritic Zr/Hf ratios occurred in Brazilian and Namibian Cretaceous complexes, and in the Oldoinyo Lengai volcano of Tanzania (Fig. 15) (Andrade et al., 2002). In the Quaternary carbonatite lava of Fort-Portal in the Toro-Ankole volcanic area, northern end of Western Rift, the Zr/Hf ratio is 78 (Eby et al., 2009). In the Namibian Kalkfeld Carbonatite Complex, associated nephelinites exhibit Zr and Hf contents close to those of Nyiragongo nephelinites (Fig. 15). In this Complex, the carbonatite melt contribution to nephelinitic magma has been demonstrated (Andrade et al., 2002). It is concluded that the Nyiragongo nephelinitic magma is mixed with a carbonatite melt.

In summary, K-basanite lavas originated from melting of a garnet- and phlogopite-bearing source. According to both garnet and phlogopite stabitity fields in the mantle, the melt depth must be between 80 and 150 km (Chakrabarti et al., 2009a). K-nephelinite series may be derived from the same source, with lower partial melting degree. But, in the Nyiragongo area, this magma has been contaminated by a carbonate component. The questions are: what is the origin of this component, and why very neighbouring volcanoes, Nyamuragira and Nyiragongo, may exhibit very different chemical composition, only one being contaminated? Chakrabarti et al. (2009a) suggest two distinct melting of a very distant heterogeneous plume. This model needs two different channelling in a very long distance for the spatially adjacent volcanoes, and also for the other Virunga volcanoes. Thus, it seems to be an improbable process. It is useful to re-examine the question of the Virunga heterogeneous source, because until now, there is no convincing model.

3.4.2. The carbonatite deal and the sources of Virunga volcanoes

Carbonate metasomatism in Nyiragongo lavas is an old hypothesis for the Virunga magma genesis to explain high alkali and lithophile element contents. Some authors also underline the possible contribution of the crust, without or with carbonatite (Higazy, 1954; Holmes, 1965; Bell and Powell, 1969). Others favour the role of a carbonatite melt (Dawson, 1964) or a volatile transfer (Sahama, 1973). Petrological analyses ruled out the crust contribution (Pouclet, 1973). The isotopic studies gave decisive data. Th isotope ratios are consistent with carbonate metasomatism beneath Nyiragongo according to Williams and Gill (1992). Nd, Sr, and Pb isotope systematics of Nyiragongo nephelinites imply that a previous fluid contamination and LILE enrichment of the source has occurred around 500 Ma ago (Vollmer and Norry, 1983; Vollmer et al., 1985) or between 750 and 850 Ma (Rogers et al., 1992). The style of enrichment could be common metasomatism by mobile fluid or, more probably, melt addition before and during magma genesis (Rogers et al., 1992; Williams and Gill, 1992). Fluid and solid inclusions in Nyiragongo melilites shows that the lava was in equilibrium with a carbonatitic liquid (Louaradi, 1994). The opportunity of carbonatitic enrichment is supported by neighbouring occurrence of the nepheline syenite-carbonatite intrusive complex of Lueshe dated at 619 ± 42 Ma by Van Overbeke et al. (1996) and at 558 ± 11 by Kramm et al. (1997). We discard the 822 ± 120 Ma date of Kampunzu et al. (1998a) having a bad mean square of weighted deviates (MSWD). Coincidently, large flakes of biotite developed close to cancrinite-bearing syenite, in the Lueshe pyrochlore-rich sövite, display a K-Ar age of 516 ±

26 Ma (Bellon and Pouclet, 1980). The Lueshe complex is associated with, at least, four alkaline syenitic intrusions of similar Late Neoproterozoic ages, in the neighbouring west-Virunga area (Kirumba, Bishusha, Fumbwe, Numbi, **Fig. 16**). The cancrinite- and sodalite-bearing syenite of Kirumba is partly rimed with a thin fringe of ankeritic carbonatite. Occurrence of pyrochlore in the alkaline syenite of Numbi suggests a close association with a carbonatite body. Hence, alkaline fluids have contaminated many parts of the sub-continental mantle in the Virunga area at the time of the carbonatite-syenite magmatic activities.

We tentatively locate the potassium-enriched mantle beneath the Virunga volcanic system as a function of magma fingerprints of the different volcanic activities. This mantle extends WSW-ENE from the south-western and western small volcanoes: Nahimbi, Rumoka, Rushayo, Suri-Turunga and Muvo (Nh, Rm, Rs, St, Mv) which are the sites of the most primitive magmas (K-limburgites and olivine-melilitites or “rushayites”) fed by independent tectonic drains unrelated to the tectonic system of the great volcanoes, to the north-east Bufumbiro Bay (Bf) small volcanoes of primitive lavas (K-limburgites or “ugandites” and K-ankaratrites or “murambites”), which were directly fed by their own drains with no magmatic relationships to the neighbouring Muhavura (Fig. 16). This mantle source area includes the more enriched carbonate core extending from Nyiragongo-Baruta to Mikeno and Visoke. The Virunga volcanism began after the uplift of the west (Tongo) and east (Muhungwe) borders, and the sinking of the Kivu and Edward basins dated around 5 Ma. We assume that the early activity took place along the SW-NE oblique zone of the anomalous mantle underlining the offset of rift axis, because the Mikeno emplaced in the middle part of this zone ca. 2 Ma.

The melting depth increased from the western uplifted rift edges (1) to the upper-middle steps (2) and the lower step (3) of the rift valley with the following magma genesis: 1) pre-Virunga sodic basalt, 2) potassic basanite of Nyamuragira and eastern volcanoes, and 3) potassic nephenilite of Nyiragongo, Mikeno and Visoke. Hence the metasomatised mantle was melted at the deepest level of magma genesis of the Virunga area. Similar melting is exhibited in the northern part of the Kivu rift, in the Toro-Ankole volcanic area characterised by highly alkaline, potassic and carbonated lavas defining the kamafungite series. The kamafungite magma genesis implied important contribution of the potassium-rich and carbonatitic component from very deep metasomatised source (Rosenthal et al., 2009).

In the eastern rift, the most K-enriched alkaline lavas are located in northern Tanzania where the rift valley becomes poorly defined in a wide zone overlapping the boundary of the Archaean Tanzanian craton and the Palaeo and Neoproterozoic Ungaran and Mozambique belts. Volcanoes emplaced on the craton and the remobilized craton margin and exhibit K-

nephelinites and melilitites similar to the Virunga ones, and also carbonatites similar to the Toro-Ankole ones (Le Bas, 1981, 1987). A carbonatite metasomatism has been evidenced from mantle xenoliths originated from the lithospheric craton root (Rudnick et al., 1993). Isotopic compositions suggest that the metasomatism occurred recently. The carbonatite was generated either by melting lithosphere that had become carbonated by asthenosphere-derived melts, or directly from the asthenosphere in relationship with the mantle plume heating.

In the Kivu rift, isotope data suggest an older carbonatitic event, may be Neoproterozoic (Vollmer and Norry, 1983; Vollmer et al., 1985; Rogers et al., 1992). But, we cannot exclude the contribution of a volatile-rich transfer from the hot upwelling asthenosphere. In the Toro-Ankole field, Nd, Sr and Hf isotope arrays suggest two time-spaced enrichments of the source: a potassic alkaline silicate metasomatism and later a carbonate-rich metasomatism (Rosenthal et al., 2009).

To comply with these data, we conclude that the distribution of geochemical variations in the Virunga area is explained by zoning of a lithosphere enrichment that has occurred during a Neoproterozoic alkaline magmatic event and by the contribution of plume-related hot and fluid-rich asthenospheric components.

4. Geochronology and history of the rift

4.1. Previous data

Reliable K-Ar geochronological data are provided by Bagdasaryan et al. (1973), Guibert et al. (1975), Bellon and Pouclet (1980), Rançon and Demange (1983), De Mulder (1985), De Mulder and Pasteels (1986), Pasteels et al. (1989), and Kampunzu et al. (1998b). Some Ar/Ar ages of the Sabinyo and Muhavura volcanoes were obtained by Rogers et al. (1998).

There is a consensus about a three stages volcanic story of the South-Kivu area. Activity began around 10 Ma with outpouring of tholeiites and olivine-tholeiites. While this tholeiitic production seems to decline, the magma evolves to an alkali basaltic composition, around 8 Ma. A new rising alkaline activity, the second stage, took place between 7 and 4 Ma. These Miocene to Pliocene activities supplied the main part of the basaltic pile of the South-Kivu area. The third stage consists of strombolian eruptions of the Tshibinda Chain, in the early Pleistocene. Around the Virunga area the Pre-Virunga activity is dated between 13 and 9 Ma. Activities of the Virunga main volcanoes are dated from 2.6 Ma to present time (see section 2.3.).

The northernmost volcanic area of Toro-Ankole, north-east of Lake Edward, is approximately dated to the Late Quaternary, with some accurate ages between 50 and 10 ka after Boven et al. (1998).

4.2. New K-Ar age data

We display a new set of 17 whole rock K-Ar determinations (Table 2). Samples locate from north and south of Idjwi Island, Bitare-Bugarama graben, Bukavu graben (Cyangugu-upper Rusizi), and western upper edge of the rift (**Fig. 17**).

We paid a special attention to the Idjwi Island where we previously obtained very old ages (Bellon and Pouclet, 1980) not supported by further studies (Pasteels and Boven, 1989; Pasteels et al., 1989).

The small outcrops of nephelinite lava were sampled north of Idjwi Island. They are residues of an old flow cover (see above). First dating yielded 28 ± 1.4 Ma, a rather old age that has been declared "not reliable" by Kampunzu et al. (1998b). Enrichment of radiogenic argon may be suspected. A new measurement (LKa4) indicates 19.98 ± 1.00 Ma. One another sample (BK8) of the same lava gives a similar age of 20.97 ± 0.56 Ma. According these new data, an early Miocene nephelinitic activity is proved. It took place between the South-Kivu area and the Virunga area, before the birth of the Lake Kivu (dated ca. 5 Ma) that separates the two areas.

The southern Idjwi Island is partly covered with tholeiitic and alkali basaltic flows belonging to the South-Kivu volcanic area. Tholeiites poured out over the crystalline basement and are overlain by alkali basalts. In two places, tholeiitic flows are linked to accumulations of hyaloclastites that are remnants of under-water volcanic cones. They are also few small outcrops of diatomite-rich lacustrine deposits that are dated to the early Holocene by their diatom composition. These last deposits were produced when the Lake Kivu has reached its highest level, between 10 and 8 ka B.P., before the digging of the Rusizi canyon (Pouclet, 1975) and thus are not related to the hyaloclastites. New ages measurements of tholeiite flows yield ages of 10.30 ± 0.35, 9.56 ± 0.48, 8.76 ± 0.44, 7.73 ± 0.30 and 6.62 ± 0.66 Ma (BK14, 19, 15, 36 and 7, respectively). An alkali basalt (BK-18) overlying the tholeiites is dated at 7.07 ± 0.51 Ma.

Finally, what could be the true age for this tholeiitic activity? An analytical study of argon behaviour in similar tholeiitic lavas from South-Idjwi has been conducted by Pasteels and Boven (1989). Apparent ages were obtained from 16.9 to 3.9 Ma. The authors concluded to

the presence of excess argon and discarded the older ages. They dated to 4.1 Ma a sample of alkali basalt overlying tholeiites, and suggested that tholeiite activity may be as young as 5 Ma. It is known that sample preparation for K-Ar analyses cannot totally eliminate xenocrystic fragments of the substratum that cause argon gain leading to old apparent ages. Conversely, alteration is responsible for potassium and radiogenic argon losses that likely make the ages younger. Unfortunately, South-Kivu tholeiites are rich in vitreous groundmass containing most of the potassium and radiogenic argon, and this groundmass is easily altered. So, young ages are not more credible than the old ones. Taking up to 7.07 Ma the age of the overlying (fresh and not vitreous) olivine basalt, the South-Idjwi tholeiites must be dated between 10.3 and 7 Ma, owing to our new datings.

To document the question of initial tholeiitic activity of South-Kivu area, tholeiites from the on-land southern prolongation of South-Idjwi lavas (RW86, 87) have been analyzed by one of us (H.B.) and age results were listed in Marcelot et al., (1989). Respectively, the following results are obtained: 8.97 ± 0.45, and 11.42 ± 0.57. These results are consistent with previous age data of tholeiites from upper Rusizi (10.0 to 7.6 Ma; Pasteels et al., 1989), and from the western edges (8.2 to 6.9 Ma; Kampunzu et al., 1998b).

Additional alkali basalts were dated in the middle part of the rift (Fig. 17): Bugarama graben (RW88, 83) 10.63 ± 0.53 and 7.75 ± 0.39 Ma, and upper Rusizi area (RW90, 89, 82, 81) 8.10 ± 0.40, 7.68 ± 0.38, 7.18 ± 0.36, and 6.33 ± 0.32 Ma. Of important are the lavas of the Kahuzi fracture zone, which are cross-cut by the main faults of the western upper steps. A dating (MM2) gives 8.19 ± 0.40 Ma (Figs. 1, 3).

4.3. Geodynamical history of the rift

Taking into account the revised and the new data, in addition to the previously published data (Bagdasaryan et al., 1973; Guibert et al., 1975; Bellon and Pouclet, 1980; Pasteels and Boven, 1989; Pasteels et al., 1989; Kampunzu et al., 1998b) there is a total of 67 K-Ar ages for South-Kivu, pre-Virunga, and Mikeno lavas (**Table 4**). We exclude the post-1 Ma young lavas. These ages are plotted on a histogram in **Figure 18**.

The earliest volcanic event happened around 21 Ma in the North-Idjwi, close to the future axis of the rift, and likely, to the western side (**Fig. 19**). It is assumed that most of the lavas of this first activity are hidden by the South-Kivu and Virunga lavas. These early Miocene lavas are strongly alkaline and nephelinitic and resulted from a very low partial melting of mantle source. At that time, the rift valley did not exist and no swell is evidenced. A large outcrop of

old nephelinites is located west of the Lake Kivu, close to an alkaline syenite intrusion (Numbi, Fig. 16) belonging to the Neoproterozoic anorogenic alkaline activity already checked in the Kahuzi area, and west of the Virunga. The alkaline intrusions are set along a NNE-SSW striking line named “the Neoproterozoic Weakness Line” (Fig. 19A). It is postulated that the initial volcanic activity of the Kivu Rift, as well as the Pre-Virunga early activity was drained by such an inherited fracture zone.

We indicate that, in the Kivu Rift, volcanism began contemporaneously with that of the Kenya Rift ca. 23 Ma (Hendrie et al., 1994) and of southern Ethiopia ca. 21 Ma (George and Rogers, 2002), though the earliest magmatism of the eastern rift is dated at 45 Ma in the main rift Ethiopia (George et al., 1998). Our data rectify common belief that the Western Rift volcanism began 5-10 m.y. after the Kenya Rift volcanism.

Pre-Virunga volcanic activity took place between 13 and 9 Ma. It is located in the Neoproterozoic Weakness Line, and controlled by NW-SE faults oblique to the rift axis (Fig.19A). The Tongo Fault was not yet active. The existence of a crustal magma chamber beneath this volcanic field is attested by the output of evolved lavas. The composition is alkaline sodic and indicates a low degree of melting of the source.

At ca. 11 Ma, tholeiitic volcanism was emplaced in the South-Kivu, along the South-Idjwi – Bitare-Bugarama structure, parallel to the rift axis (Fig. 19). Flows poured out along a north-south fracture system. Besides, the 8.2 Ma Kahuzi flow (MM2) to the edge of the upper step ran down to the west. This flow direction complies with the existence of a swell and with the absence of a rift graben. However, the tholeiitic underwater hyaloclastites and flows of South-Idjwi, which are dated around 8 Ma, involve the existence of a lacustrine basin. It must be assumed that a first, though limited graben was formed along the rift axis, at ca. 8 Ma.

Afterwards, the tholeiite magma contribution decreased until 5 Ma, but was no longer restricted to the rift axis. Last tholeiitic lavas poured out on the western upper Kahuzi step and on the Mwenga area where they are overlain by 5.8 to 2.6 Ma alkaline lavas (Fig. 19). In the same time, since 10.6 Ma or 8.5 Ma, an alkaline magma production resulted from less partial melting of a heterogeneous source. The activity was located along the Bugarama north-south tectonic axis, and then, along the N-S and NNE-SSW trending faults of the whole area. The most significant basaltic supply is dated between 8 and 7 Ma. The alkali basalt lava flew down above the western steps of the rift. Their local unconformity above the tholeiites in the Bugarama graben confirm that the rift valley was initiated around 8 Ma. Subsidence of the northern basin of Lake Kivu began ca. 5 Ma. Between 6 and 5 Ma, extrusion of evolved lavas (trachyte-phonolite), into and close to the Bukavu graben, pointed to the ponding of alkaline

magma into crustal reservoirs in a limited area. After 5 Ma, volcanic activity decreased and migrated to the south-west tectonic zone of Mwenga until 2.6 Ma, in correlation with the decreasing of the partial melting degree of the source which produced Mg-basanites. Such a timing and the magmatic feature are consistent with a rift propagation in the Mwenga branch. The last activity, around 1.7 Ma, has built the Tshibinda Chain at the edge of Mount Kahuzi. Its alkaline lavas imply a new and moderate degree of melting of a similar source. Consequently, a thermal anomaly was persisting below the higher western part of the rift in the Lake Kivu area. More recent eruptions (possibly late Pleistocene) in the Tshibinda Chain and Rwandese shore lake have been assumed by Pasteels et al. (1989) and by Ebinger (1989a). However, new accurate chronological data are needed to improve the temporal constraints of these latest eruptions.

In the Virunga area above the shelf between lakes Kivu and Edward, volcanic activity was initiated along a SW-NE fracture zone at the Mikeno area, ca. 2.6 Ma (Guibert et al., 1975), and then propagated to the SW at the Shaheru, and to the NE at the early-Visoke, early-Karisimbi, Sabinyo, Gahinga and Muhavura until to 0.1 Ma (Bagdasaryan et al., 1973; Rançon and Demange, 1983; Rogers et al., 1998). In recent time, volcanism occurred simultaneously in the eastern side at young-Visoke, Karisimbi and Muhavura (Rançon and Demange, 1983; De Mulder, 1985; Rogers et al., 1998), and in the middle area, at Baruta. Lastly, eruptions were focused in the middle Virunga at Nyiragongo, and to the west at Nyamuragira.

7. Conclusions

This study addresses the tectonic pattern, volcanic rock compositions, and age dating of the Kivu Rift in the western branch of the East African Rift system, with the aim of improving the history of the rift and deciphering the relationships between the volcano-tectonic pattern and the conditions of magma genesis.

The rift resulted from stretching of the continental lithosphere that produced thinning and passive upwelling of hot asthenosphere. The tectonic framework evolved with linking of fault segments inherited from weakness zones of the basement, and with development of isolated basins in the rift axis. Rising of the top of the asthenosphere with thinning of the lithospheric mantle initiated the decompressional driven partial melting of the lithosphere and asthenosphere, successively. This first pre-rift doming stage is portrayed with the 21 Ma nephelinites of North-Idjwi, the 13-9 Ma alkaline basalts of West-Virunga, and the 11-8 Ma

tholeiites of South-Kivu. At that time, no fault scarps were developed and the rift valley was not yet created, though a small lacustrine basin existed in the South Idjwi area owing to the occurrence of hyaloclastites. The magma composition logically evolved from highly alkaline to moderately alkaline and to sub-alkaline with increasing amount of lavas, in relationships with increasing degree of partial melting and more important contribution of the asthenospheric component. The N-S and NNW-SSE trend of the fertile fractures suggests an E-W strain field direction.

But, in the following stage, the magma production stopped in the Virunga area and completely changed in South Kivu with the outpouring of alkaline basalts, as soon as 8.5 Ma. The partial melting decreased and was limited to lithospheric mantle. One may note the lack of voluminous flood basalts, a salient component of the extensional rifting evolution in the Ethiopian-Somalian branch of the East African rift. Then, the rift valley was created and the lake basins subsided, namely around 5 Ma for the Lake Kivu. This indicates the cessation of the extensional process and the cooling of the underlying mantle, as proved by the decreasing degree of partial melting of the late Pliocene Mg-basanites of the Mwenga branch. The extrusion of differentiated lavas between 6 and 5 Ma in the Bukavu graben, points to magma storage into crustal reservoir, and to the non-existence of an opened fissural system.

Again, the Kivu rift evolution completely changed when a new highly alkaline and potassic volcanism appeared in the Virunga site around 2.6 Ma. From that time until now, this event is controlled by a transtensional constraint and the opening of a tension gash with an ENE-WSW extensional displacement. This constraint affected the South-Kivu and induced a moderate melting of the lithosphere in the Tshibinda Volcanic Chain during the Pleistocene. In the Virunga area, the magmas tapped a deep mantle source previously enriched by carbonated metasomatism. The success of the melt production is explained by the high volatile content of the mantle source which facilitated the melting. In the same structural context, a normal mantle would not melt. In return, the presence of a metasomatized mantle is the effect of a former Proterozoic magmato-tectonic event which created the structural weakness zone reactivated and used by the Kivu rift. Thereby, the existence of the outstanding Virunga volcanic province is not really fortuitous.

The history of the Kivu rift is not a smooth running of a standard rift development. It is strongly dependent on space and time distribution and changing of the surrounding driving forces in the African plate. Meanwhile, no accurate correlations can be evidenced with the eastern branch of East African Rift. Further studies and age datings are needed to attempt a more comprehensive model of the East African magmato-tectonic evolving constraints.

1018 .

1019 **Acknowledgments**

1020

1021 We gratefully acknowledge Peter Kunkel, director of the “Institut pour la Recherche en
1022 Afrique Centrale”, the former “Centre de Recherches en Sciences Naturelles“ (CRSN), for
1023 providing facilities during the four years of field studies and for his warmful support. We
1024 thank Andrew Conly and Alfred Wittaker for improving the English text.

1025

1026 **References**

1027

1028 Agassiz, J.F., 1954. Géologie et pegmatites stannifères de la région de Mumba-Numbi.
1029 Comité National du Kivu (Congo) N.S. n° 7, 78 pp.
1030 Andrade, F.R.D. de, Möller, P., Dulski P., 2002. Zr/Hf in carbonatites and alkaline rocks:
1031 New data and a re-evaluation. Revista Brasileira de Geociências 32, 361-370.
1032 Auchapt, A., 1987. Les elements traces dans les basalts des rifts continentaux : exemple de la
1033 province du Sud Kivu (Zaïre) dans le rift Est-Africain. Documents et Travaux du Centre
1034 Géologique et Géophysique de Montpellier, France, n° 12, 99 pp.
1035 Auchapt, A., Dupuy, C., Dostal, J., Kanika, M., 1987. Geochemistry and petrogenesis of rift-
1036 related volcanics from South Kivu (Zaire). Journal of Volcanological and Geothermal
1037 Research 31, 33-46.
1038 Bagdasaryan, G.P., Gerasimovskiy, V.I., Polyakov, A.I., Gukasyan, R.K.H., 1973. Age of
1039 volcanic rocks in the rift zones of East Africa. Geochemistry International 10, 66-71.
1040 Bell, K., Powell, J.L., 1969. Strontium isotopic studies of alkalic rocks: The potassium-rich
1041 lavas of the Birunga and Toro-Ankole. Journal of Petrology 10, 536-572.
1042 Bellon, H., Pouclet, A., 1980. Datations K-Ar de quelques laves du rift-ouest de l’Afrique
1043 Centrale; implications sur l’évolution magmatique et structurale. Geologische Rundschau
1044 69, 49-62.
1045 Bellon H., Quoc Buü N., Chaumont J. and Philippet J.C., 1981. Implantation ionique d'argon
1046 dans une cible support: application au traçage isotopique de l'argon contenu dans les
1047 minéraux et les roches. Comptes Rendus de l'Académie des Sciences, Paris (France),
1048 Série II, 292, 977-980.
1049 Boven, A., Pasteels, P., Punzalan, L.E., Yamba, T.K., Musisi, J.H., 1998. Quaternary
1050 perpotassic magmatism in Uganda (Toro-Ankole Volcanic Province): age assessment and

1051 significance for magmatic evolution along the East African Rift. Journal of African Earth
1052 Sciences 26, 463-476.
1053 Boven, A., Theunissen, K., Sklyarov, E., Klerkx, J., Melnikov, A., Mruma, A., Punzalan, L.,
1054 1999. Timing of exhumation of a high-pressure mafic granulite terrane of the
1055 Paleoproterozoic Ubende belt (West Tanzania). Precambrian Research 93, 119-137.
1056 Brousse, R., Lubala, R.T., Katabarwa, J.-B., 1983. Découverte d'une formation de nuées
1057 ardentes dans la région de Ruhengeri au flanc sud du volcan Sabyinyo (chaîne volcanique
1058 des Birunga-Rwanda). Comptes Rendus de l'Académie des Sciences, Paris (France), Série
1059 II, 297, 623 – 626.
1060 Chakrabarti, R., Basu, A.R., Santo, A.P., Tedesco, D., Vaselli, O., 2009a. Isotopic and
1061 geochemical evidence for a heterogeneous mantle plume origin of the Virunga volcanics,
1062 Western rift, East African Rift system. Chemical Geology 259, 273-289.
1063 Chakrabarti, R., Sims, K.W.W., Basu, A.R., Reagan, M., Durieux, J., 2009b. Timescales of
1064 magmatic processes and eruption ages of the Nyiragongo volcanics from ^{238}U-^{230}Th-^{226}Ra-
1065 ^{210}Pb disequilibria. Earth and Planetary Science Letters 288,149-157.
1066 Dawson, J.B., 1964. Reactivity of the cations in carbonate magmas. Proceedings Geological
1067 Association of Canada 15, 103-113.
1068 Degens, E.T., Von Herzen, R.P., Wong, H.-K., Deuser, W.G., Jannash, H.W., 1973. Lake
1069 Kivu: structure, chemistry and biology of an East African rift lake. Geologische Rundschau
1070 62, 245-277.
1071 De La Vallée-Poussin, J., 1933. Découverte de nouveaux gisements de lave au Kivu. Bulletin
1072 de la Société Belge de Géologie 43, 74-75.
1073 Demant, A., Lestrade, P., Lubala, R.T., Kampunzu, A.B., Durieux, J., 1994. Volcanological,
1074 and petrological evolution of Nyiragongo volcano, Virunga volcanic field, Zaire. Bulletin
1075 of Volcanology 56, 47-61.
1076 De Mulder, M., 1985. The Karisimbi volcano (Virunga). Musée Royal de l'Afrique Centrale,
1077 Tervuren, Belgique, Annales, Série in-8°, Sciences géologiques n° 90, 101 pp.
1078 De Mulder, M., Pasteels, P., 1986. K-Ar geochronology of the Karisimbi volcano (Virunga,
1079 Rwanda-Zaire). Journal of African Earth Sciences 5, 575-579.
1080 De Mulder, M., Hertogen, J., Deutsch, S., André, L., 1986. The role of crustal contamination
1081 in the potassic suite of the Karisimbi volcano (Virunga, African Rift Valley). Chemical
1082 Geology 57, 117-136.
1083 Denaeyer, M.-E., 1954. Les anciens volcans sous-lacustres de la bordure nord du lac Kivu.
1084 Bulletin de la Société Belge de Géologie 63, 280-298.

Denaeyer, M.-E., 1960. Les laves de la bordure occidentale du fossé tectonique du Kivu, à l'ouest des Virunga. Bulletin de l'Académie Royale Sciences Outre-Mer de Belgique N. S. 6, 1074-1085.

Denaeyer, M.-E., 1972. Les laves du fossé tectonique de l'Afrique Centrale (Kivu, Rwanda, Toro-Ankole). I. – Supplément au recueil d'analyses de 1965, II. – Magmatologie, III. – Magmatogenèse. Annales du Musée Royal de l'Afrique Centrale, Tervuren, Belgique, Série in-8°, Sciences Géologiques n° 72, 134 pp.

Denaeyer, M.-E., Schellinck, F., Coppez, A., 1965. Recueil d'analyses des laves du fossé tectonique de l'Afrique Centrale (Kivu, Rwanda, Toro-Ankole). Annales du Musée Royal Afrique Centrale, Tervuren, Belgique, Série in-8°, Sciences Géologiques n° 49, 234 pp.

De Paepe, P., Fernandez-Alonso, M., 1981. Contribution à la connaissance du volcanisme du Sud-Kivu : la région de Cyangugu-Bugarama (Rwanda). Musée Royal de l'Afrique Centrale, Tervuren, Belgique, Dépt. Géologie et Minéralogie, Rapport annuel 1980, 111-126.

Dupuy, C., Liotard, J.M., Dostal, J., 1992. Zr/Hf fractionation in intraplate basaltic rocks: Carbonate metasomatism in the mantle source. Geochimica et Cosmichimica Acta 56, 2417-2423.

Ebinger, C.J., 1989a. Geometric and kinematic development of border faults and accommodation zones, Kivu-Rusizi rift, Africa. Tectonics 8, 117-133.

Ebinger, C.J., 1989b. Tectonic development of the western branch of the East African rift system. Bulletin of the Geological Society of America 101, 885-903.

Ebinger, C.J., Sleep, N.H., 1998. Cenozoic magmatism throughout east Africa resulting from impact of a single plume. Nature 395, 788-791.

Ebinger, C.J., Bechtel, T.D., Forsyth, D.W., Bowin, C.O., 1989. Effective elastic plate thickness beneath the East African and Afar Plateaus and dynamic compensation of the uplifts., J. Geophys. Res. 94, 2883-2901.

Ebinger, C.J., Jackson, J.A., Foster, A.N., Hayward, N.J., 1999. Extensional basin geometry and the elastic lithosphere. Phil. Trans. R. Soc. London A 357, 741-765.

Eby, G.N., Lloyd, F.E., Woolley, A.R., 2009. Geochemistry and petrogenesis of the Fort Portal, Uganda, extrusive carbonatite. Lithos 113, 785-800.

Evrard, P., Jones, L., 1963. Etude gravimétrique du graben de l'Afrique centrale. La région des volcans Nyiragongo et Nyamuragira. Mémoire de l'Académie royale des Sciences d'Outre-Mer de Belgique, Sciences et techniques 15(5), 1-71.

Felton, A.A., Russell, J.M., Cohen, A.S., Baker, M.E., Chesley, J.T., Lezzar, K.E., McGlue, M.M., Pigati, J.S., Quade, J., Stager, J.C., Tiercelin, J.J., 2007. Paleolimnological evidence for the onset and termination of glacial aridity from Lake Tanganyika, Tropical East Africa. Palaeogeography, Palaeoclimatology, Palaeoecology 252, 405-423.

Furman, T., 2007. Geochemistry of East African Rift basalts: An overview. Journal of African Earth Sciences 48, 147-160.

Furman, T., Graham, D., 1999. Erosion of lithospheric mantle beneath the East African Rift system: geochemical evidence from the Kivu volcanic province. Lithos 48, 237-262.

Furman, T., Bryce, J.G., Karson, J., Iotti A., 2004. East African Rift System (EARS) plume structure: Insights from Quaternary mafic lavas of Turkana, Kenya. Journal of Petrology 45, 1069-1088.

Furman, T, Kaleta, K.M., Bryce, J.G., Hanan, B.B., 2006. Tertiary mafic lavas of Turkana, Kenya: Constraints on East African plume structure and the occurrence of High-μ volcanism in Africa. Journal of Petrology 47, 1221-1244.

George, R.M., Rogers, N.W., 2002. Plume dynamics beneath the African Plate inferred from the geochemistry of the Tertiary basalts of southern Ethiopia. Contributions to Mineralogy and Petrology 144, 286-304.

George, R., Rogers, N., Kelley, S., 1998. Earliest magmatism in Ethiopia: evidence for two mantle plumes in one flood basalt province. Geology 26, 923-926.

Green, D.H., 1969. The origin of basaltic and nephelinitic magmas in the Earth's mantle. Tectonophysics 7, 409-432.

Guibert, P., 1977. Contribution à l'étude du volcanisme du sud Kivu (Zaïre). Archives des Sciences (Genève, Suisse) 30, 15-43.

Guibert, P., Delaloye, M., Hunziker, J., 1975. Contribution à l'étude géologique du volcan Mikeno, Chaîne des Virunga (République du Zaïre) I: Données géochronologiques K/Ar. II: Données isotopiques Rb/Sr. Comptes Rendus Séances Société Physique Histoire Naturelle 10, 57-66.

Haberyan, K.A., Hecky, R.E., 1987. The late Pleistocene and Holocene stratigraphy and paleolimnology of Lakes Kivu and Tanganyika. Palaeogeography, Palaeoclimatology, Palaeoecology 61, 169-197.

Hendrie, D.B., Kusznir, N.J., Morley, C.K., Ebinger, C.J., 1994. Cenozoic extension in northern Kenya: a quantitative model of rift basin development in the Turkana region. Tectonophysics 236, 409-438.

Hertogen, J., Vanlerberghe, L., Namegabe, M.R., 1985. Geochemical evolution of the Nyiragongo Volcano (Virunga, Western African Rift, Zaire). Bulletin Geological Society of Finland 57, 21-35.

Higazy, R.A., 1954. Trace elements of volcanic ultrabasic potassic rocks of southwestern Uganda and adjoining part of the Belgian Congo. Bulletin Geological Society of America 65, 39-70.

Holmes, A., 1965. Principles of physical geology. Ronald Press, New-York, 2nd edition.

Kampunzu, A., Pottier, Y., Vellutini, P.-J., 1979. A propos des produits volcaniques de Cibinda, région de Bukavu (Sud-Kivu, Zaïre). Annales de la Faculté des Sciences de Lubumbashi, Université nationale du Zaïre 2, 21-30.

Kampunzu, A.B., Lubala, R.T., Caron, J.P.H., Vellutini, P.-J., 1983. Sur l'existence de deux cycles volcaniques précédant le volcanisme actuel des Virunga (Nord Kivu-Zaïre). Comptes Rendus de l'Académie des Sciences, Paris (France), Série II, 296, 839-844.

Kampunzu, A.B., Lubala, R.T., Makutu, M.N., Caron, J.-P.H., Rocci, G., Vellutini, P.-J., 1985. Les complexes alcalins de la région interlacustre à l'Est du Zaïre et au Burundi: un exemple de massifs anorogéniques de relaxation. Journal of African Earth Sciences 3, 151-167.

Kampunzu, A.B., Kramers, J.D., Makutu, M.N., 1998a. Rb-Sr whole rock ages of the Lueshe, Kirumba and Numbi igneous complexes (Kivu, Democratic Republic of Congo) and the break-up of the Rodinia supercontinent. Journal of African Earth Sciences 26, 29-36.

Kampunzu, A.B., Bonhomme, M.G., Kanika, M., 1998b. Geochronology of volcanic rocks and evolution of the Cenozoic Western Branch of the East African Rift System. Journal of African Earth Sciences 26, 441-46.

Kanika, M., Kampunzu, A.B., Caron, J.P.H., Vellutini, P.J., 1981. Données nouvelles sur le volcanisme de la Haute Ruzizi (Sud Kivu, Zaïre). Comptes Rendus de l'Académie des Sciences, Paris (France), série II, 292, 1277-1282.

Kinzler, R.J., 1997. Melting of mantle peridotite at pressures approaching the spinel to garnet transition: application to mid-ocean ridge basalt petrogenesis. Journal of Geophysical Research 102, 853-874.

Komorowski, J.-C., Tedesco, D., Kasereka, M., Allard, P., Papale, P., Vaselli, O., Durieux, J., Baxter, P., Halbwachs, M., Akumbe, M., Baluku, B., Briole, P., Ciraba, M., Dupin, J.-C., Etoy, O., Garcin, D., Hamaguchi, H., Houlie, N., Kavotha, K.S., Lemarchand, A., Lockwood, J., Lukaya, N., Mavonga, G., de Michele, M., Mpore, S., Mukambilwa, K., Munyololo, F., Newhall, C., Ruch, J., Yalire, M., Wafula, M., 2002. The January 2002

1185 flank eruption of Nyiragongo volcano (Democratic Republic of Congo): chronology,
1186 evidence for a tectonic rift trigger, and impact of lava flows on the city of Goma. Acta
1187 Vulcanologica 14-15, 27-62.
1188 Kramm, U., Maravic, H.V., Morteani, G., 1997. Neodymium and Sr isotopic constraints on
1189 the petrogenetic relationships between carbonatites and cancrinite syenites from the Lueshe
1190 Alkaline Complex, east Zaire. Journal of African Earth Sciences 25, 55-76.
1191 Kusznir, N.J., Ziegler, P.A., 1992. The mechanics of continental extension and sedimentary
1192 basin formation: A simple-shear/pure-shear flexural cantilever model. Tectonophysics 215,
1193 117-131.
1194 Le Bas, M.J., 1981. Carbonatite magmas. Mineralogical Magazine 44, 133-140.
1195 Le Bas, M.J., 1987. Nephelinites and carbonatites. In Fitton, J.G., Upton, B.G.J. (Eds)
1196 Alkaline igneous rocks: Geological Society of London, Special Publication vol. 30, pp. 53-
1197 83.
1198 Ledent, D., Cahen, L., 1965. Quelques données géochronologiques nouvelles sur les minéraux
1199 des roches du Kivu méridional. Musée Royal de l'Afrique Centrale, Tervuren (Belgique),
1200 Rapport annuel 1964, 94-95.
1201 Louaradi, D., 1994. Etude isotopique (carbone, oxygène) et microthermométrique (inclusions
1202 fluides et vitreuses) des magmas alcalins et carbonatitiques du rift est africain et de la
1203 presqu'île de Kola. Ph. D. Thesis, University of Paris VII, France.
1204 Lubala, R.T., 1981. Etude géologique du massif de Biega (Kivu, Zaïre). Structure,
1205 géochronologie et signification géotectonique. Ph. D. Thesis, Univ. Zaïre, Lubumbashi,
1206 308 pp.
1207 Lubala, R.T., Kampunzu, A.R., Caron, J.P.H., Vellutini, P.J., 1982. Sur la nature et la
1208 signification possible des basaltes de la Lugulu au Sud-Kivu (Zaïre). Comptes Rendus de
1209 l'Académie des Sciences, Paris, Série II, 294, 325-328.
1210 Lubala, R.T., Kampunzu, A.R., Caron, J.P.H., Vellutini, P.J., 1984. Minéralogie des basaltes
1211 saturés tertiaires du Kahuzi-Biéga (Rift du Kivu, Zaïre). Annales de la Société Géologique
1212 de Belgique 107, 125-134.
1213 Lubala, R.T., Kampunzu, A.R., Caron, J.P.H., Vellutini, P.J., 1987. Petrology and
1214 geodynamic significance of the Tertiary alkaline lavas from the Kahuzi-Biega region,
1215 Western rift, Kivu, Zaire. In: Bowden, P. and Kinnaird, J. (Eds) African geology reviews,
1216 Geological journal 22, pp. 515-535.

1217 Mahood G. and Drake R. E. 1982. K-Ar dating young rhyolite rocks : a case study of the
1218 Sierra La Primavera, Jalisco, Mexico, Geological Society of America Bulletin 93, 1232-
1219 1241.
1220 Marcelot, G., Dupuy, C., Dostal, J., Rançon, J.P., Pouclet, A., 1989. Geochemistry of mafic
1221 volcanic rocks from the Lake Kivu (Zaire and Rwanda) section of the western branch of
1222 the African rift. Journal of Volcanology and Geothermal Research 39, 73-88.
1223 Meyer, A., 1953. Notes vulcanologiques. Les basaltes du Kivu méridional. Mémoires du
1224 Service géologique du Congo belge et du Ruanda Urundi 2, 25-52.
1225 Meyer, A., Burette, H., 1957. Nouveaux phénomènes volcaniques au sud-Kivu. Bulletin du
1226 Service Géologique du Congo belge 7 (4), 1-15.
1227 Mitchell, R.H., Bell, K., 1976. Rare Earth element geochemistry of potassic lavas from the
1228 Birunga and Toro-Ankole regions of Uganda, Africa. Contributions to Mineralogy and
1229 Petrology 58, 293-303.
1230 Ongendangenda, T., 1992. Le magmatisme potassique du volcan Visoke (Chaîne des Virunga,
1231 Rift Est Africain) : aspects volcanologiques, pétrologiques et géochimiques. Ph. D. Thesis,
1232 University of Aix-Marseille III, France, 304 pp.
1233 Pasteels, P., Boven, A., 1989. Excès d'argon dans les basaltes de la zone volcanique d'Idjwi
1234 sud (Kivu, Zaïre). Musée Royal de l'Afrique Centrale, Tervuren (Belgique), Département
1235 de Géologie et Minéralogie, Rapport annuel 1987-1988, 101-107.
1236 Pasteels, P., Villeneuve, M., De Paepe, P., Klerkx, J., 1989. Timing of the volcanism of the
1237 southern Kivu province: implications for the evolution of the western branch of the East
1238 African Rift system. Earth and Planetary Science Letters 94, 353-363.
1239 Platz, T., Foley, S.F., André, L., 2004. Low-pressure fractionation of the Nyiragongo volcanic
1240 rocks, Virunga Province, D.R. Congo. Journal of Volcanology and Geothermal Research
1241 136, 269-295.
1242 Pottier, Y., 1978. Première éruption historique du Nyiragongo et manifestations adventives
1243 simultanées du volcan Nyamulagira (Chaîne des Virunga – Kivu – Zaïre : Déc. 76 – Juin
1244 77). Musée Royal de l'Afrique Centrale, Tervuren (Belgique), Département de Géologie et
1245 Minéralogie, Rapport annuel 1977, 157-175.
1246 Pouclet, A., 1973. Contribution à la connaissance du Volcan Nyiragongo (Rift ouest-africain).
1247 Les éruptions intra-cratérales de juillet 1971 à avril 1972. Bulletin Volcanologique 37-1,
1248 37-72.

Pouclet, A., 1975. Histoire des grands lacs de l'Afrique Centrale. Mise au point des connaissances actuelles. Revue de Géographie physique et de Géologie dynamique (2) 17, 475-482.

Pouclet, A. 1976. Volcanologie du rift de l'Afrique Centrale. Le Nyamuragira dans les Virunga. Essai de magmatologie du rift. Ph. D. Thesis, University of Paris-Sud, France, 610 pp.

Pouclet, A., 1977. Contribution à l'étude structurale de l'aire volcanique des Virunga, rift de l'Afrique Centrale. Revue de Géographie physique et de Géologie dynamique (2) 19, 115-124.

Pouclet, A., 1978. Les communications entre les grands lacs de l'Afrique Centrale. Implications sur la structure du rift occidental. Musée Royal de l'Afrique Centrale, Tervuren (Belgique), Département de Géologie et Minéralogie, Rapport annuel 1977, 145-155.

Pouclet, A., 1980. Contribution à la systématique des laves alcalines, les laves du rift de l'Afrique Centrale (Zaïre-Uganda). Bulletin Volcanologique 43-3, 527-540.

Pouclet, A., Villeneuve, M., 1972. L'éruption du Rugarama (mars-mai 1971) au volcan Nyamuragira (Rép. Zaïre). Bulletin Volcanologique 36-1, 200-221.

Pouclet, A., Ménot, R.P., Piboule, M., 1981. Classement par l'analyse factorielle discriminante des laves du rift de l'Afrique Centrale (Zaïre, Rwanda, Uganda). Comptes Rendus de l'Académie des Sciences, Paris (France) 292 (série II), 679-684.

Pouclet, A., Ménot, R.P., Piboule, M., 1983. Le magmatisme alcalin potassique de l'aire volcanique des Virunga (Rift occidental de l'Afrique de l'Est). Une approche statistique dans la recherche des filiations magmatiques et des mécanismes de différenciation. Bulletin de Minéralogie 106, 607-622.

Pouclet, A., Ménot, R.P., Piboule, M., 1984. Différenciation des laves de l'Afrique Centrale (Rift Ouest). Contribution de l'analyse statistique multivariée. Neues Jahrbuch für Mineralogie Abhandlungen 149, 283-308.

Rançon, J.P., Demange, J., 1983. Reconnaissance géothermique de la République du Rwanda. Bureau de Recherches Géologiques et Minières, rapport 83 SGN 192GTH, 130 pp.

Rogers, N.W., De Mulder, M., Hawkesworth, C.J., 1992. An enriched mantle source for potassic basanites: evidence from Karisimbi volcano, Virunga volcanic province, Rwanda. Contribution to Mineralogy and Petrology 111, 543-556.

Rogers, N.W., James, D., Kelley, S.P., De Mulder, M., 1998. The generation of potassic lavas from the Eastern Virunga Province, Rwanda. J. Petrology 39, 1223-1247.

1283 Rogers, N.W., Macdonald, R., Fitton, J.G., George, R., Smith, M., Barreiro, B., 2000. Two
1284 mantle plumes beneath the East African Rift system: Sr, Nd and Pb isotope evidence from
1285 Kenya rift basalts. Earth Planet. Sci. Lett. 176, 387-400.
1286 Rollinson, H., 1993. Using geochemical data: Evaluation, presentation, interpretation.
1287 Longman Group UK Limited, 352 pp.
1288 Rosenthal, A., Foley, S.F., Pearson, D.G., Nowell, G.M., Tappe, S., 2009. Petrogenesis of
1289 strongly alkaline primitive volcanic rocks at the propagating tip of the western branch of
1290 the East African Rift. Earth and Planetary Science Letters 284, 236-248.
1291 Rooney, T.O., 2010. Geochemical evidence of lithospheric thinning in the southern Main
1292 Ethiopia Rift. Lithos 117, 33-48.
1293 Rudnick, R.L., McDonough, W.F., Chappell, B.W., 1993. Carbonatite metasomatism in the
1294 northern Tanzanian mantle: petrographic and geochemical characteristics. Earth and
1295 Planetary Science Letters 114, 463-475.
1296 Sahama, Th.G., 1973. Evolution of the Nyiragongo magma. Journal of Petrology 14, 33-48.
1297 Sahama, Th.G., 1978. The Nyiragongo main cone. Musée Royal de l'Afrique Centrale,
1298 Tervuren (Belgique), Annales, Sciences géologiques 81, 88pp.
1299 Steiger, R.H., Jäger, E., 1977. Subcomission of geochronology: convention on the use of
1300 decay constants in geo- and cosmochronology. Earth and Planetary Science Letters 36,
1301 359-362.
1302 Stracke, A., Hofmann, A.W., Hart, S.R., 2005. FOZO, HIMU, and the rest of the mantle zoo.
1303 Geochemistry Geophysics Geosystem 6 (5), 1-20.
1304 Sun, S.S., McDonough, W.F., 1989. Chemical and isotopic systematics of oceanic basalts:
1305 Implications for mantle composition and processes. In: Saunders, A.D. and Norry, M.J.
1306 (Eds), Magmatism in the ocean basins: Geological Society of London, Special Publication
1307 vol. 42, pp. 313-345.
1308 Tack, L., De Paepe, P., 1983. Le volcanisme du Sud-Kivu dans le nord de la plaine de la
1309 Rusizi au Burundi et ses relations avec les formations géologiques avoisinantes. Musée
1310 Royal de l'Afrique Centrale, Tervuren, Belgique, Département de Géologie et Minéralogie,
1311 Rapport annuel 1981-1982, 137-145.
1312 Tack, L., Wingate, M.T.D., De Waele, B., Meert, J., Belousova, E., Griffin, B., Tahon, A.,
1313 Fernandez-Alonso, M., 2010. The 1375 Ma "Kibaran event" in Central Africa: Prominent
1314 emplacement of bimodal magmatism under extensional regime. Precambrian Research
1315 180, 63-84.

1316 Tanaka, K., 1983. Seismicity and focal mechanism of the volcanic earthquakes in the Virunga
1317 Volcanic Region. In: Hamagushi, H. (Ed.), Volcanoes Nyiragongo and Nyamuragira:
1318 Geophysical Aspects. Tohoku University, Sendai, Japan, pp. 19-28.
1319 Thornton, C.P., Tuttle, O.F., 1960. Chemistry of igneous rocks. I, differentiation index.
1320 American Journal of Sciences 253, 664-684.
1321 Toscani, L., Capedri, S., Oddone, M., 1990. New chemical and petrographic data of some
1322 undersaturated lavas from Nyiragongo and Mikeno (Virunga-Western African Rift –
1323 Zaire). Neues Jahrbuch Miner. Abh. 161, 287-302.
1324 Van Overbeke, A.-C., Demaiffe, D., Verkaeren, J., 1996. The syenite-carbonatite complex of
1325 Lueshe (N-E Zaïre): petrography, geochemistry and Rb-Sr chronology. In: Demaiffe, D.
1326 (Ed.), Petrology and Geochemistry of magmatic suites of rocks in the continental and
1327 oceanic crusts. Université libre de Bruxelles and Royal Museum for Central Africa
1328 (Tervuren, Belgique) pp. 355-370.
1329 Verhaeghe, M.A.P., 1958. Eruption du volcan Mugogo au Kivu. Comptes Rendus de
1330 l'Académie des Sciences, Paris (France), 246, 2917-2920.
1331 Villeneuve, M., 1978. Les centres d'émissions volcaniques du rift africain au sud du lac Kivu
1332 (République du Zaïre). Revue de Géographie physique et de Géologie dynamique (2) 20,
1333 323-334.
1334 Villeneuve, M., 1987. Géologie du synclinal de l'Itombwe (Zaïre oriental) et le problème de
1335 l'existence d'un sillon plissé Pan-africain. Journal of African Earth Sciences 6, 869-880.
1336 Villeneuve, M., Chorowicz, J., 2004. Les sillons plissés du Burundien supérieur dans la
1337 chaîne Kibarienne d'Afrique centrale. Comptes rendus Géoscience 336, 807-814.
1338 Vollmer, R., Norry, M.J., 1983. Possible origin of K-rich volcanic rocks from Virunga, East
1339 Africa, by metasomatism of continental crust material: Pb, Nd and Sr isotope evidence.
1340 Earth and Planetary Science Letters 64, 374-386.
1341 Vollmer, R., Nixon, P.H., Condliffe, E., 1985. Petrology and geochemistry of a U and Th
1342 enriched nephelinite from Mt. Nyiragongo, Zaire: Its bearing on ancient mantle
1343 metasomatism. Bulletin Geological Society of Finland 57, 37-46.
1344 Walter, M.J., 1998. Melting of garnet peridotite and the origin of komatiite and depleted
1345 lithosphere. Journal of Petrology 39, 29-60.
1346 Williams, R.W., Gill, J.B., 1992. Th isotope and U-series disequilibria in some alkali basalts.
1347 Geophysical Research Letters 19, 139-142.
1348 Wong, H.-K., Von Herzen, R.P., 1974. A geophysical study of Lake Kivu, East Africa.
1349 Geophysical Journal of the Royal Astronomy Society 37, 371-389.

Yoder, H.S., Tilley, C.E., 1962. Origin of basalt magmas: an experimental study of natural and synthetic rock systems. Journal of Petrology 3, 342-532.

Caption

Fig. 1 - Tectonic pattern of the western branch of the Eastern Africa rift system in the Lake Kivu region, after Pouclet (1976) slightly modified. Map of the South-Kivu and Virunga volcanic areas. Volcanoes of Virunga: Nyamuragira (N), Nyiragongo (Ny), Mikeno (M), Karisimbi (K), Visoke (V), Sabinyo (S), Gahinga (G), and Muhavura (Mh).

Fig. 2 - Tectonic map of the Lake Kivu and altitude of rift steps in metres. This new map is drawn after the bathymetric map and the geophysical data of Degens et al. (1973) and Wong and Von Herzen (1974), which were acquired during two cruises of the Woods Hole Oceanographic Institution in 1971 and 1972. The sub-water volcanoes were discovered using echo sounder and magnetometer records. A-B and C-C, interpreted cross-sections in the northern and southern basins, respectively. Sub-lacustrine volcanoes of the northern lake side are linked to the Late Pleistocene activity of Virunga during the high level stage (Pouclet, 1975). The South-Idjwi sub-lacustrine volcanoes are much older (Miocene), see section 4.2. Mineral hot springs deposited thick travertine terraces or sinters in the Holocene. The up-lifting points are localized using topographical data. They mark the westward and eastward tilting of the horst steps, in the west side and the east side, respectively.

Fig. 3 - Geological sketch map of the Mount Kahuzi area showing the birth of tholeiitic Lugulu flows (new map). The MM2 basaltic lava is dated at 8.19 ± 0.40 Ma (new dating, Table 2). This lava flow westward poured out during the doming stage of the Kivu Rift, before the rift valley formation. Igneous intrusions are dated to Neoproterozoic and consist of quartz-porphyry microgranite in Mount Kahuzi and of acmite-riebeckite-bearing granites and syenites in the other areas (ref. in the text).

Fig. 4 - Map of strombolian cones of the Tchibinda Volcanic Chain (new map) and location of the analysed lavas. The CRSN ”Centre de Recherches en Sciences Naturelles”, formerly IRSAC “Institut pour la Recherche Scientifique en Afrique Centrale” is located at Lwiro.

Sample numbers refer to analysed rocks (Table 1). Full dots are dated samples: TB4 = 1.9 Ma ; MM1 = 1.7 Ma ; KT1 = 1.6 Ma (Table 4); MM2 = 8.19 Ma (Table 2).

Fig. 5 - Map of the Virunga Volcanic area locating the Plio-Quaternary volcanic activities after Pouclet (1977) completed with the recent volcanic centres. Main edifices: Nyamuragira (N), Nyiragongo (Ny) and its two "elder brothers" Shaheru (Sh) and Baruta (B), Mikeno (M), Karisimbi (K) and its older craters Branca (Br) and Muntango (Mt), Visoke (V), Sabinyo (S), Gahinga (G), and Muhavura (Mh). Lithology of the surrounding substratum is specified. Red dots, flank or parasitic cones; red diamonds, historical parasitic activities.

Fig. 6 - Map of the Bishusha-Tongo area (new map). Outcrops of the Miocene lavas. Altitudes of the Tongo uplifted Pleistocene terraces in metres.

Fig. 7 - Qtz-Ab+Or-Hy-Ol-Ne combined ternary diagrams of the Kivu basaltic lavas. Data after Meyer (1953), Meyer and Burette (1957), Denaeyer et al. (1965), Denaeyer (1972), Pouclet (1976), Guibert (1977), Villeneuve (1978), Kampunzu et al. (1979, 1983, 1998b), Bellon and Pouclet (1980), De Paepe and Fernandez-Alonso (1981), Kanika et al. (1981), Lubala (1981), Lubala et al. (1982, 1984, 1987), Tack and De Paepe (1983), Auchapt (1987), Auchapt et al. (1987), Marcelot et al. (1989), Pasteels et al. (1989), Furman and Graham (1999), and new analyses (Table 1). Normative nomenclature: T, tholeiite (Qtz); Ol-T, olivine-tholeiite (Ol and > 15% Hy); Ol-B, olivine basalt (Ol and < 15% Hy); Alk-B, alkali basalt (0.01% < Ne < 5%); Bs, basanite (5% < Ne < 15%); Neph, nephelinite (Ne > 15%).

Fig. 8 - Primitive Mantle normalized incompatible element diagram of the South-Kivu tholeiitic and alkali basaltic lavas. Tholeiitic and basaltic areas drawn after the analytical data set. New analyses of (A) Miocene lavas, and (B) Pleistocene lavas of the Tchibinda Volcanic Chain from Table 1. Normalizing values after Sun and McDonough (1989).

Fig. 9 - Yb vs. La/Yb and La/Sm vs. Sm/Yb diagrams for determining the enrichment of the source and the partial melting degrees of mantle source. (A) The Yb vs. La/Yb diagram indicates an increase of partial melting, from basanites to tholeiites, and/or varying enrichment of sources compared with the average OIB-type source. (B) Batch melting of

the enriched source C1 and of the less enriched source C2. Melt curves are drawn for spinel-lherzolite, garnet-lherzolite and a 50:50 mixture of spinel- and garnet-lherzolite. Modal compositions of spinel-lherzolite (olivine 53%, OPX 27%, CPX 17%, spinel 3%) and garnet-lherzolite (olivine 60%, OPX 20%, CPX 10%, garnet 10%) are after Kinzler (1997) and Walter (1998). Mineral/melt partition coefficients for basaltic liquids are after compilation of Rollinson (1993). Tholeiites may have resulted from ca. 10% of partial melting of spinel-lherzolite from a moderately enriched source. Basaltic and alkaline lavas resulted from lower degrees of partial melting (10% to 2%) of a spinel- and garnet-lherzolite mixture of varying amount of spinel and garnet.
OIB, Primitive Mantle, N-MORB, and E-MORB compositions are from Sun and McDonough (1989).

Fig. 10 - Nb/Yb vs. Th/Yb diagram to test crustal contamination. Same symbols as for Figure 9. OIB, Primitive Mantle, and N-MORB compositions are from Sun and McDonough (1989). All the lavas plot in the mantle array, precluding any perceptible crustal contamination.

Fig. 11 - (A) La vs. Yb, (B) Ba vs. La, and (C) Nb vs. Zr covariation diagrams. Same symbols as for Figure 9. Tsh, Tshibinda Volcanic Chain; Lem, Leymera; PM, partial melting curves; FC, fractional crystallization; trend # 1, low-Yb, high-La, high-Ba, and low-Zr curves evolving from basanites to olivine basalts (enriched source); trend # 2, low-La, low-Ba, and high-Zr curves characterizing the tholeiites and some olivine basalts (less enriched source); trend # 3, intermediate high-Ba and high-La pattern, and intermediate Nb and Zr feature (intermediate or mixed source). The pattern of these trends attests for the contribution of two sources. The trend # 1, best exposed by the Tshibinda Chain lavas, derived from an enriched source. The trend # 2 derived from a less enriched source. These two sources are documented by isotopic studies (see text). The enriched source is lithospheric, while the less enriched source can be mixed lithospheric and asthenospheric materials.

Fig. 12 - Primitive Mantle normalized incompatible element diagram of North-Idjwi and Pre-Virunga lavas. These sodic-rich lavas are more fractionated than the basaltic lavas of South-Kivu. Normalizing values after Sun and McDonough (1989).

Fig. 13 - Primitive Mantle normalized incompatible element diagram of (A) Nyamuragira lavas compared with South-Kivu lavas, (B) the other basanitic volcanoes of Virunga, (C) Nyiragongo lavas compared with Nyamuragira lavas, and (D) the other leucite-nephelinitic volcanoes of Virunga.

Fig. 14 - La/Sm vs. Sm/Yb diagram of Virunga mafic lavas. Batch melting of the enriched source C1. Melt curves as in Figure 9. The Virunga magma can be originated from a garnet- and a few spinel-bearing lherzolite source. The degree of partial melting is higher for the basanite magma than for the nephelinite magma. Same symbols as for Figure 13.

Fig. 15 - Zr/Hf vs. Hf diagram of mafic lavas of Virunga. Hf and Zr/Hf chondritic values of K-basanites of Nyamuragira, Karisimbi, and eastern volcanoes are consistent with partial melting of common mantle. High Zr/Hf ratios in the Nyiragongo lavas imply the contribution of Hf-poor carbonatite component, as shown by the Namibian nephelinite-carbonatite association. Same symbols as for Figure 13.

Fig. 16 - Inferred location of the metasomatized and carbonated mantle in the sub-lithospheric mantle of the Virunga area, after geochemical signatures of the Plio-Quaternary volcanoes. Normal mantle is suspected below the Miocene volcanic area.
Small red stars are the eruptive centers of the most primitive lavas unrelated to the magma chambers of the large volcanoes (St, Suri-Turunga; Mv, Muvo; Nh, Nahimbi; Rm, Rumoka; Rs, Rushayo; Bf, Bufumbiro). Large star is the Lueshe carbonatite. Circled stars are Late Neoproterozoic intrusions of nephelinitic syenites (N, Numbi; F, Fumbwe; B, Bishusha; K, Kirumba).

Fig. 17 - Location of the new geochronological data in the Lake Kivu and South-Kivu volcanic area. Data in Table 2.

Fig. 18 - Histogram of all the geochronological data. Volcanic activity initiated south of the future Lake Kivu trough, at 21 Ma, with alkaline sodic nephelinite. It evolved to sodic basanite in the Pre-Virunga region, between 13 and 9 Ma. A distinct tholeiitic volcanism appeared in the South-Kivu region at 11 Ma, and is progressively replaced by alkaline activity until the last pulse in the Tshibinda Chain ca. 1.7 Ma. The oldest activity of the Virunga area is dated at 2.6 Ma in the Mikeno volcano.

Fig. 19 - Geographical distribution of the volcanic activity

(A) Data from 21 to 9 Ma. The initial activity is nephelinitic and is limited to the middle part of the future Lake Kivu. In the Virunga area, the rift valley did not exist during the Pre-Virunga activity. In the South-Kivu area, the activity is tholeiitic and located along N-S fractures of the future rift axis. Late Neoproterozoic alkaline intrusions: L, Lueshe; K, Kirumba; B, Bishusha; F, Fumbwe; N, Numbi; Kz, Kahuzi; Bg, Biega. The layout of these intrusions suggests a structural weakness line.

(B) Data from 9 Ma to Present. In the Virunga area, activity began ca. 2.6 Ma in the middle of the oblique rift segment. In South-Kivu, activity extended to the whole area along N-S and NNE-SSW fractures and changed from tholeiitic to alkaline between 8.5 and 5.9 Ma. Activity occurred to the south-west along the NE-SW fractures of Mwenga, ca. 5.8 to 2.6 Ma, and, finally, to the west, in the Tshibinda Chain, ca. 1.7 Ma.

Table 1 - New analyses and analyses of dated samples from Marcelot et al. (1989). Alk-B, alkali basalt; Ol-B, olivine basalt; Bs, basanite; Na-Bs, sodic basanite; Benm, benmoreite; H, hawaiite; Mug, mugearite; Neph, nephelinite; T, tholeiite.

Analytical method and laboratory: H = atomic absorption spectrometry (AA) for the major elements and instrumental neutron activation (INAA) and X-ray fluorescence (XRF) for the minor elements at the University of Halifax (Canada); O = inductively-coupled plasma spectrometry (ICP-OES) at the analytical laboratory of the University and CNRS of Orléans (France); P = atomic absorption spectrometry at the Department of Petrography-Volcanology of the University of Paris-Sud; T = XRF at the Musée Royal de l'Afrique Centrale of Tervuren (Belgique).

Ages are from Tables 2 and 4.

Table 2 - New K-Ar geochronological analyses. Most of potassium-argon ages were measured at the "Université de Bretagne Occidentale" in Brest (France) on grains of whole-rock, 0.3 to 0.15 mm in size, obtained after crushing and subsequent sieving of the solid samples. One aliquot of grains was powdered in an agate grinder for chemical attack of around 0.1 g of powder by 4 cc of hydrofluoric acid, before its analysis of K content by AAS (Atomic Absorption Spectrometry). A second aliquot of grains was reserved for argon analysis. About 0.7 g to 0.8 g of grains were heated and fused under vacuum in a molybdenum crucible, using a high frequency generator. Released gases during this step

1519 were cleaned successively on three quartz traps containing titanium sponge when their
1520 temperature was decreasing from 800°C to the ambient one, during 10 minutes; at the final
1521 step the remaining gas fraction was ultra-purified using a Al-Zr SAES getter. Isotopic
1522 compositions of argon and concentrations of radiogenic argon $^{40}Ar^{*}$ were measured in a
1523 stainless steel mass spectrometer with a 180° geometry and a permanent magnetic field.
1524 Isotopic dilution was realized during the fusion step, using precise concentrations of ^{38}Ar
1525 buried as ions in aluminium targets (Bellon et al., 1981). Ages are calculated using Steiger
1526 and Jäger's (1977) constants and errors, following the equation of Mahood and Drake
1527 (1982).
1528
1529 **Table 3 -** Trace element composition of the South-Kivu magma sources according to Auchapt
1530 (1987).
1531
1532 **Table 4 –** K-Ar geochronological data for the Lake Kivu area lavas (Western Branch of the
1533 East African Rift) excluding the post-1 Ma lavas. References: 1, Bagdasaryan et al. (1973);
1534 2, Guibert et al. (1975); 3, Bellon and Pouclet (1980); 4, Pasteels and Boven (1989); 5,
1535 Pasteels et al. (1989); 6, Kampunzu et al. (1998b); 7, this work.

Table 1

Location	Kahuzi	Bukavu	Bukavu	Upper-Rusizi		South-Idjwi				
#	MM2	BK24	BK24'	RW82	RW89	BK7	BK14	BK15	BK19	BK20
Method	T-O	T-O	H	H	H	O	O	T-O	P-O	P-O
Rock	Alk-B	Bs	Bs	Bs	Alk-B	T	T	T	T	T
Age (Ma)	8.19	7		7.18	7.68	6.62	10.30	8.76	9.56	
SiO_2	44.09	45.43	46.45	45.65	47.62	50.22	50.03	49.41	50.91	51.44
TiO_2	2.28	2.07	2.04	2.06	2.33	1.90	1.69	2.24	2.03	1.58
Al_2O_3	14.48	14.57	13.80	14.45	14.35	15.40	15.42	14.70	14.41	14.99
Fe_2O_3 t	13.33	10.46	10.90	10.85	11.50	11.01	10.73	13.64	12.19	11.48
MnO	0.16	0.19	0.18	0.20	0.15	0.15	0.17	0.17	0.14	0.15
MgO	10.19	8.66	8.61	7.17	6.70	6.13	6.30	6.52	6.74	5.77
CaO	10.83	10.93	10.90	11.54	10.66	9.94	10.15	6.86	9.35	9.13
Na_2O	2.53	3.56	3.67	3.63	3.00	2.52	2.65	3.20	2.77	2.68
K_2O	0.91	1.24	1.55	1.56	1.35	0.28	0.30	0.55	0.45	0.20
$P2O_5$	0.90	0.76	0.87	1.00	0.86	0.19	0.13	0.39	0.10	0.04
LOI	1.75	2.51	1.15	1.03	1.36	2.55	2.64	2.90	1.88	2.97
Total	101.45	100.38	100.12	99.14	99.88	100.29	100.21	100.58	100.97	100.43
Rb	21	31	35	43	30		8			
Sr	733	1178	1152	1107	890		255			
Y	35	30	32	37	34		27			
Zr	198	252	224	243	235		101			
Nb	99	120	125	170	137		21			
Ba	857	998	10.38	1340	908		150			
Hf	4.1	5.5	4.3	4.9	4.9		2.5			
Ta	5.0	6.1					1.3			
Th	10.6	12	11.6	14.2	10.6		2			
La	75.1	92.2	94.6	111	79.2		17.5			
Ce	132	169	178	197	152		32.2			
Pr	12.8	17.5					3.9			
Nd	40.2	58.9	65.0	67.2	60.9		15.5			
Sm	8.6	9.8	10.4	11.5	10.3		3.9			
Eu	2.4	2.99	3.04	3.31	3.04		1.4			
Gd	7.7	7.9					4.6			
Tb	1.1	1.1	1.11	1.21	1.20		0.8			
Dy	6.3	6.2					4.5			
Yb	2.7	2.4	2.4	2.78	2.81		2.1			
Lu			0.37	0.44	0.40					

Table 1 (continued 1)

Location	South-Idjwi		Bitare		Bugarama		Tshibinda Chain (from south to north)			
#	BK36	BK18	RW86	RW87	RW83	RW88	MM1	TB4	TB4'	TB4a
Method	T-O	O	H	H	H	H	T-O	P-O	H	T-O
Rock	T	Alk-B	T	T	Bs	Bs	Bs	Bs	Na-Bs	Bs
Age (Ma)	7.73	7.07	8.97	11.42	7.75	10.63	1.7	1.9		
SiO_2	52.64	46.23	52.57	49.68	46.60	43.90	46.58	45.67	46.84	48.50
TiO_2	1.63	2.01	1.57	1.59	2.12	2.87	1.82	1.53	1.53	1.46
Al_2O_3	15.49	15.12	13.98	13.75	14.10	14.94	15.08	14.04	13.56	12.76
Fe_2O_3 t	12.36	12.55	10.86	13.26	10.95	12.88	10.21	12.41	11.20	10.61
MnO	0.11	0.20	0.14	0.30	0.21	0.18	0.22	0.17	0.18	0.19
MgO	5.47	9.24	6.90	7.00	8.40	8.80	10.23	9.08	8.87	9.56
CaO	9.11	9.87	8.23	8.86	10.70	9.85	9.38	12.12	11.59	10.90
Na_2O	2.43	3.05	2.64	2.61	3.45	3.33	3.24	2.65	3.52	3.84
K_2O	0.30	0.99	0.95	0.62	1.22	1.40	1.36	1.21	1.60	1.06
$P2O_5$	0.21	0.54	0.24	0.24	0.89	0.96	0.54	0.40	0.70	0.55
LOI	1.65	1.11	1.14	1.54	0.51	0.98	2.45	1.22	1.00	0.94
Total	101.40	100.91	99.22	99.45	99.15	100.09	101.11	100.50	100.59	100.37
Rb	25	27	16	30	36	50		46	50	
Sr	532	254	247	1050	702	725		772	770	
Y	31			31	36	28		30	30	
Zr	162			210	282	165		143	145	
Nb	62			109	67	88		93	90	
Ba	640			996	614	1012		1123	1100	
Hf	3.7	3.0	2.7	4.2	5.8	3.6		3.0	3.1	
Ta	3.7					3.9			4.2	
Th	6.6	6	3	9.6	4.7	12		13	13	
La	45.5	27.5	20.3	81.2	45.4	70.8		72.3	72	
Ce	85.2	50.4	38.1	151	94.3	110		123	121	
Pr	8.7					12.6			12.5	
Nd	25.1	18.1	17.2	59.1	46.8	40.1		40.6	40.2	
Sm	6.4	4.53	4.11	9.64	10.20	7.2		7.39	7.3	
Eu	2.1	1.48	1.46	2.89	3.27	2.0		2.10	2.1	
Gd	6.2					5.4			5.4	
Tb	0.95	0.79	0.75	1.05	1.35	0.87		0.88	0.87	
Dy	5.9					4.8			4.9	
Yb	2.55	2.20	2.09	2.40	2.85	2.4		2.50	2.4	
Lu		0.35	0.35	0.38	0.40			0.40		

Table 1 (continued 2)

Location	Tshibinda Chain (from south to north)									
#	KT1	KT1'	KT1a	KT26	KT23	KT21	KT16	KT14	KT12	KT11
Method	P-O	H	T-O	T-O	T-O	T-O	T-O	T-O	T-O	T-O
Rock	Ol-B	Ol-B	Ol-B	Na-Bs	Ol-B	Alk-B	Alk-B	Alk-B	Alk-B	Alk-B
Age (Ma)	1.6									
SiO_2	50.00	48.98	49.42	44.79	49.00	45.63	46.30	46.01	46.99	46.82
TiO_2	1.07	1.17	1.17	1.87	1.32	1.18	2.08	1.51	1.46	1.48
Al_2O_3	13.50	13.55	14.92	15.25	15.36	14.40	16.50	15.60	15.08	15.41
Fe_2O_3 t	9.71	10.57	10.67	10.22	10.55	10.54	13.83	9.45	10.85	10.76
MnO	0.15	0.16	0.13	0.22	0.18	0.18	0.19	0.20	0.17	0.19
MgO	9.98	10.68	9.23	9.63	9.00	11.11	6.96	9.20	10.18	9.36
CaO	10.08	10.10	10.36	10.08	9.38	9.91	9.33	10.60	10.01	10.27
Na_2O	2.78	2.56	2.72	4.14	3.13	2.87	3.01	2.38	2.79	2.87
K_2O	1.12	1.14	1.04	1.09	0.90	0.83	1.15	1.21	1.00	1.12
$P2O_5$	0.52	0.44	0.43	0.60	0.47	0.56	0.94	0.64	0.36	0.46
LOI	2.16	0.31	0.52	0.98	1.24	2.94	2.40	4.29	2.07	1.71
Total	101.07	99.66	100.61	98.87	100.53	100.15	102.69	101.09	100.96	100.45
Rb	28	26		62				35		
Sr	509	495		902				720		
Y	24	22		29				30		
Zr	116	104		172				157		
Nb	65	62		101				95		
Ba	751	740		1290				802		
Hf	2.5	2.1		3.7				3.1		
Ta	3.5			4.9				4.0		
Th	9.8	9.8		14				12		
La	48.1	45.6		81.1				62.2		
Ce	78.0	74.1		130				119		
Pr	9.1			14.2				12.6		
Nd	25.8	24.9		46.5				40.2		
Sm	4.6	4.43		7.3				7.0		
Eu	1.5	1.45		2.2				2.1		
Gd	5.2			6.3				5.5		
Tb	0.7	0.62		1.1				0.9		
Dy	3.8			6.1				4.8		
Yb	2.2	2.00		2.7				2.4		
Lu		0.31								

Table 1 (continued 3)

Location	Tshibinda Chain		North-Idjwi							
#	KT9	KT8	LKA4	LKA4'	BK8	N370	N-573	N373	N373'	N378
Method	T-O	T-O	P-O	H	O	P-O	P-O	P-O	H	P-O
Rock	Alk-B	Ol-B	Neph	Neph	Neph	Na-Bs	Na-Bs	Haw	Haw	Na-Bs
Age (Ma)				19.98	20.97			12.6		8.9
SiO_2	45.72	47.89	42.41	42.76	42.97	47.30	43.92	47.84	46.90	45.35
TiO_2	1.49	1.46	1.66	1.77	1.60	1.40	1.50	1.64	1.66	1.49
Al_2O_3	15.67	15.66	11.98	11.68	12.15	14.67	16.12	13.87	16.19	17.54
Fe_2O_3 t	11.00	10.78	10.50	10.47	9.87	11.36	11.56	17.27	11.62	10.93
MnO	0.20	0.19	0.16	0.17	0.16	0.04	0.10	0.03	0.21	0.03
MgO	10.36	9.80	12.41	12.11	12.44	5.97	6.35	3.56	5.05	4.46
CaO	9.84	9.75	13.55	12.90	13.23	11.43	11.46	8.89	8.81	11.19
Na_2O	2.61	2.75	3.57	3.64	3.49	4.44	4.27	4.07	3.66	4.21
K_2O	0.97	0.90	0.69	0.97	1.02	0.50	0.97	0.96	1.45	1.49
$P2O_5$	0.41	0.41	0.44	1.14	1.05	0.17	0.44	0.07	1.25	0.06
LOI	2.42	1.77	2.37	2.00	2.12	4.02	3.19	3.46	2.30	3.01
Total	100.69	101.36	99.74	99.61	100.10	101.30	99.88	101.66	99.10	99.76
Rb	32	32	33	56	40		Rb	49		104
Sr	682	1620	1650	1904	1400		Sr	1890		940
Y	25	30	28	34	36		Y	35		31
Zr	166	192	199	260	273		Zr	265		297
Nb	74	129	120	174	190		Nb	237		124
Ba	733	1311	1299	1770	1482		Ba	1710		1250
Hf	3.6	3.2	3.5	4.2	4.4		Hf	4.0		6.9
Ta	4.0		6.9	7.6			Ta			5.9
Th	9.1	16.8	16	20	22.1		Th	17.3		13
La	51	135	129	137	141		La	132		87.8
Ce	89.5	252	245	289	257		Ce	266		169
Pr	9.8		27.3	30.2			Pr			16.6
Nd	29.0	92.1	91.3	102.0	84.2		Nd	93.0		54.5
Sm	5.9	12.90	12.7	13.5	11.60		Sm	12.70		10.3
Eu	1.8	3.77	3.6	3.9	3.32		Eu	3.70		3.3
Gd	5.4		8.0	8.7			Gd			6.1
Tb	0.84	1.07	1.1	1.8	1.05		Tb	1.00		1.2
Dy	4.0		5.6	5.7			Dy			6.1
Yb	2.2	2.02	2.0	2.8	3.07		Yb	3.00		2.6
Lu		0.31			0.44		Lu	0.41		

Table 1 (continued 4)

Location	Tongo					Mweso	West-Nyamuragira									
#	N378'	N379	N377(2)	N377(4)	N373'	N337	N46	N341	N346a	N363	N404	N556	N572	N2		
Method	H	T-O	T-O	P	P-O	P	P-O	P	P	P	P	P	P-O	H		
Rock	Bs	Mug	Benm	Ol-B	K-Bs	K-Bs	K-Bs	K-Bs	K-Bs	K-Bs	K-Bs	K-Bs	K-Bs	K-Bs		
Age (Ma)																
SiO_2	44.13	53.16	57.86	48.93	46.24	45.42	45.93	46.01	46.55	44.54			SiO2	45.88	44.90	
TiO_2	1.53	1.04	1.13	2.38	2.75	3.55	2.75	3.16	2.71	2.73			TiO2	3.10	3.37	
Al_2O_3	15.72	16.98	19.10	15.17	15.53	15.06	12.73	14.94	13.95	10.78			Al2O3	14.53	13.55	
Fe_2O_3 t	11.08	8.27	4.41	12.51	11.12	12.77	11.38	12.58	11.25	12.71			Fe2O3 t	13.63	12.80	
MnO	0.22	0.17	0.06	0.04	0.20	0.03	0.03	0.03	0.03	0.08			MnO	0.08	0.18	
MgO	6.52	3.36	1.36	7.24	7.76	5.62	9.89	6.37	8.54	11.15			MgO	6.79	7.50	
CaO	10.92	5.44	4.27	8.29	10.12	10.77	11.13	10.08	10.97	11.85			CaO	10.44	10.70	
Na_2O	3.80	4.60	5.28	2.41	3.29	2.83	2.59	2.56	3.17	2.12			Na2O	2.86	2.80	
K_2O	1.15	3.55	4.00	2.00	3.16	2.50	2.70	2.51	2.68	1.97			K2O	2.82	2.90	
$P2O_5$	1.12	0.57	0.56	0.06	0.00	0.06	0.06	0.08	0.07	0.32			P2O5	0.34	0.57	
LOI	2.84	2.75	2.73	1.15	0.19	1.56	0.67	0.77	0.27	1.19			LOI	0.94		
Total	99.03	99.89	100.76	100.18	100.36	100.17	99.86	99.09	100.19	99.44			Total	101.41	99.27	
Rb	49				104								Rb	89	80	
Sr	1890				940								Sr	887	873	
Y	35				31								Y	30	28	
Zr	265				297								Zr	305	278	
Nb	237				124								Nb	131	100	
Ba	1710				1250								Ba	1106	1079	
Hf	4.0				6.9								Hf	6.3	6.0	
Ta					5.9								Ta	6.1		
Th	17.3				13								Th	12	10	
La	132				87.8								La	70.3	66.8	
Ce	266				169								Ce	147.2	138.0	
Pr					16.6								Pr	14.7		
Nd	93.0				54.5								Nd	52.9	56.4	
Sm	12.70				10.3								Sm	10.0	9.47	
Eu	3.70				3.3								Eu	3.1	2.72	
Gd					8.5								Gd	8.4		
Tb	1.00				1.2								Tb	1.1	0.95	
Dy					6.1								Dy	5.9		
Yb	3.00				2.6								Yb	2.3	2.22	
Lu	0.41												Lu		0.34	

Table 1 (continued 5)

Table 2 Whole rock K-Ar age dating

Location	Sample #	Rock type	Fused mass (g)	K_2O (wt%)	$^{40}Ar^*$ (10^{-7} cc/g)	$^{40}Ar^*/^{40}Ar_t$	Age (Ma) ± 1 σ
North-Idjwi	BK8	Nephelinite	0.7137	1.46	9.82	42.6	20.74 ± 0.56
			0.7094	1.46	10.04	57.9	21.21 ± 0.52
						Mean age	20.97 ± 0.56
North-Idjwi	LKA4	Nephelinite	1.0160	1.27	8.23	50.7	19.98 ± 1.00
Bitare	RW87	Tholeiite	1.0108	0.55	2.03	27.0	11.42 ± 0.57
Bugarama	RW88	Basanite	1.0023	1.25	4.29	52.7	10.63 ± 0.53
South-Idjwi	BK14	Tholeiite	0.7007	0.43	1.43	28.4	10.30 ± 0.35
South-Idjwi	BK19	Tholeiite	1.0049	0.68	2.10	27.8	9.56 ± 0.48
Bitare	RW86	Tholeiite	1.0009	0.90	2.61	37.3	8.97 ± 0.45
South-Idjwi	BK15	Tholeiite	1.0145	0.66	1.87	19.3	8.76 ± 0.44
Kahuzi	MM2	Alkaline basalt	1.0171	0.87	2.23	41.1	7.92 ± 0.21
			0.7039	0.87	2.38	38.6	8.47 ± 0.24
						Mean age	8.19 ± 0.40
Upper Ruzizi	RW90	Olivine basalt	1.0130	0.76	1.99	26.6	8.10 ± 0.40
Bugarama	RW83	Basanite	1.0115	1.15	2.88	39.8	7.75 ± 0.39
South-Idjwi	BK36	Tholeiite	0.7154	0.38	0.95	16.5	7.73 ± 0.30
Upper Ruzizi	RW89	Alkaline basalt	1.0022	1.20	2.98	32.7	7.68 ± 0.38
Bukavu	RW82	Basanite	1.0072	1.56	3.62	44.3	7.18 ± 0.36
South-Idjwi	BK18	Alkaline basalt	0.7101	1.00	2.28	10.8	7.07 ± 0.51
South-Idjwi	BK7	Tholeiite	0.7007	0.43	0.92	9.7	6.62 ± 0.66
Bukavu	RW81	Basanite	1.0086	1.45	2.96	43.0	6.33 ± 0.32

Table 3 Trace element composition of the South-Kivu magma sources

	C1	**C2**
Sr	51	45
Y	7.5	7.2
Zr	19	25
Nb	3.3	3.3
Ba	38	26
Hf	0.48	0.62
Th	0.52	0.26
La	3.80	2.33
Ce	7.10	5.05
Nd	3.10	2.90
Sm	0.84	0.80
Eu	0.30	0.30
Tb	0.16	0.16
Yb	0.67	0.66

Table 4 K-Ar geochronological data for the Lake Kivu area lavas

Location	Sample #	Rock type	Age	Ref.	Location	Sample #	Rock type	Age	Ref.
North-Idjwi	BK8	Nephelinite	20.97 ± 0.56	7	Burundi	19	Tholeiite	7.6 ± 0.5	5
North-Idjwi	LKA4	Nephelinite	19.98 ± 1.00	7	South-Idjwi	18	Tholeiite	7.6 ± 0.3	5
Bishusha	N373	Hawaiite	12.6 ± 0.7	3	West-Bukavu	2	Basanite	7.3 ± 0.3	5
Tongo	TRK4	Benmoreite	11.8 ± 0.8	6	Upper-Rusizi	RW82	Basanite	7.18 ± 0.36	7
Bitare	RW87	Tholeiite	11.42 ± 0.57	7	South-Idjwi	BK18	Alk-Basalt	7.07 ± 0.51	7
Bishusha	TR44	Ol-Tholeiite	11.0 ± 0.5	6	Bukavu	BK24	Basanite	7.00 ± 0.35	3
Bishusha	TR50	Ol-Tholeiite	10.8 ± 1.7	6	Kahuzi	AK486	Ol-Tholeiite	6.90 ± 0.35	6
Bishusha	TR5	Ol-Basalt	10.7 ± 0.7	6	Upper-Rusizi	11	Alk-Basalt	6.7 ± 0.5	5
Bugarama	RW88	Basanite	10.63 ± 0.53	7	South-Idjwi	BK7	Tholeiite	6.62 ± 0.66	7
South-Idjwi	BK14	Tholeiite	10.30 ± 0.35	7	Upper-Rusizi	12	Hawaiite	6.45 ± 0.90	5
Tongo	TRK2a	Benmoreite	10.2 ± 0.7	6	Upper-Rusizi	RW81	Basanite	6.33 ± 0.32	7
Lower-Rusizi	27	Tholeiite	10.0 ± 2.0	5	Upper-Rusizi	10	Hawaiite	6.2 ± 0.3	5
Bugarama	17	Tholeiite	10.0 ± 0.6	5	Upper-Rusizi	22	Benmoreite	6.14 ± 0.30	5
Bishusha	TR1b	Hawaiite	9.9 ± 1.2	6	West-Bugarama	9	Hawaiite	6.06 ± 0.27	5
Bishusha	TR12	Basanite	9.7 ± 1.3	6	Bugarama	13	Hawaiite	5.9 ± 0.5	5
South-Idjwi	BK19	Tholeiite	9.56 ± 0.48	7	Upper-Rusizi	5	Basanite	5.9 ± 0.4	5
Bishusha	TR24	Mugearite	9.2 ± 1.0	6	Kahuzi	RTL180	Ol-Tholeiite	5.9 ± 0.3	6
East-Cyangugu	14	Ol-Tholeiite	9.0 ± 0.6	5	Mwenga	K157	Ol-Basalt	5.8 ± 1.1	6
Bitare	RW86	Tholeiite	8.97 ± 0.45	7	Upper-Rusizi	25	Trachyte	5.74 ± 0.23	5
Tongo	N378	Basanite	8.9 ± 0.5	3	Upper-Rusizi	23	Trachyte	5.74 ± 0.09	5
South-Idjwi	BK15	Tholeiite	8.76 ± 0.44	7	Upper-Rusizi	4	Basanite	5.7 ± 0.4	5
W-Bukavu	1	Alk-Basalt	8.5 ± 0.5	5	Upper-Rusizi	21	Phonolite	5.7 ± 0.3	5
East-Cyangugu	20	Tholeiite	8.4 ± 0.3	5	North-Mushaka	7	Hawaiite	5.65 ± 0.23	5
Upper-Rusizi		Ol-Basalt	8.3 ± 1.1	1	Bugarama	15	Hawaiite	5.6 ± 0.3	5
Kahuzi	AK256	Alk-Basalt	8.2 ± 0.4	6	Upper-Rusizi	24	Trachyte	5.05 ± 0.4	5
Kahuzi	MM2	Alk-Basalt	8.19 ± 0.40	7	Mwenga	K40	Alk-Basalt	4.2 ± 1.1	6
Upper-Rusizi	RW90	Ol-basalt	8.10 ± 0.40	7	South-Idjwi	I-84-30	Ol-Basalt	4.1 ± 1	4
Upper-Rusizi	26	Tholeiite	8.0 ± 1.0	5	NW-Bukavu	6	Basanite	4.06 ± 0.21	5
Mushaka	3	Basanite	7.99 ± 0.24	5	Mwenga	K58	Basanite	2.6 ± 1.6	6
Bugarama	RW83	Basanite	7.75 ± 0.39	7	Mikeno		Trachyte	2.6 ± 0.4	2
South-Idjwi	BK36	Tholeiite	7.73 ± 0.30	7	Tshibinda	TB4	Basanite	1.9 ± 0.1	3
Upper-Rusizi	RW89	Alk-Basalt	7.68 ± 0.38	7	Tshibinda	MM1	Basanite	1.7 ± 0.2	3
Burundi	28	Tholeiite	7.6 ± 1.4	5	Tshibinda	KT1	Ol-Basalt	1.6 ± 0.3	3
Upper-Rusizi		Ol-Basalt	7.6 ± 0.5	1					

Fig. 1

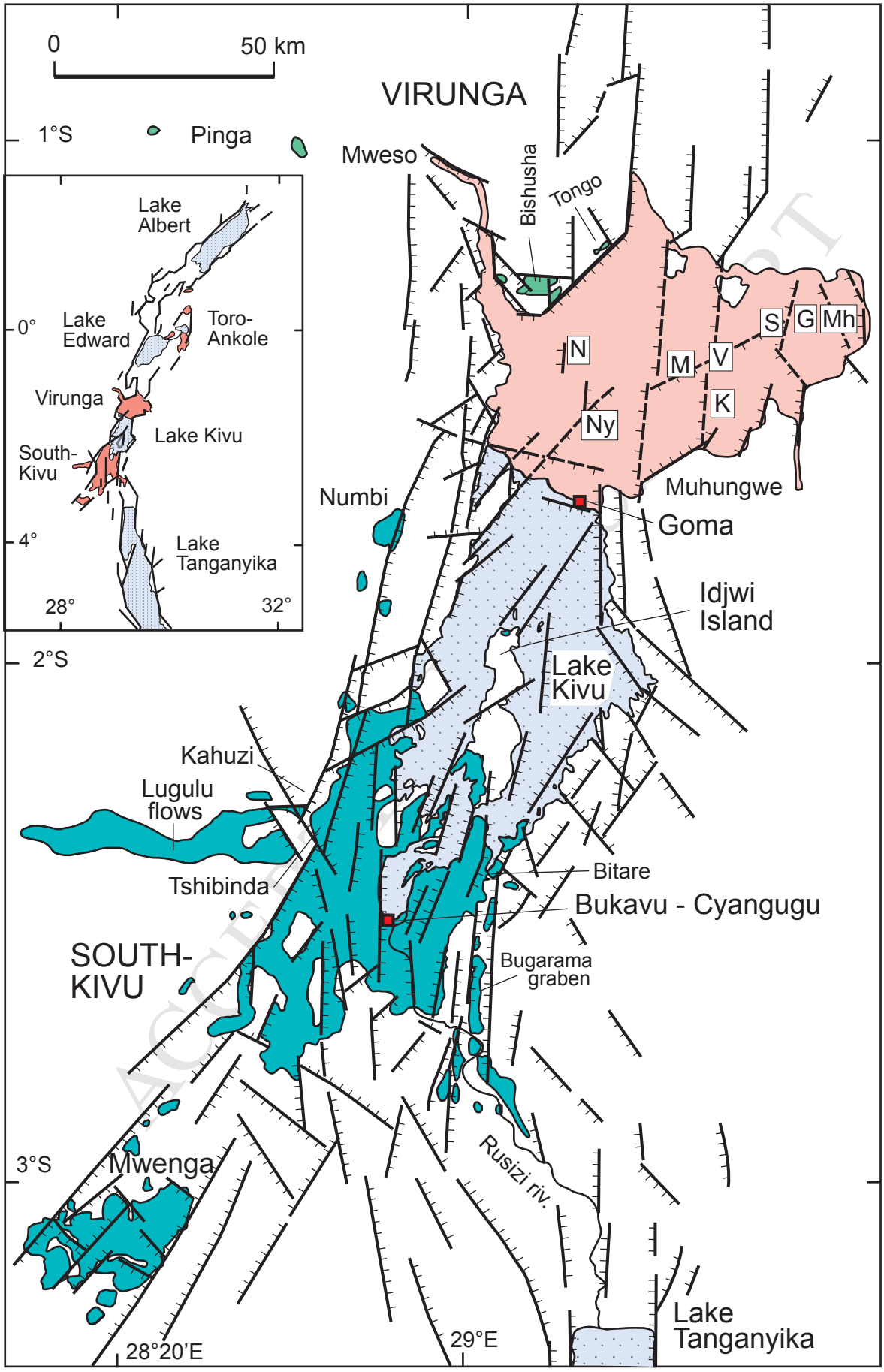

Fig. 2

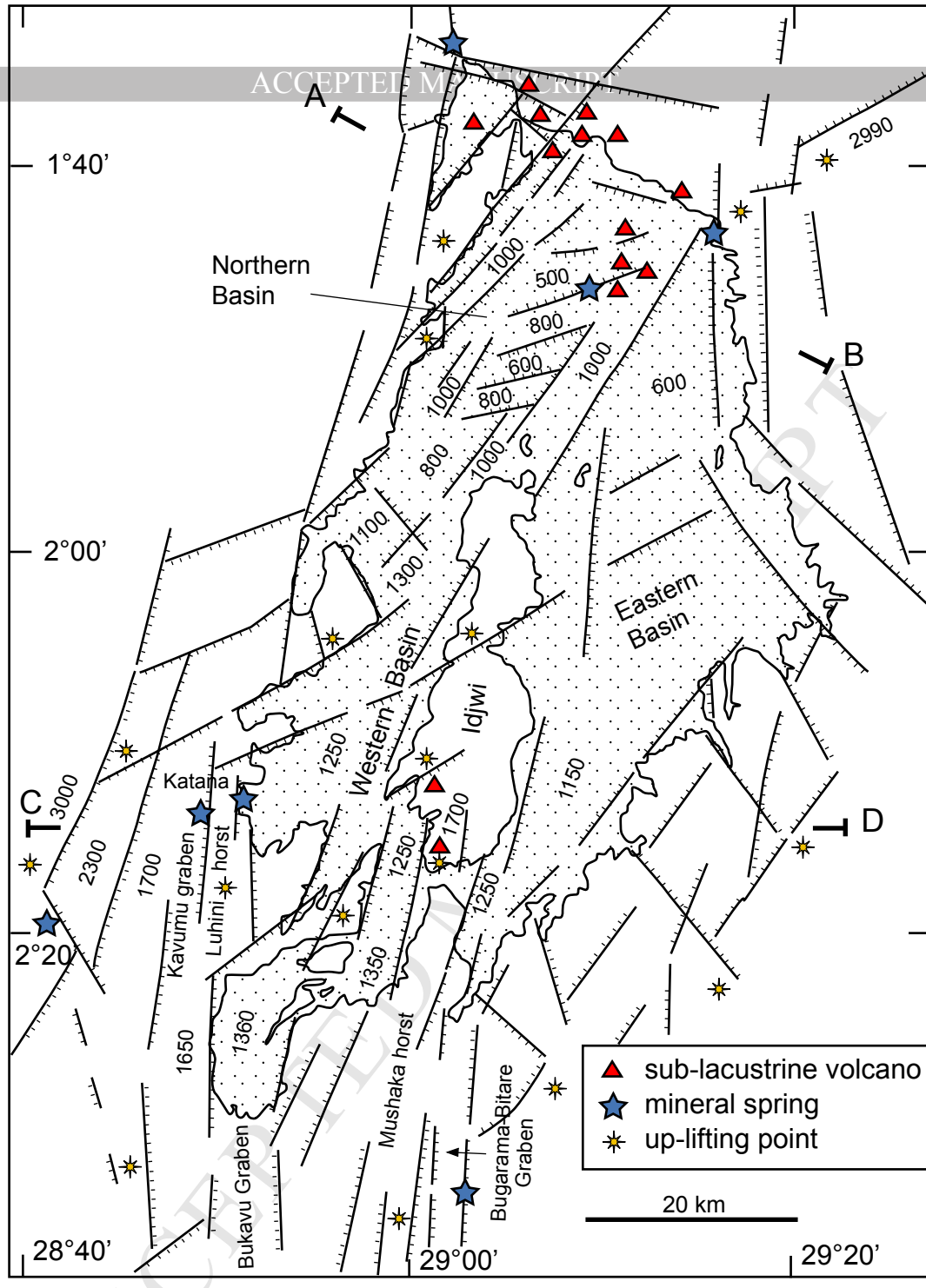

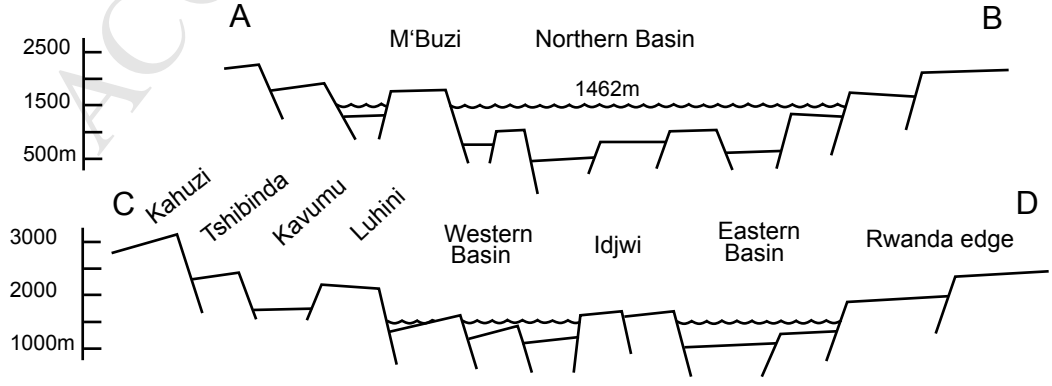

Fig. 3

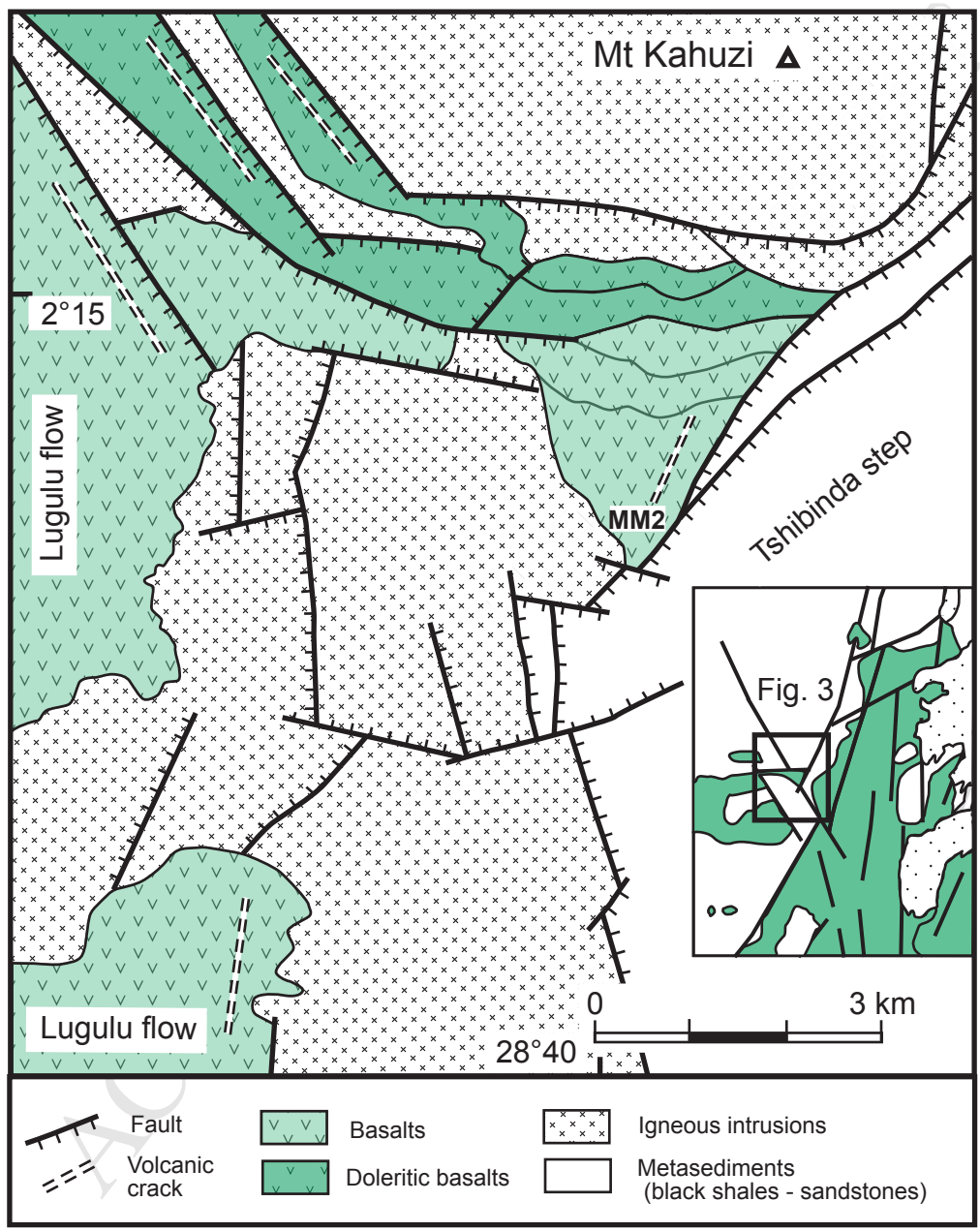
Mt Kahuzi
2°15
Lugulu flow
MM2
Tshibinda step
Fig. 3
0
3 km
28°40
Lugulu flow
Fault
Volcanic crack
Basalts
Doleritic basalts
Igneous intrusions
Metasediments (black shales - sandstones)

Fig. 4

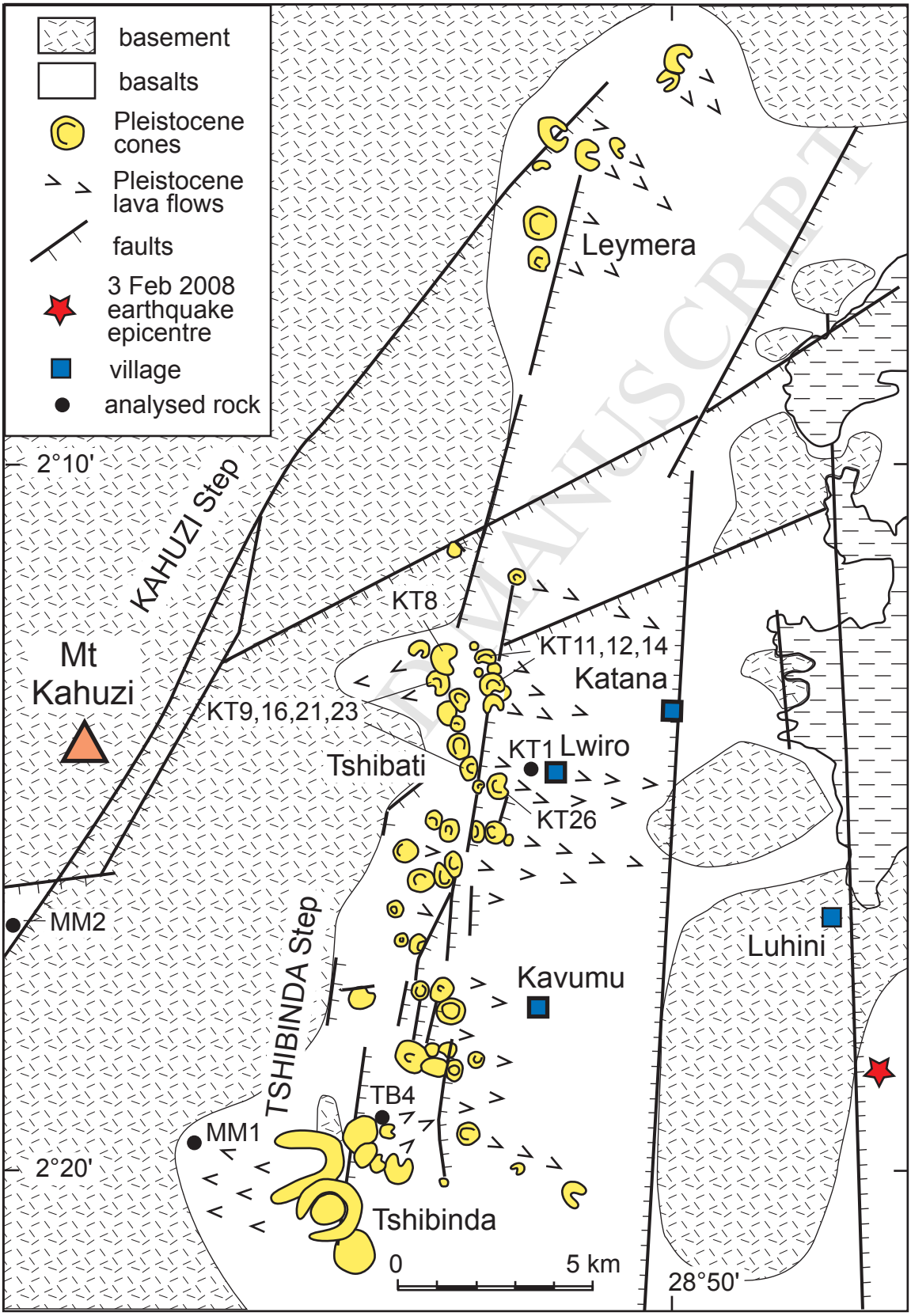
basement
basalts
Pleistocene cones
Pleistocene lava flows
faults
3 Feb 2008 earthquake epicentre
village
analysed rock
2°10'
KAHUZI Step
Mt Kahuzi
KT8
KT11,12,14
Katana
KT9,16,21,23
KT1
Lwiro
Tshibati
KT26
Leymera
MM2
TSHIBINDA Step
Kavumu
Luhini
TB4
MM1
2°20'
Tshibinda
0
5 km
28°50'

Fig. 5

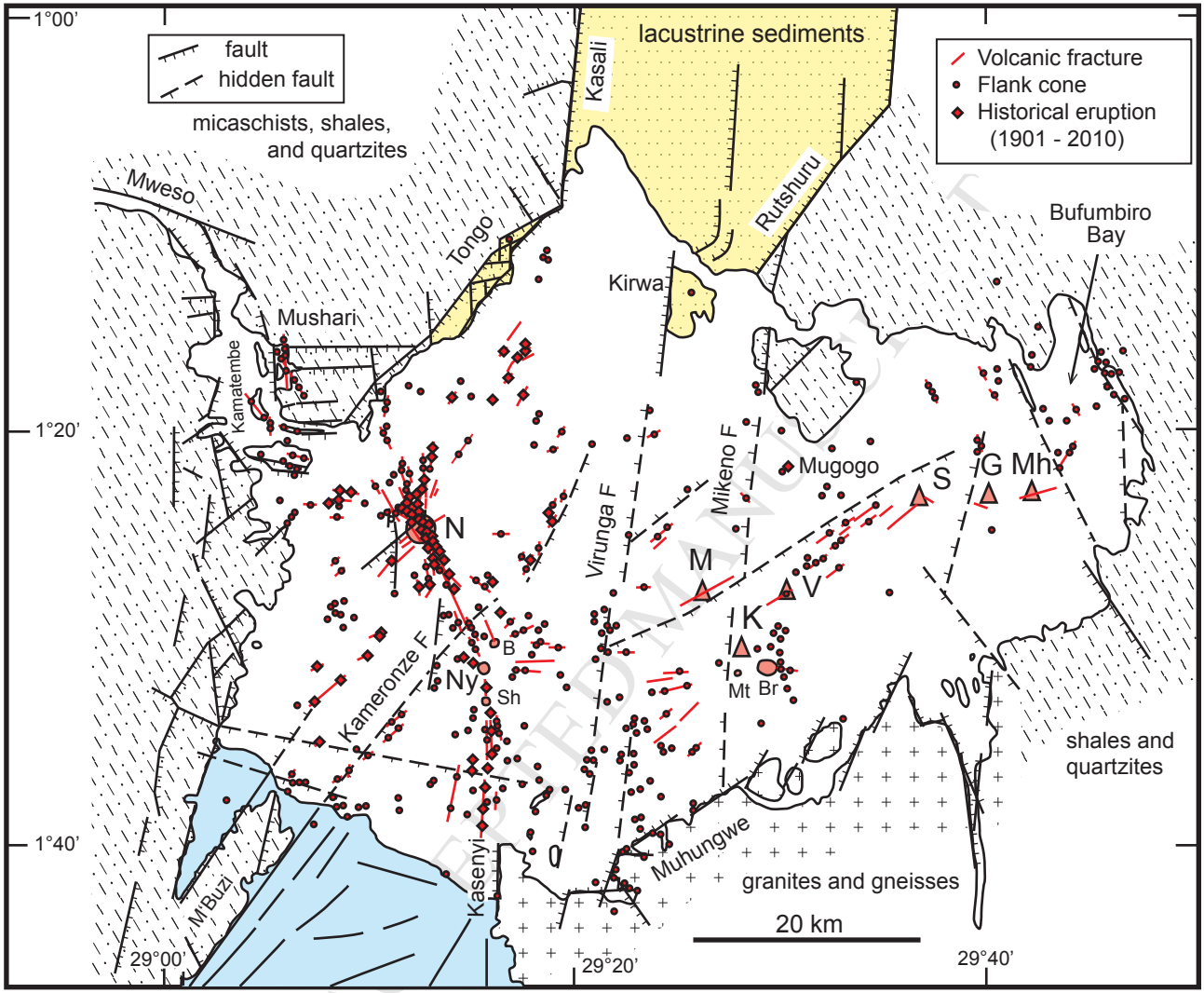

Fig. 6

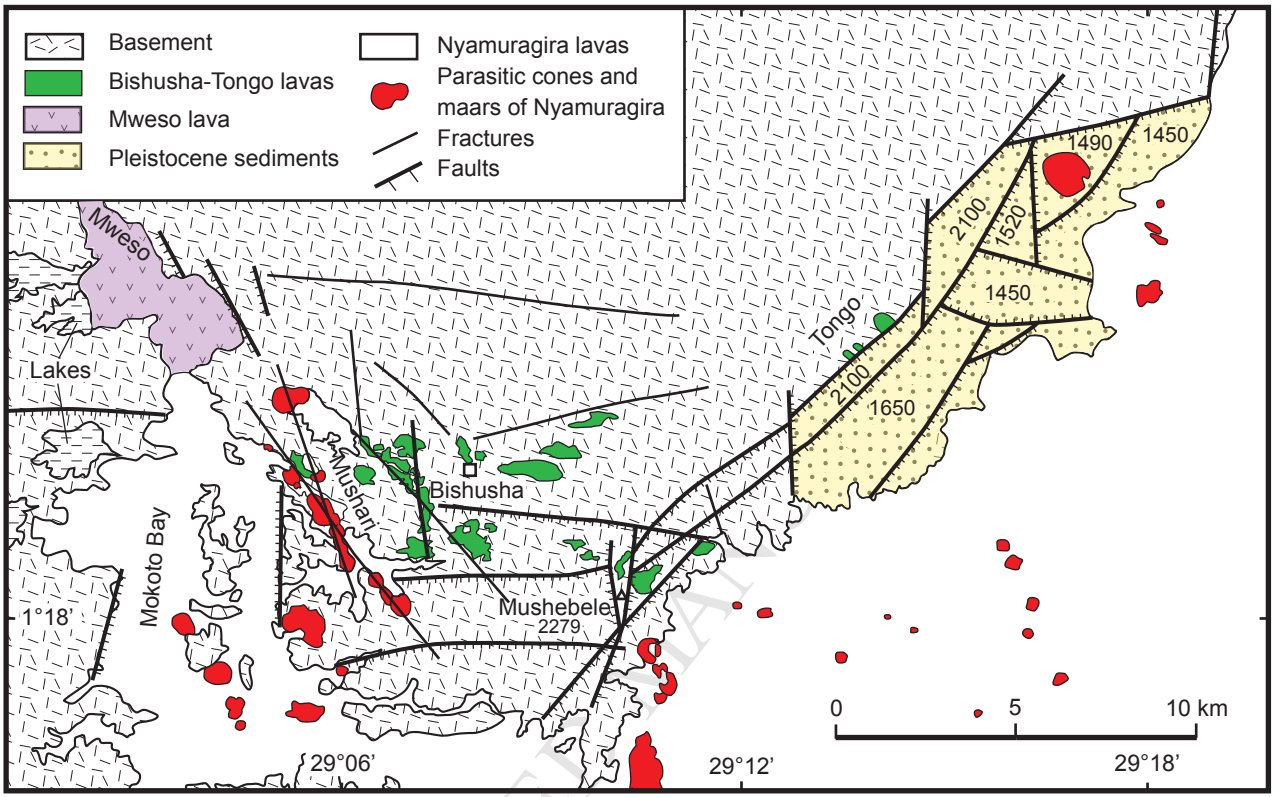

Fig. 7

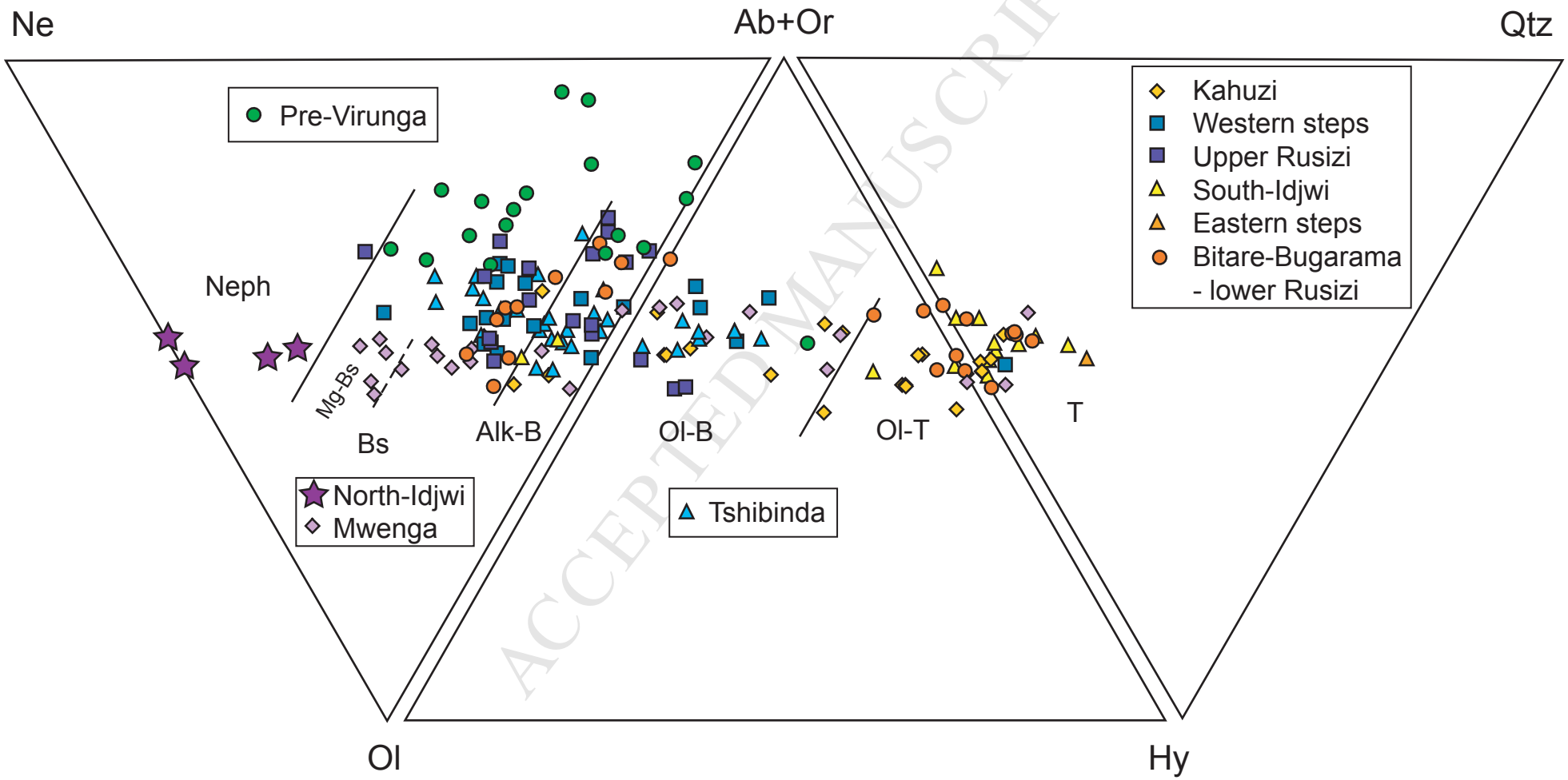

Fig. 8

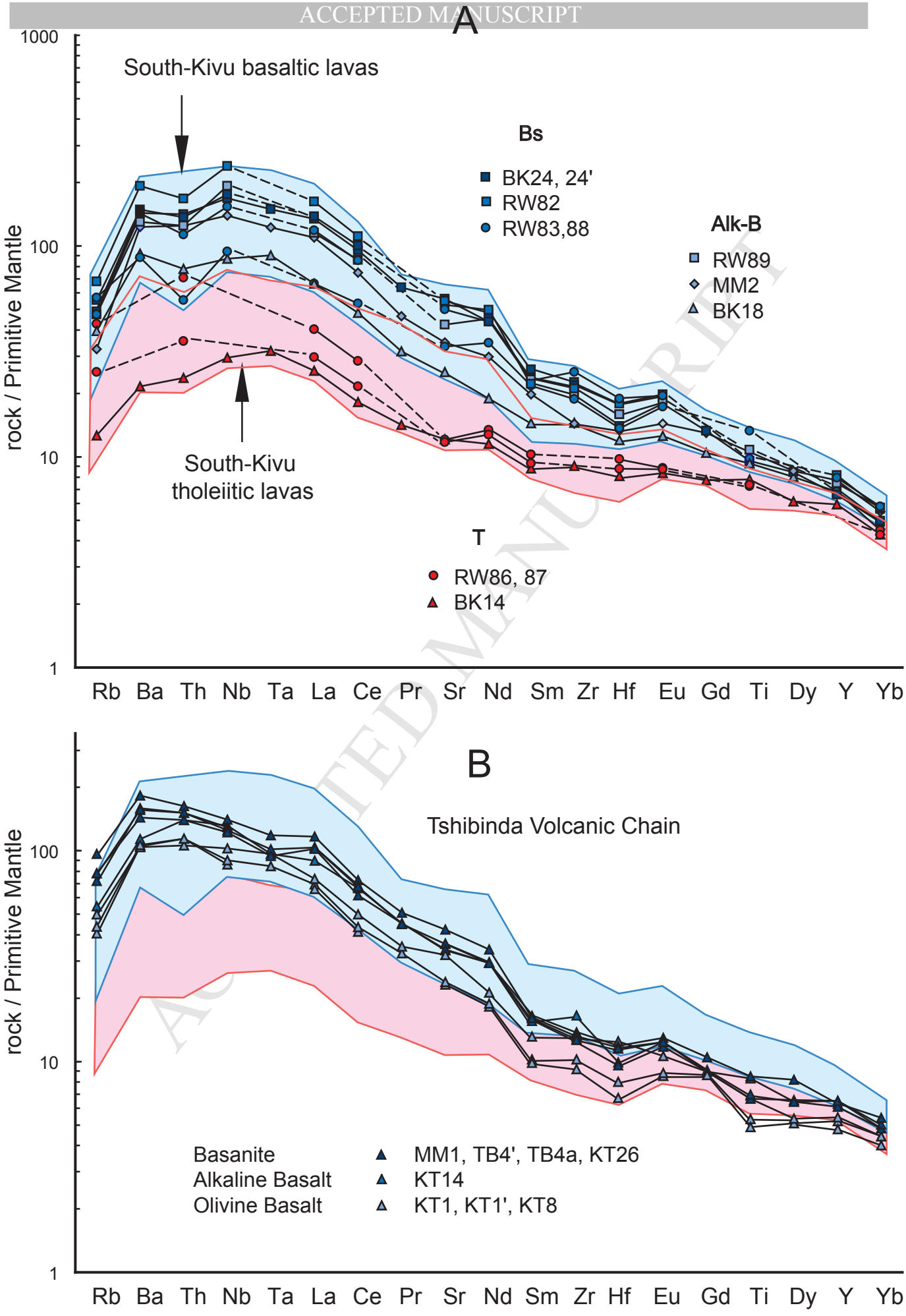

Fig. 9

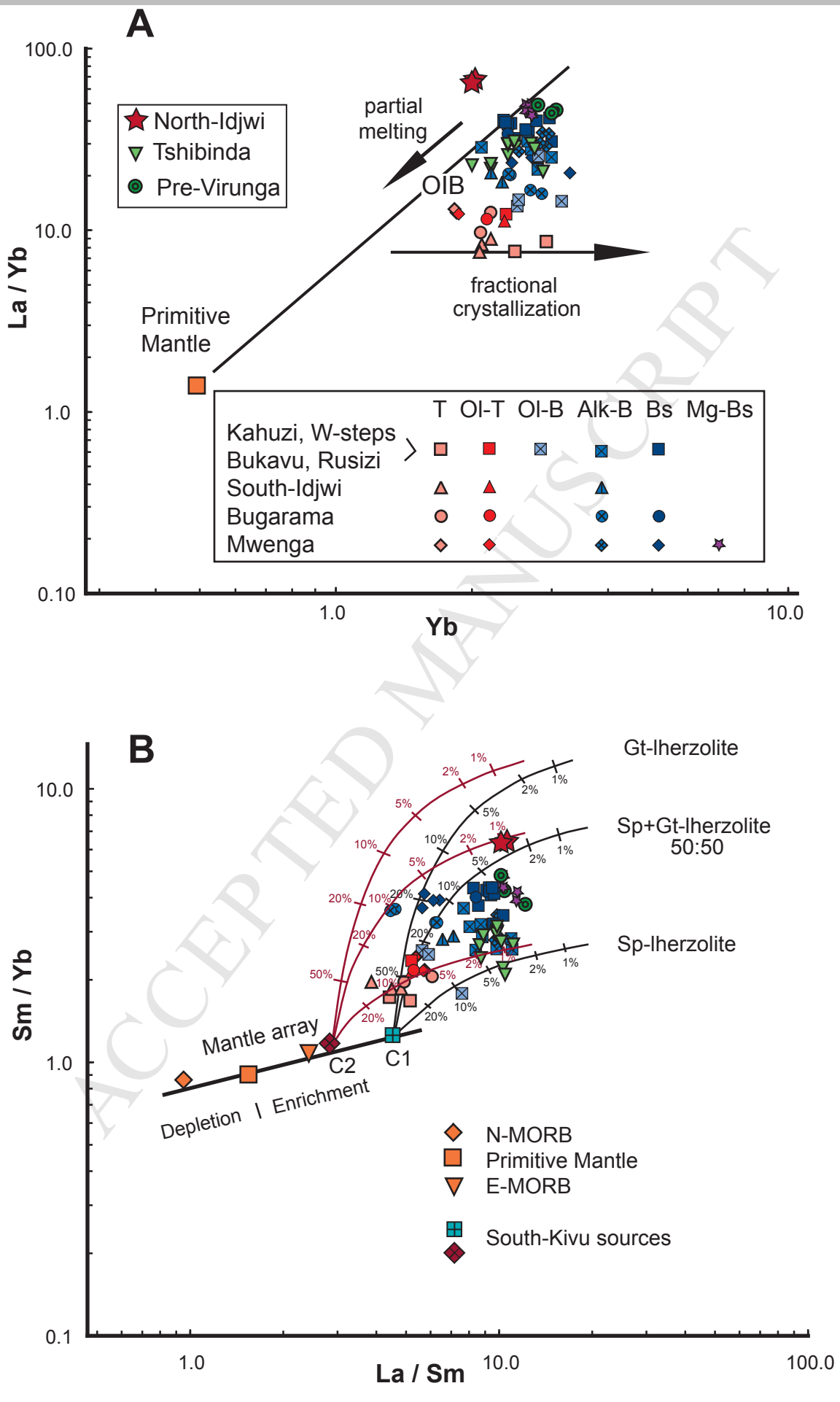

Fig. 10

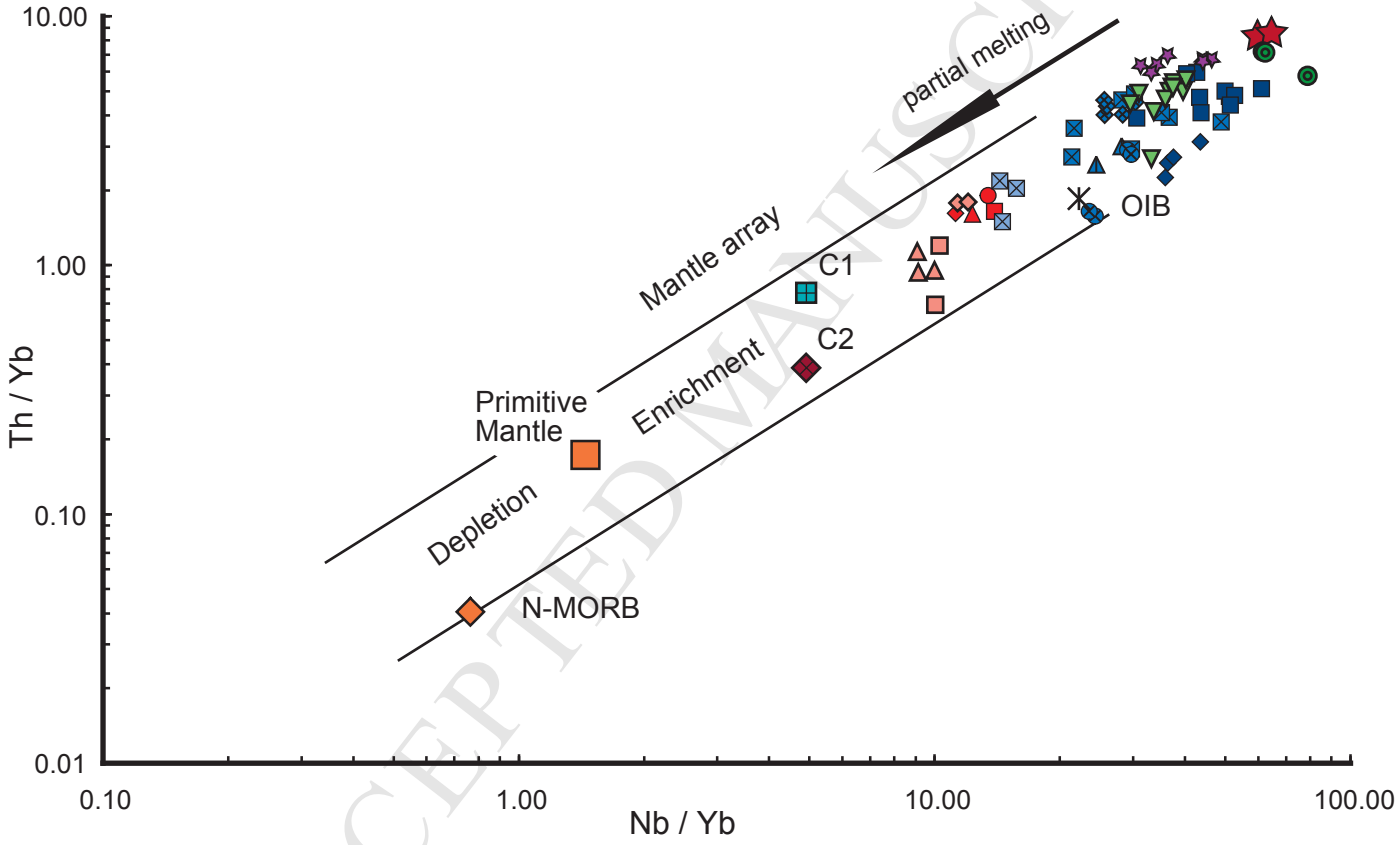

Fig. 11

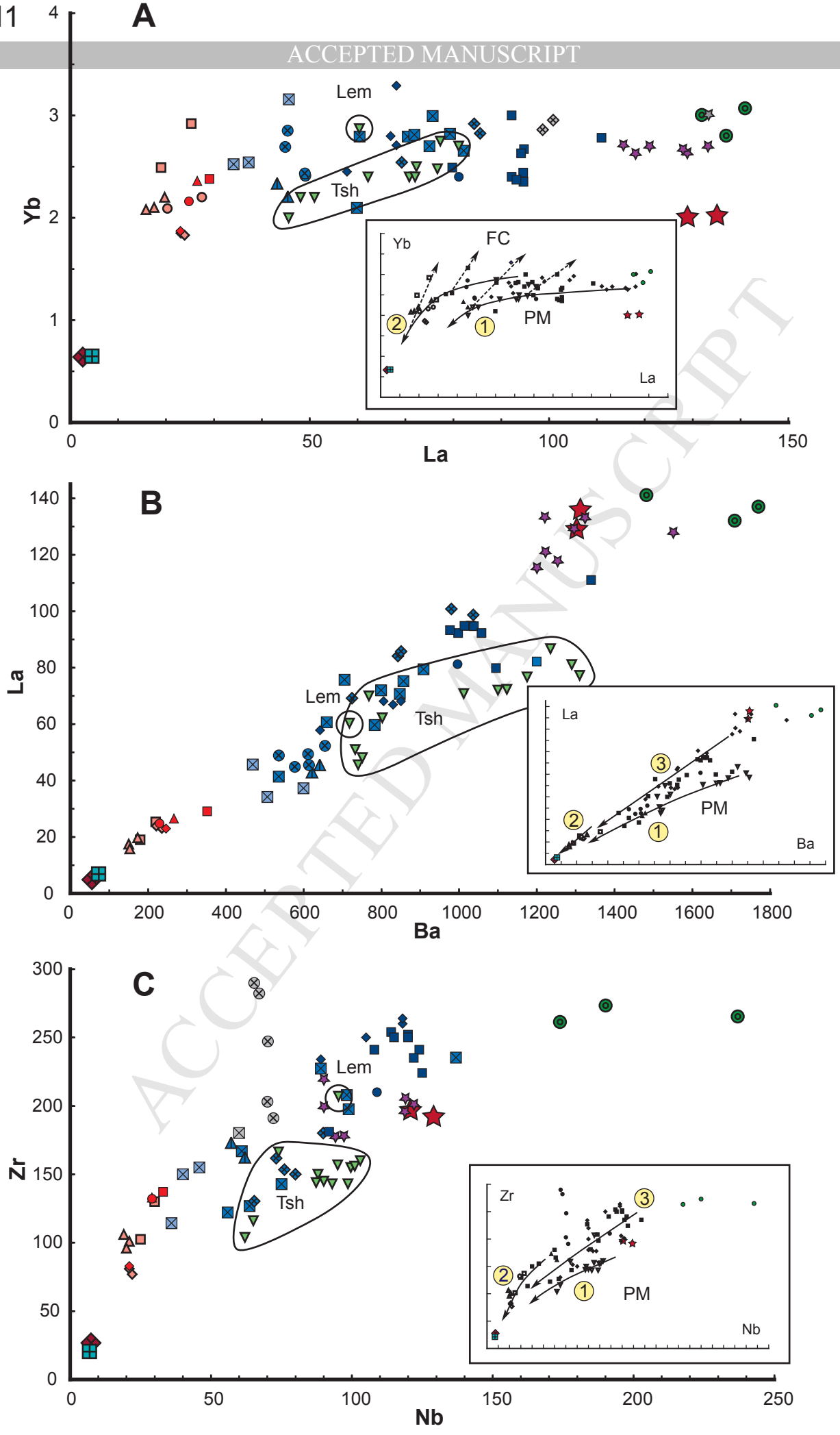

Fig. 12

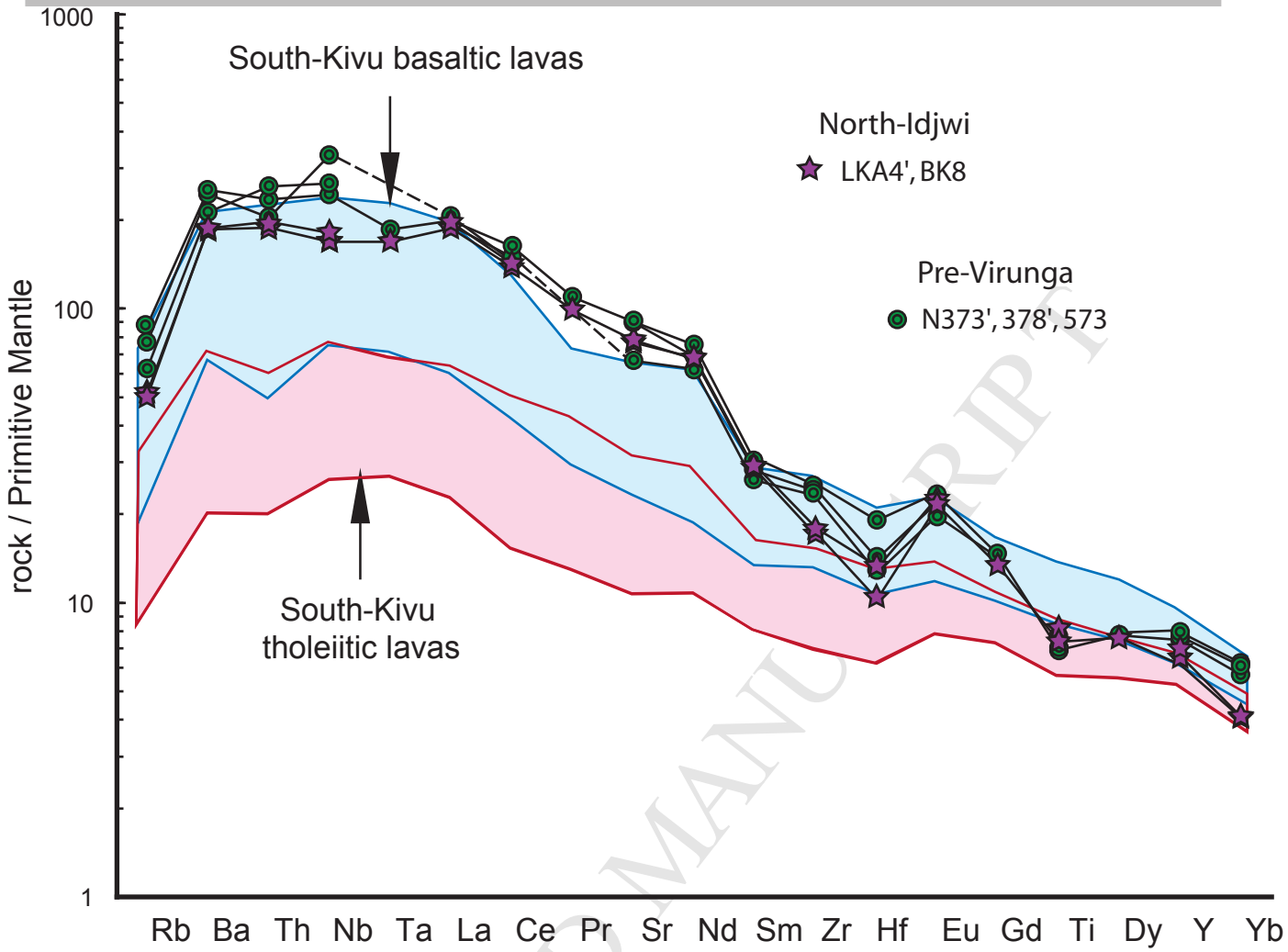

Fig. 13A, B

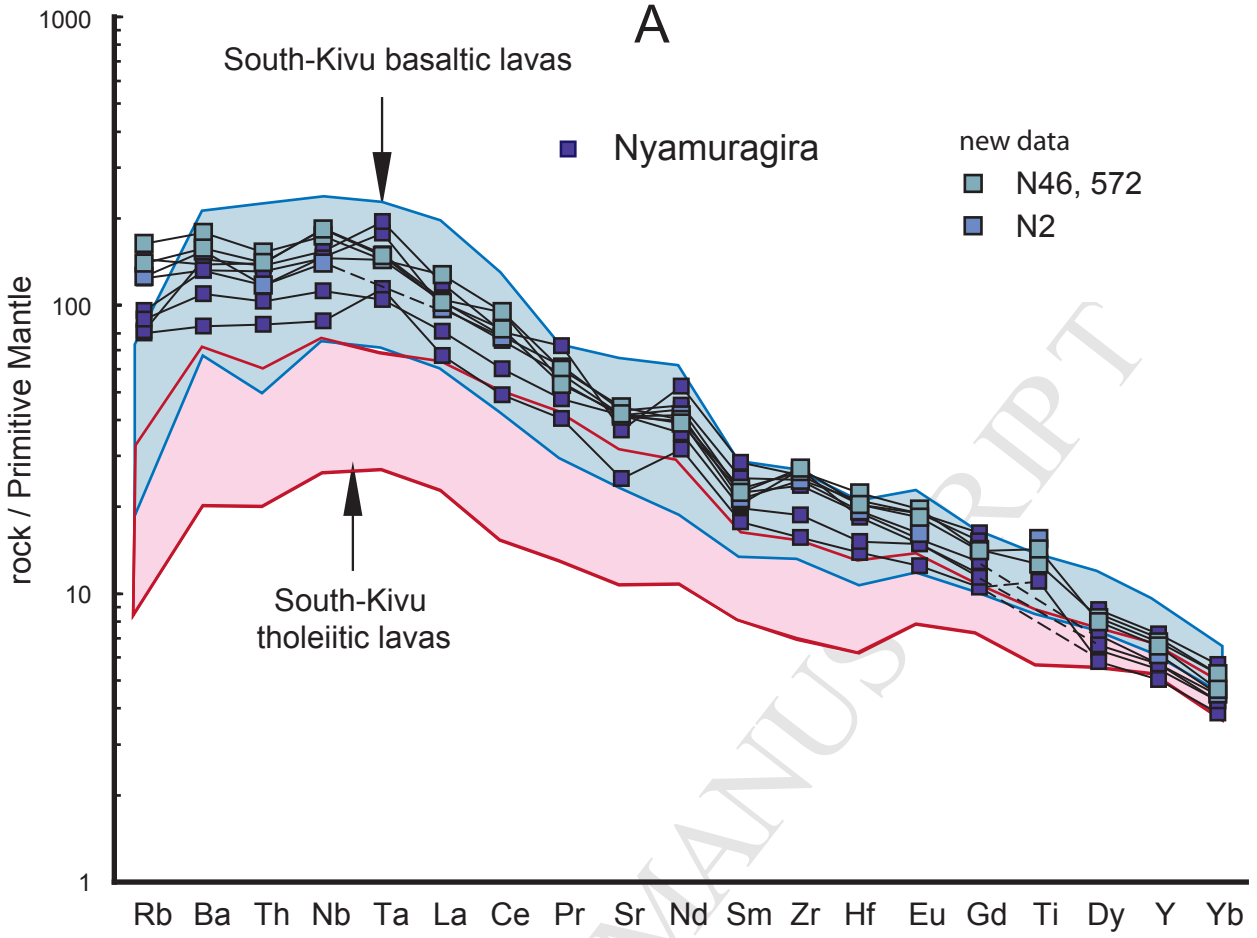

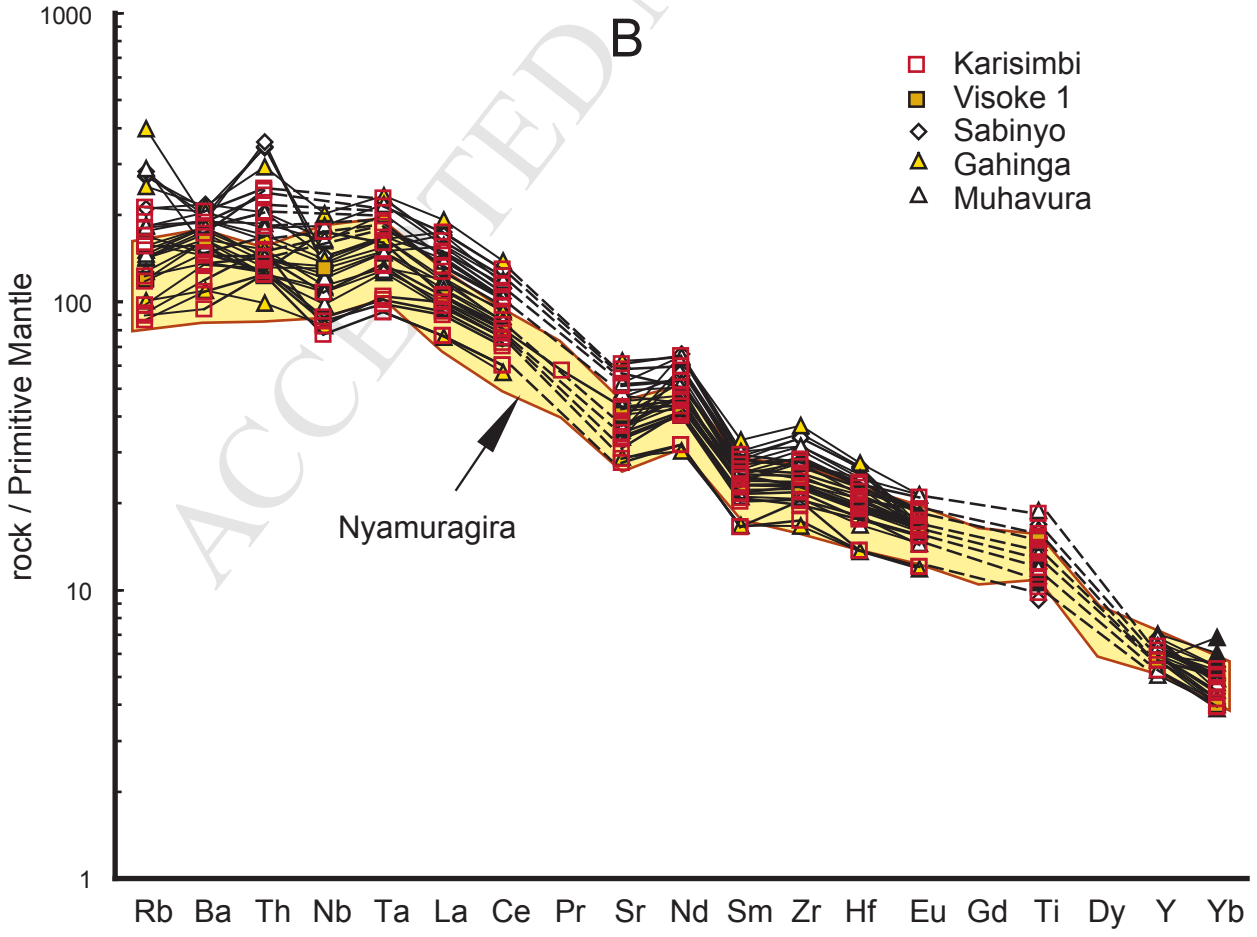

Fig. 13C, D

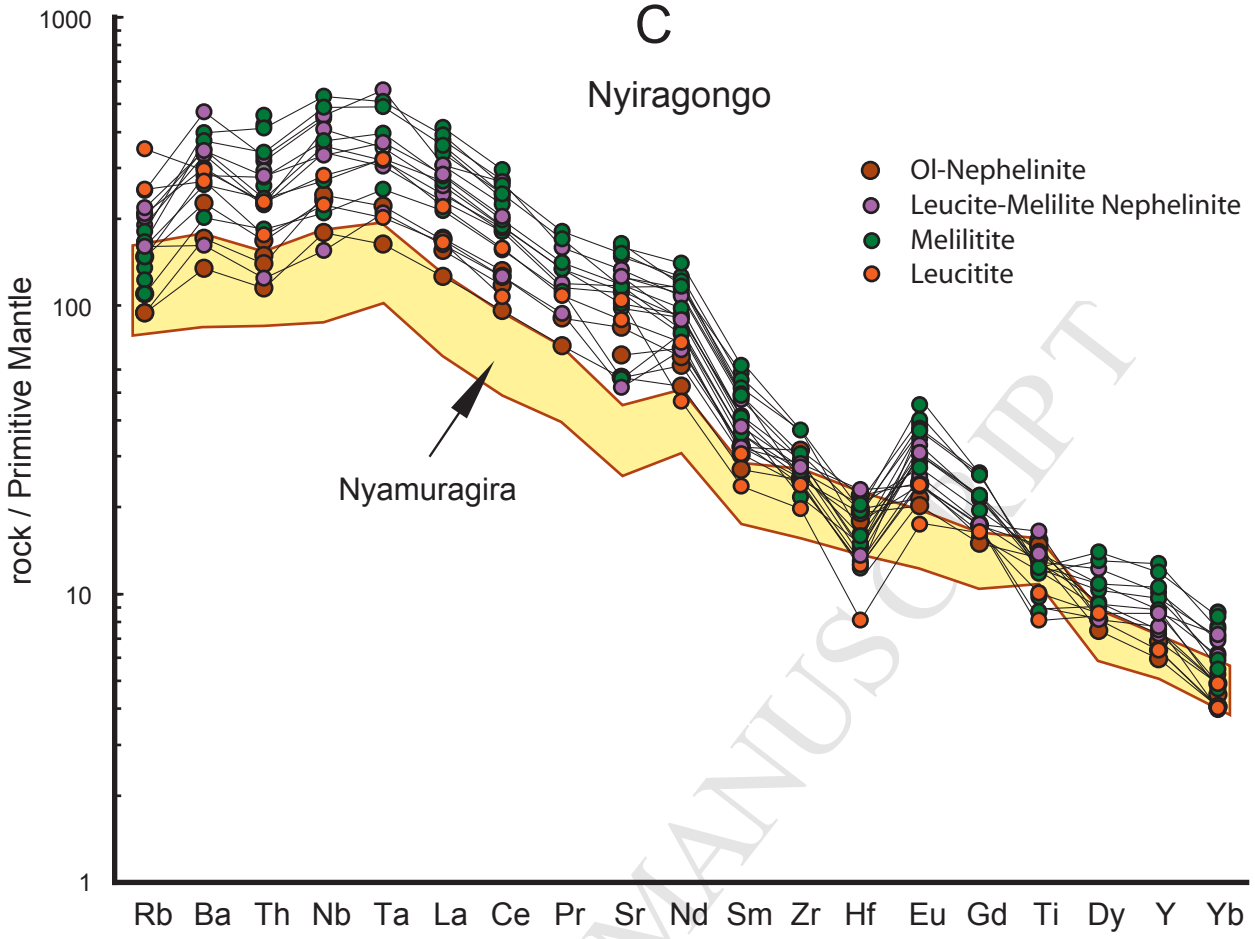

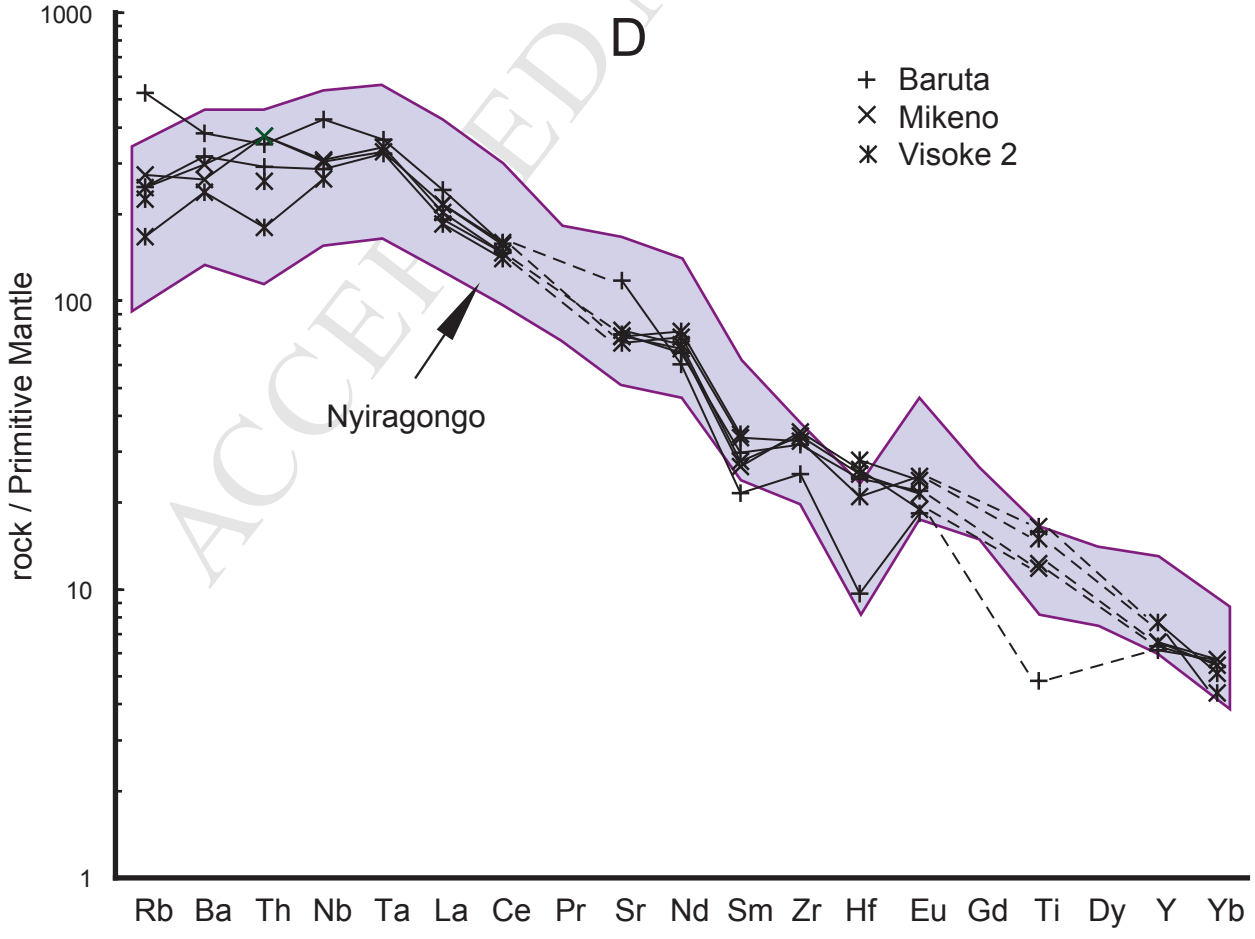

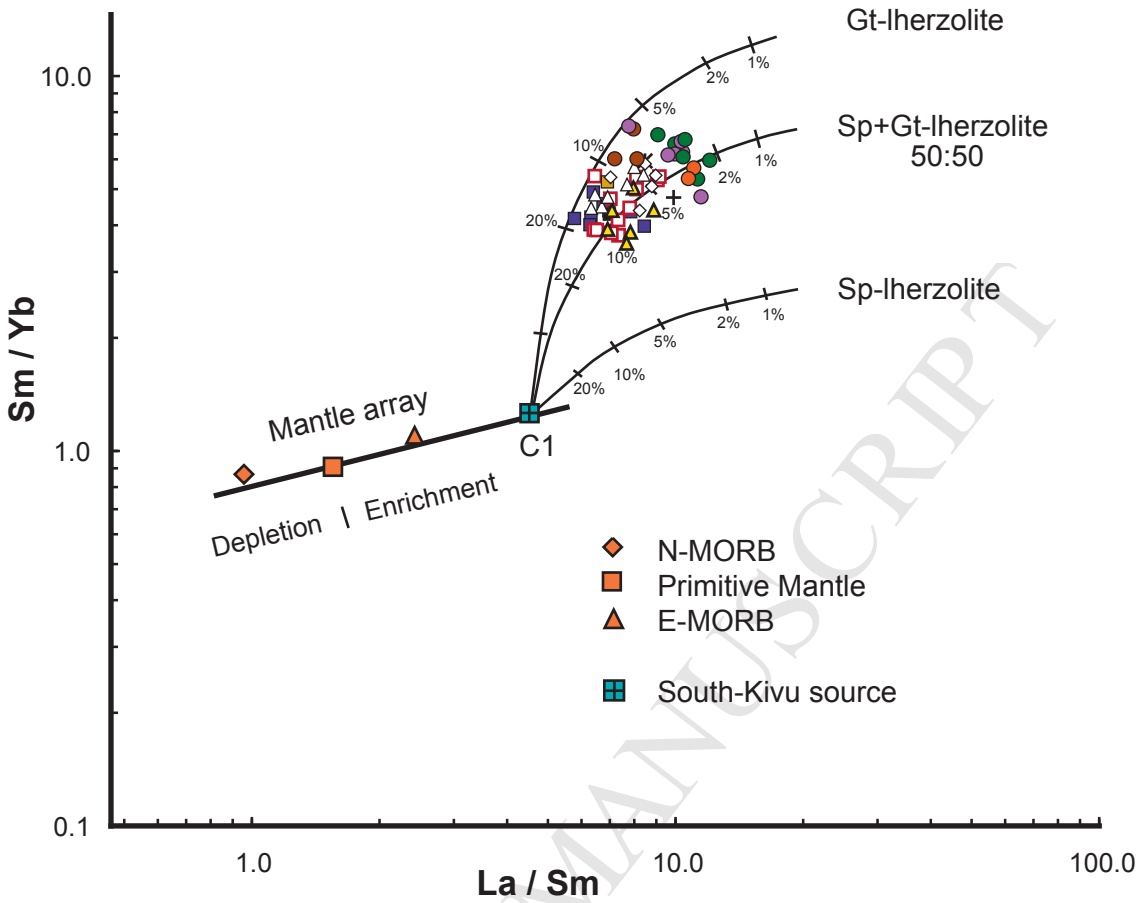

Fig. 15

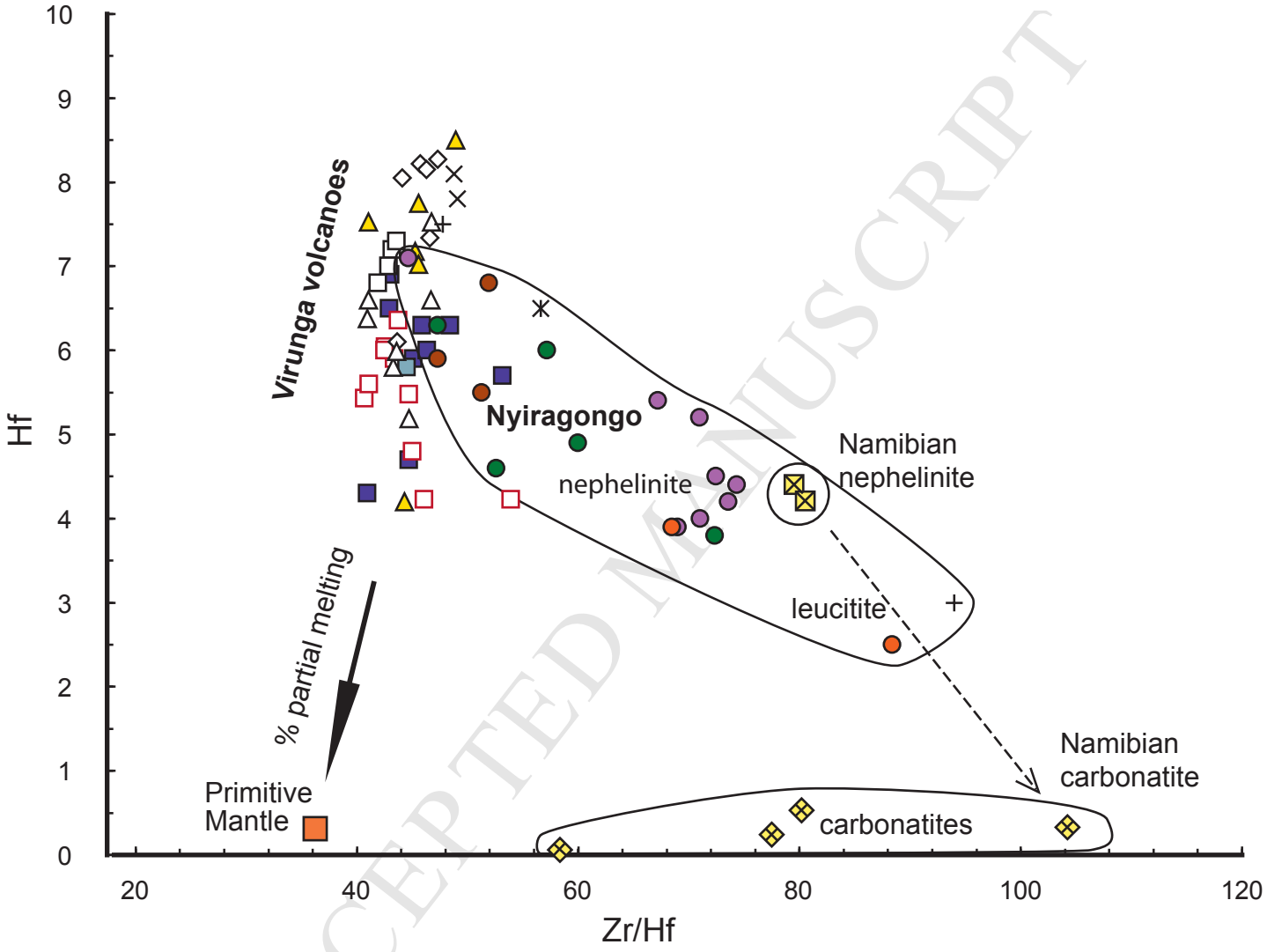

Fig. 16

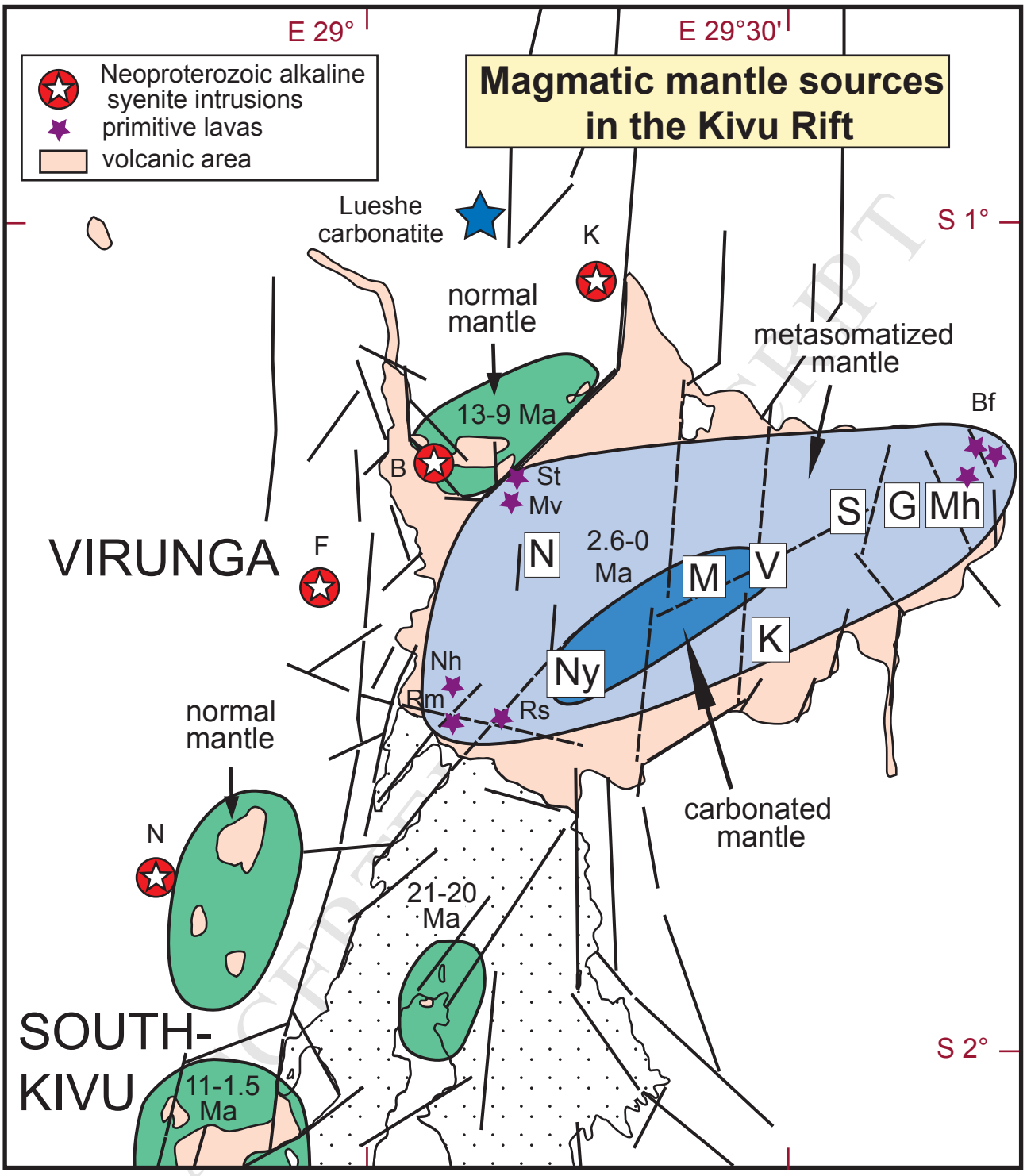
E 29°
E 29°30'
Neoproterozoic alkaline syenite intrusions
primitive lavas
volcanic area
Magmatic mantle sources in the Kivu Rift
Lueshe carbonatite
K
S 1°
normal mantle
metasomatized mantle
13-9 Ma
Bf
B
St
Mv
S
G
Mh
VIRUNGA
F
N
2.6-0 Ma
M
V
K
Nh
Ny
Rm
Rs
normal mantle
carbonated mantle
N
21-20 Ma
SOUTH-KIVU
11-1.5 Ma
S 2°

Fig. 17

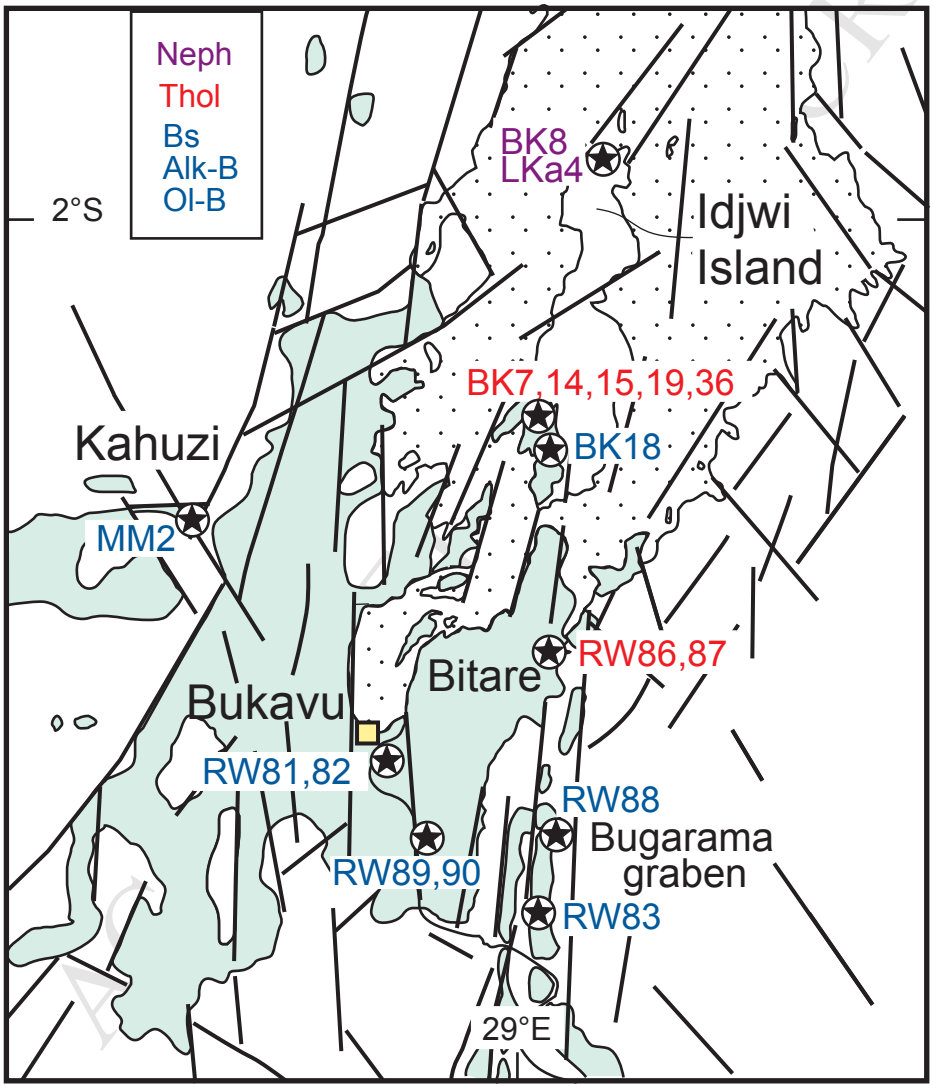
Neph
Thol
Bs
Alk-B
Ol-B
2°S
BK8
LKa4
Idjwi
Island
BK7,14,15,19,36
BK18
Kahuzi
MM2
RW86,87
Bitare
Bukavu
RW81,82
RW88
Bugarama
graben
RW89,90
RW83
29°E

Fig. 18

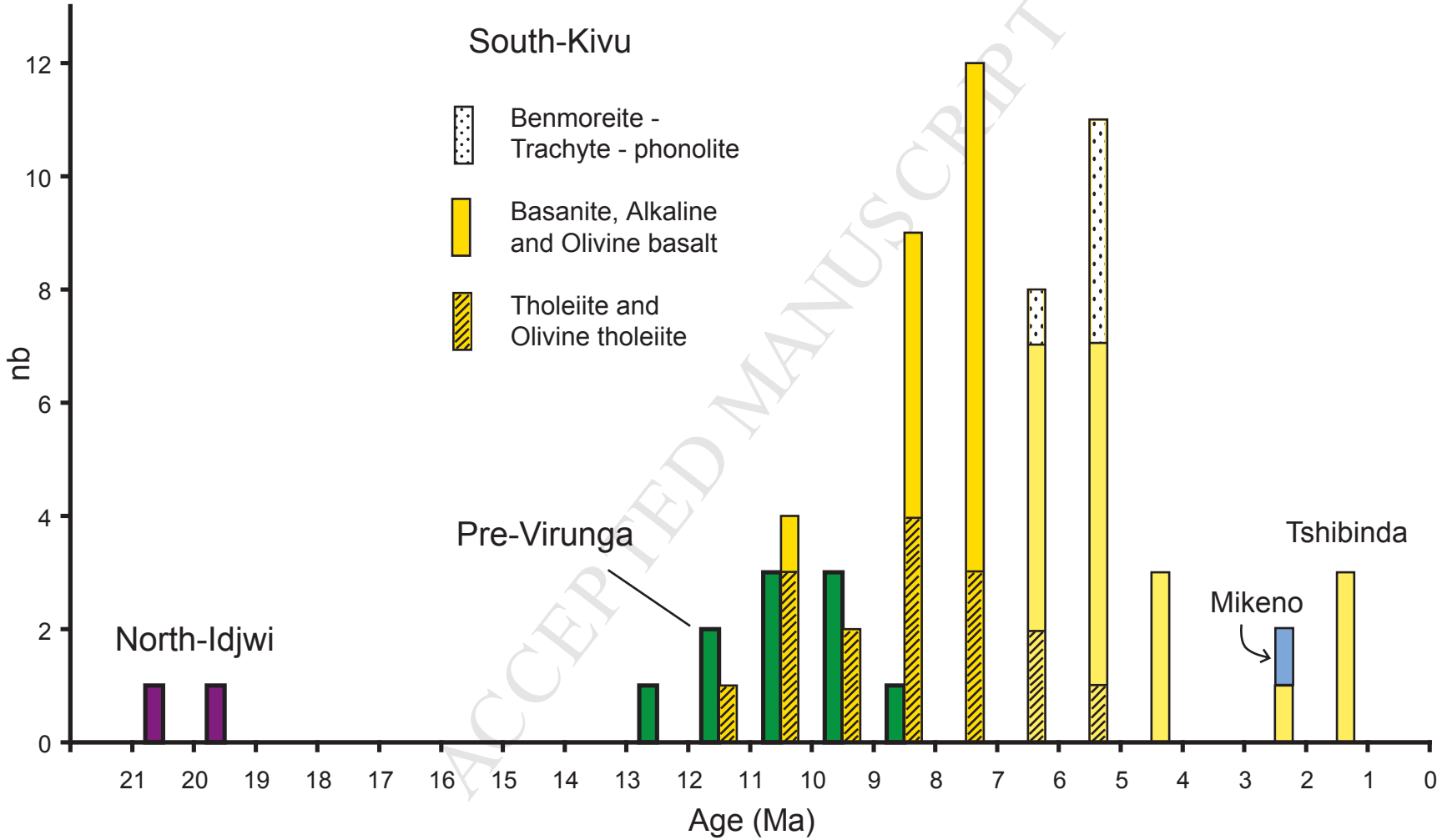

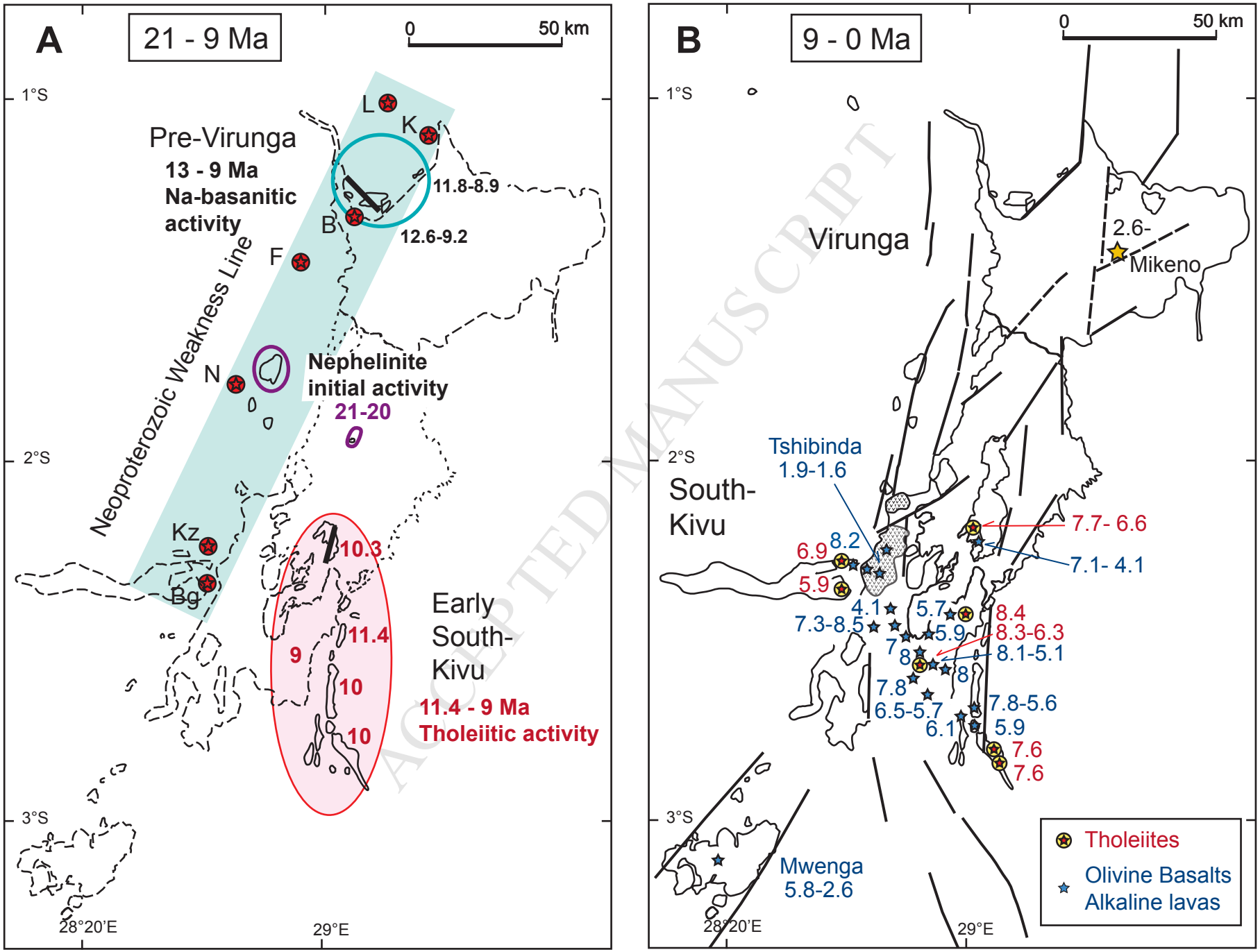

Fig. 19

Highlights

The pre-rift doming stage of the Kivu rift (East African Rift system) is dated at 21 Ma by nephelinites.

Tholeiite lavas initiate the extensional stage between 11 and 9 Ma.

In the Pliocene, alkali basalts indicate decreasing of the extensional process and cooling of the mantle.

Quaternary renewal of the activity in the Virunga is linked to a tension gash with an ENE-WSW extension.